Adsorptive Removal of Selected Halogenated Pharmaceuticals from Water Using Iron-Modified Kenyan Natural Zeolite: An Experimental Study

Jack Kikuvi

A thesis submitted in partial fulfillment for the requirement of the degree of Master of Science in Chemistry of Masinde Muliro University of Science and Technology

November 2025

DECLARATION

Declaration by Candidate

This thesis is my original work prepared with no other than the indicated sources and support and has not been presented elsewhere for a degree or any other award.

Signed..... Date….....

Jack Kikuvi

SCH/G/01-70042/2022

Declaration by Supervisors

The undersigned certify that they have read and hereby recommend for acceptance of Masinde Muliro University of Science and Technology a thesis entitled "**Adsorptive Removal of Selected Halogenated Pharmaceuticals from Water using iron-modified Kenyan natural Zeolite: An Experimental Study**"

Signed..... Date….....

Prof. Francis Orata,
Department of Pure and Applied Chemistry,
Masinde Muliro University of Science and Technology

Signed..... Date….....

Dr. Gershom Mutua,
Department of Pure and Applied Chemistry,
Masinde Muliro University of Science and Technology.

STATEMENT OF PLAGIARISM

Student's Declaration

1. I hereby declare that I understand that this thesis must be my own work.
2. I know that the incorporation of materials from other works or a paraphrase of such material without acknowledgement will be treated as plagiarism according to the rules and regulations of Masinde Muliro University of Science and Technology.
3. I know that plagiarism is an academic dishonesty and that if I commit any act of plagiarism my thesis can be assigned grade "F".
4. I further understand that I may be suspended or expelled from the University for Academic Dishonesty.

Signature..... Date….....

Jack Kikuvi SCH/G/01-70042/2022

Supervisors' Declaration

We hereby approve the examination of this thesis. The thesis has been subjected to plagiarism test and its Similarity index is not above 20 %.

Prof. Francis Orata

Signature..... Date.....

Dr. Gershom Mutua

Signature..... Date.....

COPYRIGHT

DEDICATION

I dedicate this work to my beloved family. To my mum Esther Kikuvi, my siblings Wambua, Mtesh, Hum, Tish, Eddy, Bob, Wayne, Yolanda and Ben. Thank you.

ACKNOWLEDGEMENTS

Firstly, my gratitude is to God Almighty for in Him do I live, move and have my being. I would also like to express my sincere thanks to my supervisors Dr. Gershom Mutua and Prof. Francis Orata for their tireless support, valuable criticism, encouragement, guidance and motivation throughout the period of this study. Special appreciation also goes to Robert Gembo (University of Johannesburg – South Africa) who helped with the adsorbent characterization. I would like to express my sincere appreciation to all staff from the department of Pure and Applied Chemistry, Masinde Muliro University of Science and Technology. Big thanks to my peers Josephat Mabuko, Nebert Shiyoya, Ben Bulimo, Edna Achola and Agnes Muyale whose support made the journey bearable.

Special thanks go to Rev. Ian Harris whose support throughout this journey can never be repaid in word or deed. Great thanks to my family for their endless support throughout the course of my studies.

ABSTRACT

A worldwide basic human right is the availability of affordable, trustworthy, and safe water. Pollutants of emerging concern like halogenated pharmaceuticals have been documented in all environmental matrices. Their adverse effects on humans and biota necessitate the need for their removal from water. The remediation of pharmaceuticals from water is a growing concern since conventional wastewater treatment plants are not equipped effectively for the task. Owing to its simplicity of use, affordability, and environmental friendliness, adsorption using natural and modified adsorbents appeals as a method of remediation. This study investigated the adsorptive potential of iron-modified Kenyan zeolite by varying contact time, initial pollutant concentration, temperature, and pH, while employing spectrophotometric monitoring. Adsorbent characterization using EDS, XRD, SEM, FTIR, and point of zero charge analyses provided insights into the structural and chemical changes brought by iron modification. The sorption capacity of unmodified zeolite was 7.71, 4.35, and 5.19 mg/g for Chloramphenicol, Ciprofloxacin, and Diclofenac potassium, respectively, while iron- modified zeolite exhibited significantly higher capacities of 22.49, 18.43, and 15.70 mg/g, respectively. Kinetic studies revealed that Chloramphenicol adsorption followed a *pseudo*-first order model, while Ciprofloxacin and Diclofenac potassium adhered to a *pseudo*-second order model. Isothermal analyses indicated that Chloramphenicol and Diclofenac potassium adsorption better fitted to the Freundlich model, whereas Ciprofloxacin was well described by the Temkin model. Thermodynamic analysis confirmed that adsorption onto iron-modified zeolite was spontaneous and feasible for all pollutants, with adsorption of Chloramphenicol and Diclofenac potassium being exothermic and Ciprofloxacin's showed endothermic characteristics. These findings highlight the superior performance of iron-modified Kenyan zeolite as an affordable and efficient adsorbent for pharmaceutical pollutant removal, offering a promising solution for water treatment.

Keywords: Iron-modified zeolite, Diclofenac potassium, Chloramphenicol, Ciprofloxacin

TABLE OF CONTENTS

LIST OF FIGURES

LIST OF TABLES

LIST OF APPENDICES

LIST OF ABBREVIATIONS AND ACRONYMS

$(R_{adj})^2$	Adjusted R-Squared
AOPs	Advanced Oxidation Processes
ImZe	Iron-Modified Zeolite
B3LYP	Becke, 3-parameter, Lee-Yang-Parr
C_e	Equilibrium concentration
EDS	Energy Dispersive Spectroscopy
FTIR	Fourier Transform Infrared Spectroscopy
HOMO	Highest Occupied Molecular Orbit
IPD	Intraparticle diffusion
log K_{ow}	octanol-water partition coefficient
LUMO	Lowest Unoccupied Molecular Orbit
NZe	Natural Zeolite
PFO	*Pseudo*-First Order
pH_{pzc}	Point of Zero Charge
PSO	*Pseudo*-Second Order
Q_e	Equilibrium Adsorption Capacity
Q_{max}	Maximum Adsorption Capacity
RMSE	Root Mean Squared Error
SEM	Scanning Electron Microscope
UNESCO	United Nations Educational, Scientific and Cultural Organization
WWTPs	Waste Water Treatment Plants
XRD	X-ray diffraction
ZSM-5	Zeolite Socony Mobil-5
χ^2	Chi-Squared Test

CHAPTER ONE

INTRODUCTION

1.1 Background information

Life on earth is dependent on water. It is the undisputed thread that binds life together, an elemental force essential for the very fabric of biological, ecological, and geological existence. From the microscopic realms of cellular biology to the vast expanses of our planet's diverse ecosystems, the significance of water resonates through every facet of life (Alberts et al., 2015). Water covers about two-thirds of planet earth with the oceans harbouring 97.5%. Given that not all of the water is suitable for consumption, freshwater is a finite resource. The improvement of life quality and the prevention of diseases heavily depend on the availability of safe drinking water. Every person has a fundamental right to suitable, affordable, safe, and sufficient water for residential use, according to the United Nations (United Nations, 2010). Despite governments and organizations all over the world trying to guarantee availability of safe water, pollution has been a major issue. Water pollution stands as a pervasive and escalating disaster, transcending geographical boundaries and threatening the very essence of life. With the increase of anthropogenic activities such as industrialization and agricultural activities, the once pristine waters that sustain ecosystems and communities are increasingly becoming repositories of contamination, heralding a crisis of unprecedented magnitude (UNEP, 2016). Pollutants in water can affect human health, destroy marine species, and upset the ecological cycle (Prüss-Ustün et al., 2019).

Water pollutants have been classified as either conventional or emerging (Ahamad et al., 2020). Conventional pollutants have been well-recognized and extensively studied. They include suspended solids, heavy metals, nutrients, and pathogens (Baste, 2021). Conversely,

pharmaceuticals and personal hygiene items, endocrine-disrupting compounds, microplastics, per- and polyfluoroalkyl compounds, and pesticides are examples of emerging pollutants, also referred to as micropollutants (Ahamad et al., 2020). Emerging pollutants have been detected in water and are linked with detrimental effects on biota. This explains the shift in the recent past, to study their remediation. Pharmaceuticals cause the greatest concern amongst micropollutants (Arman et al., 2021).

Pharmaceuticals are medicinal chemical compounds used with the intention of providing a therapeutic effect on the body at small doses (Gonzalez Pena et al., 2021). They particularly attract attention due to their low-biodegradability and high persistence (Patel et al., 2019). Pharmaceuticals and their metabolic byproducts have been detected in effluents from wastewater treatment plants (WWTPs), surface and ground waters, and drinking water (K'oreje et al., 2016). Halogenation is increasingly applied in pharmaceuticals in a bid to improve their bioavailability (Xu et al., 2014). However, this chemical modification also makes these drugs more persistent and difficult to remediate from water systems (Straub et al., 2023).

For example, Diclofenac is an analgesic used to treat inflammation and pain. It is considered as an emerging concern pollutant and was added by Decision 2015/495 to the European Union's Watch List (Sousa et al., 2019). Because of its stability and hydrophilic qualities, it is more persistent in aquatic systems (Madikizela & Chimuka, 2017). Similarly, Chloramphenicol is an emerging antibiotic pollutant that is stable and highly polar (Gu et al., 2021; Hong et al., 2023). It is a broad-spectrum antibiotic for combating both gram-positive and gram- negative bacteria (Bayrakci et al., 2021). It had been extensively utilized in food-producing animals prior to being outlawed in the European Union, some Asian countries, Australia, Canada, and Brazil (Wang et al., 2021).

Ciprofloxacin is an antibiotic of the fluoroquinolone class prescribed to manage bacterial illnesses including pneumonia and infections of the urinary tract (Sharma et al., 2010). It has been classified as an emerging antibiotic pollutant in the third Watch List under the Water Framework Directive by the Commission Implementing Decision European Union 2018/840 (Gomez Cortes et al., 2022). Aquatic organisms' health, population, and diversity are threatened by ciprofloxacin and its metabolite residues in water systems (Yan et al., 2019).

Pharmaceuticals are bioactive molecules that are life-threatening pollutants that require mitigation when present in water. One of the favoured methods for their removal from water is by adsorption. In the recent past, adsorption technology using locally available materials has attracted attention. Zeolites, especially offer a good alternative for use in the remediation of micropollutants. Zeolites are crystalline aluminosilicates characterized by a microporous framework composed of TO_4 tetrahedrons connected through shared oxygen atoms. Their structure obeys the Lowenstein rule (Pang et al., 2021). The negative charges in the zeolite frameworks, resulting from the substitution of Al^{3+} for Si^{4+}, are typically quenched by extra-framework mono or divalent cations, which can be readily exchanged with other cations (Li et al., 2017). Zeolites' extraordinary properties are due to their crystalline framework and distinct pore structure. This affords it properties like heat and hydrothermal stability, shape selectivity, acidity, catalytic activity, diffusion, adsorption and ion exchange performance. The bridging Al-OH-Si group attached to the framework has a great affinity for water and the Si-OH group on the zeolite's exterior renders the surface polar (Windeck et al., 2024). To solve the shortcomings of natural aluminosilicates, heteroatom isomorphism is widely utilized to substitute or modify the aluminium and silicon framework components of the zeolites (Pang et al., 2021).

Modification of zeolites is a practical approach for enhancing their performance in hydrophobic adsorption and catalytic applications (Li et al., 2015). In addition to the intrinsic capabilities supplied by the zeolitic structure, transition metal elements can be added to zeolites to provide them with catalytic oxidation properties. Iron, in comparison to other transition metal elements, is more readily incorporated into the zeolitic framework due to it favourable ionic radius (Yi et al., 2020) and its charge compatibility with tetrahedral sites (van Bokhoven & Lamberti, 2014) thereby improving the zeolites' hydrophobicity, acidity, and redox characteristics. It has been reported that modifying zeolite with iron enhances the adsorptive capacity of zeolites. In the current study, Iron-modified Kenyan natural zeolite was employed in the adsorptive removal of Diclofenac potassium, Chloramphenicol and Ciprofloxacin from water.

1.2 Statement of the problem

Pollution of the aquatic environment with synthetic chemicals is a global issue (UNESCO, 2023). Antibiotics such as Ciprofloxacin and Chloramphenicol have been reported in local surface waters at levels exceeding their predicted no-effect concentrations, potentially fostering antibiotic resistance (Kairigo et al., 2020). Additionally, Diclofenac persists in water and harms aquatic life by causing endocrine disruption and digestive organ damage in fish (Guiloski et al., 2017). The adverse effects of pharmaceuticals in water, even at trace concentrations, on aquatic biota as well as on human health is a wakeup call on the urgent need to remove them with great efficiency from water.

Developing countries such as Kenya have addressed the water pollution problem using conventional wastewater treatment plants (WWTPs). Although the conventional WWTPs have been efficient in the remediation of conventional pollutants, they have however proven counterproductive in the mitigation of micropollutants which include pharmaceuticals. According to estimates, only up to 50% micropollutant load is eliminated by conventional

WWTPs through degradation and sorption to sludge while the polar ones remain in water as they have no affinity for sludge (Luo et al., 2014). This has led to WWTPs being listed as the main source point for biota exposure to micropollutants hence the recommendation to add to the WWTPs a tertiary treatment to deal with pollutants of emerging concern hence increasing their efficiency (Orata, 2018). Owing to conventional WWTPs ineffectiveness in eliminating micropollutants from water alternative technologies such as Advanced Oxidation Processes (AOPs), Electro-oxidative degradation, Membrane Technology and Ultrafiltration have been exploited with reasonable success. However, these techniques are associated with high initial and operational costs and the generation of even more toxic metabolites during oxidation and degradation processes (Patel et al., 2019).

Natural zeolites, while possessing benefits like widespread availability, affordability and high surface area are limited in their capability to adsorb large hydrophobic organic compounds due to their small pore sizes and hydrophilic surfaces (Wanyonyi et al., 2020). There is a need to modify these zeolites to transform their surface properties and enhance pore accessibility, thereby significantly boosting their performance as adsorbents for halogenated pharmaceuticals and a broader range of organic compounds (Xie et al., 2012).

1.3 General objectives

To assess the efficacy of iron-modified Kenyan zeolite in removing selected halogenated pharmaceuticals from model wastewater by adsorption.

1.4 Specific objectives

i. To study the effect of process parameters on the adsorption of Chloramphenicol, Ciprofloxacin and Diclofenac potassium from water using iron-modified Kenyan zeolite.

ii. To determine the kinetics and isotherms of adsorption process of the selected pharmaceuticals onto iron-modified Kenyan zeolite from water.

iii. To determine the thermodynamics and propose mechanisms of the adsorption process of the selected pharmaceuticals onto iron-modified Kenyan zeolite from water.

1.5 Justification

The selected halogenated pharmaceuticals (Chloramphenicol, Ciprofloxacin, and Diclofenac) are heavily consumed for the treatment of different ailments in Kenya. They are persistent in the environment and have reported negative effects on flora and fauna, with antimicrobial resistance reported for Chloramphenicol and Ciprofloxacin (Kairigo et al., 2020). They have all been listed under European Union Watchlist as pollutants of emerging concern. The use of zeolites is informed by its availability locally, reusability, non-toxicity, stability and its potential for use as an adsorbent (Jiang et al., 2018). Modification of zeolites with metal ions has been reported to its increase their adsorption capacity and selectivity thus increasing their efficiency in decontaminating polluted water (Jannat Abadi et al., 2019). Adsorption unlike other conventional methods of removing pollutants from water stands out as affordable, efficient and environmentally safe (Rashid et al., 2021). This study is justified by its alignment with UN Sustainable Development Goals 6 (Clean Water and Sanitation) and 14 (Life Below Water), as it aims to address critical challenges in ensuring access to safe water and protecting aquatic ecosystems for sustainable development.

1.6 Significance of Study

This study is important in many ways. The findings of this research will benefit stakeholders in water resource management, water quality and pollution control. Additionally, this research will benefit manufacturers and hospitals in controlling water pollution. The utilization of zeolites for water purification will lead to improved water quality and the well-being of the population as

locals will utilize zeolites to make potable water purification systems and increased economic benefits along the value chain. The results on adsorption efficiency will help in the design of efficient waste water treatment plants. Data on the efficacy of iron-modified Kenyan zeolite for pharmaceutical elimination will add to scientific understanding, and the results will aid in policy formulation.

1.7. Scope of Study

This study investigated key process parameters influencing adsorption i.e., contact time, initial pollutant concentration, temperature and pH to optimize the process. The study characterized the zeolite's physico-chemical properties by applying Energy dispersive spectroscopy, X-ray diffractometry, scanning electron microscopy, Fourier-transform infrared spectroscopy, point of zero charge analysis and thermogravimetric analysis to understand its structural and surface properties. Additionally, the adsorption kinetics, isotherms, and thermodynamics were analyzed to elucidate the adsorption mechanisms, capacity, and practical feasibility of the adsorbent for pharmaceutical removal. The research was aimed at providing insights into the practical application of iron modified zeolite for wastewater treatment by running experimental laboratory study using spiked deionized water samples.

CHAPTER TWO

LITERATURE REVIEW

2.1 Introduction

Water, the most vital compound for life on Earth and industrial processes, is under threat from pollution. This pollution not only damages the environment but also has serious implications for public health. Among the many identified pollutants, a new class, micropollutants, that include pharmaceutical active compounds, are gaining attention because of their resistance to degradation and their potential for toxic effects at even low concentrations (Yang et al., 2021). The potential harm to human health and their detrimental effects on biota due to their presence in water systems is a cause for concern.

Pharmaceutical products are intended for therapeutic activities, and therefore, many of them are relatively chemically stable, enabling them to withstand degradation processes and consequently accumulate in water bodies (Bavumiragira & Yin, 2022). They are released into the water systems in many ways such as dumping of hazardous waste, and effluents from treatment plants. Consequently, pharmaceuticals have increasingly been found in municipal water systems among other water bodies, and this poses questions about their effects on aquatic life and human beings (Wada & Olawade, 2025).

2.1.1 Water pollution

Water pollution is a term used to describe the contamination of water systems with toxicants that can harm human health, destroy marine life, and disrupt the ecological cycle (Ahamad et al., 2020). Water resource pollution endangers both the current and future supply, impedes economic growth at the local, regional, and national levels, presents unknown and known

health risks to the public, and further disrupts the ecosystem's already severely upset equilibrium (Madhav et al., 2020).

Any chemical, biological or physical contaminant that has an unfavorable aesthetic impact on aquatic life and consumers of the water is considered a water pollutant (Madhav et al., 2020). Conventional pollutants include nutrients (NO_3^- and PO_4^-), organic pollutants, heavy metals, and microbial pollutants while emerging pollutants include personal care products, pharmaceuticals, pesticides and endocrine-disrupting compounds (Ahamad et al., 2020; Orata, 2018). Emerging pollutants, have especially attracted special interest among researchers with pharmaceuticals being at the core.

2.2. Pharmaceuticals

Pharmaceuticals are molecules often bioactive at low doses designed to have a healing impact on the body. They stay in the body for an extended period in their activated state until they have a therapeutic effect on the target (Bottoni et al., 2010). Pharmaceuticals, particularly draw attention due to their high persistence and low biodegradability; while not all pharmaceutical compounds are persistent, most are classified as "*pseudo*-persistent" since they are continuously released into the environment (Dai et al., 2011).

Prescription drugs and their metabolic by-products have been detected in WWTP effluents and other water systems (Massano et al., 2023). Concerns about the potential effects on human health have been raised by reports of analgesics, antibiotics, psychiatric, and antiretroviral medications in drinking, surface, and ground waters (K'oreje et al., 2016). Pharmaceuticals, even in trace levels, pose a significant threat to public health and the aquatic ecosystem (Patel et al., 2019).

Pharmaceuticals have been increasingly halogenated to improve their bioavailability and consequently their efficiency (Cao et al., 2025). This has been, however characterized as an

impediment to their biodegradation which results in their persistence and buildup in the environment, particularly in aquatic systems (Straub et al., 2023). Some of the halogenated pharmaceuticals include Diclofenac, Ciprofloxacin and Chloramphenicol. An understanding of the transformation of pharmaceuticals in the host body is essential in solving the problem of their presence in water.

2.2.1. Pharmacological Metabolism within the Host's Body

After administration, pharmaceuticals undergo metabolic transformations caused by either host's enzymes or gut bacteria before excretion (Zimmermann et al., 2019). These changes usually take place in two stages. During the first phase, the parent pharmaceutical compound is modified into metabolites with increased polarity by reduction, oxidation and hydrolysis reactions. During the second phase, conjugation reactions transform either the original active pharmaceutical ingredient or the compounds generated in the first phase into hydrophobic derivatives. These byproducts are more readily enzymatically degraded and excreted. Fecal matter and urine are the primary pathways by which the parent pharmaceutical, both metabolized and unmetabolized, are released into the environment. The percentages of unmetabolized medications excreted as the original active pharmaceutical ingredient of the selected halogenated drugs are displayed in Table 2.1.

Table 2.1: An estimated percentage of a pharmaceuticals that passes through the human body unmetabolized and enters the sewage system after ingestion.

Drug	% Excreted	Reference
Chloramphenicol	5 – 15	(Oong & Tadi, 2020)
Ciprofloxacin	40 – 50	(Thai et al., 2023)
Diclofenac	5 – 35	(Altman et al., 2015)

Pharmaceuticals are frequently detected in the environment, and studying their sources is crucial for effective remediation.

2.2.2. Sources of Pharmaceuticals and their Pathways in the Environment

Pharmaceuticals and their derivatives are continuously discharged into the environment via both point and nonpoint sources. Point sources include hospital waste and effluent from the pharmaceutical manufacturing industry. Nonpoint sources include agricultural soil runoff, urban runoff, and leaching from landfills. All environmental matrices have pharmaceuticals reported in them due to anthropogenic activities (Aus der Beek et al., 2016). A review of literature available agrees that pharmaceutical concentration in environmental compartments follow this sequence: drinking water, ground water, surface water, WWTP effluents, hospital effluents and pharmaceutical industrial effluent ranked from the lowest to the highest (Patel et al., 2019).

Pharmaceutical transport in the water environment has been modelled by the source-pathway-receptor scheme (Stuart et al., 2012) as shown in Figure 2.1. The model takes into account the receptor, the pathway that medicines have taken as well as their source. Aquatic transport, and food chain transportation are the primary methods of environmental transportation. Upon release into the environment, pharmaceuticals are transported through a variety of physical and chemical processes, including sorption, desorption, leaching, and degradation. Pharmaceuticals' physicochemical characteristics and the surrounding environmental factors influence their mobility and transit in the sediment-water matrices (Kathuria et al., 2023).

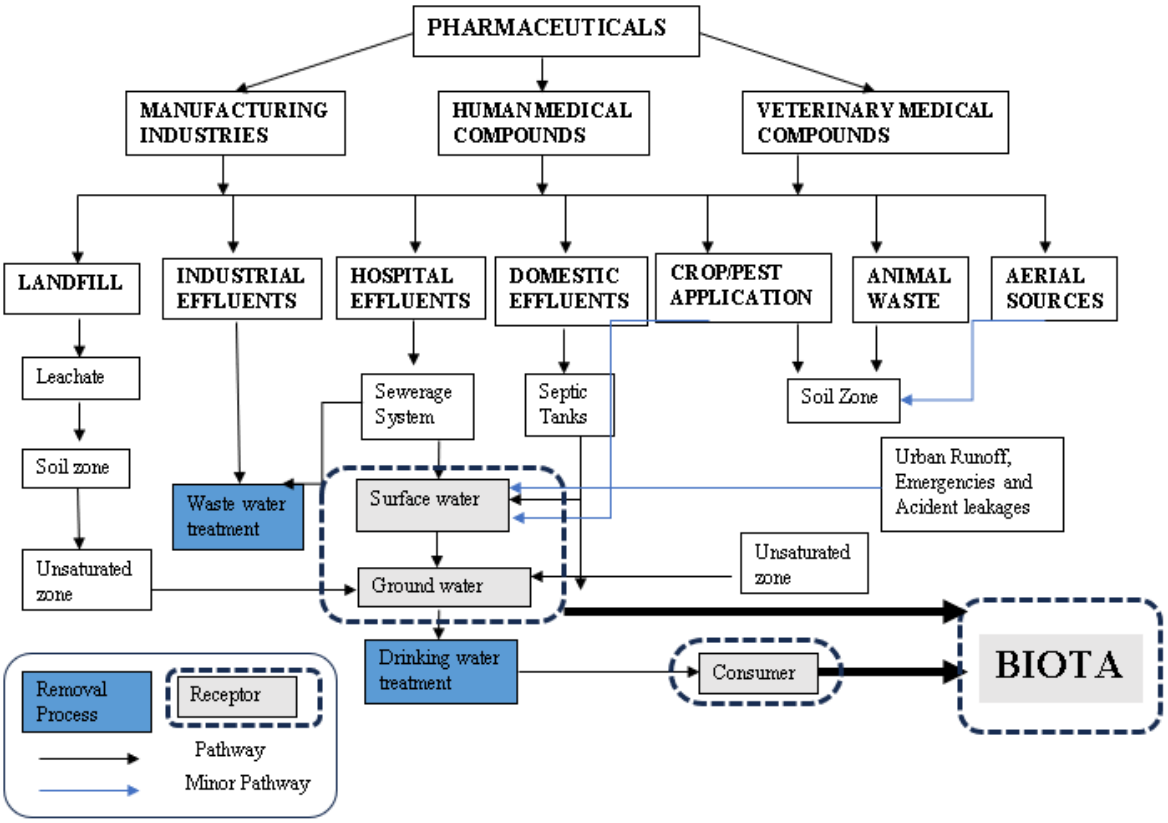

Figure 2.1: The source – pathway − receptor model (Patel et al., 2019)

2.2.3. The Transformation and Fate of Pharmaceuticals in the Aquatic Environment

Pharmaceuticals are made to be stable chemically since stability boosts their effectiveness. They, however, can undergo physicochemical and biotic transformations, which lowers environmental stabilities (Kalyva, 2017). In order to increase stability and bioavailability in patients, halogenation has been applied to many pharmaceutical products (Küster & Adler, 2014) which in turn increases their environmental stability. *Pseudo*-persistent drugs are said to have greater environmental persistence than other pollutants since they are continuously replenished despite undergoing biodegradation, photodegradation, and particle sorption. Continuous influx of pharmaceuticals into the environment therefore, makes them *pseudo*-persistent (Ebele et al., 2017). A pharmaceutical's physicochemical properties i.e.,

water solubility, dissociation constants and biodegradability are key in prediction of its fate in aquatic environment.

2.2.4. Pathways for Pharmaceutical Transformation in the Environment

Temperature, pH, water salinity, and sunlight are all environmental factors that catalyze various degradation processes of pharmaceuticals hence affecting their transformation. Figure 2.2 is a schematic representation illustrating the pathways of pharmaceutical transformation in the environment as they move through humans and animals into wastewater treatment, and finally into the environment. When pharmaceuticals are administered to humans and animals, the body metabolizes them, using a portion for therapeutic purposes while excreting the rest. These compounds and their metabolites then enter wastewater treatment systems, undergoing both abiotic and biotic transformations. The treated wastewater then releases these compounds and products into the environment, where additional abiotic transformations and biodegradation occur, influencing their persistence and environmental fate. The cyclic arrows indicate a continuous process, suggesting that pharmaceutical compounds and their transformation products can re-enter the cycle, perpetuating their presence and transformation in the environment.

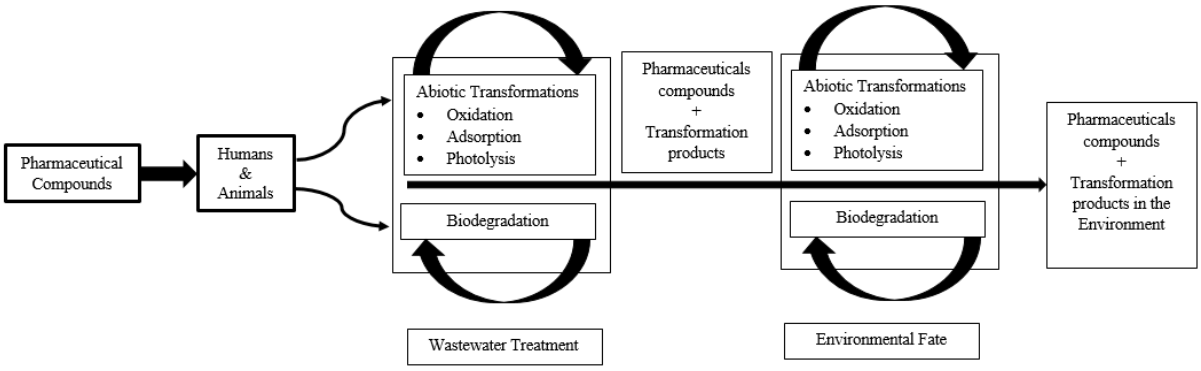

Figure 2.2: General schematic representation of pharmaceutical transformation in the Environment (Rehman et al., 2015)

Sorption onto sediments and sludge as well as photodegradation and biodegradation are essential pathways for eliminating pharmaceuticals from surface water. Drugs, especially antibiotics are designed to eliminate microbes. This in turn, reduces the concentration of pharmaceuticals that is eliminated through microbial biodegradation. Photodegradation is a significant surface water elimination route for many pharmaceuticals that contain photosensitive functional groups (Bavumiragira & Yin, 2022). For example, Diclofenac directly photodegrades under ultraviolet irradiation generating 13 transformation products (Muñoz et al., 2025). Fluoroquinolones photodegrades to form piperazine ring opening products (Lu et al., 2021). Majority of antibiotics biodegrade relatively slowly, with the biodegradation of fluoroquinolones in aquatic systems reported to be negligible (Rusch et al., 2019). Planar aromatic pharmaceuticals readily intercalate with clay minerals (Kümmerer, 2009).

2.3. Halogenated Pharmaceuticals and their Environmental Risks

Drugs are designed for the treatment of infections in both human and animals. They act by binding to particular receptors in the target organism. In the recent past, pharmaceuticals have been increasingly halogenated to improve their bioavailability hence increasing their efficiency. It has been shown that non-therapeutic exposure to pharmaceuticals has detrimental effects on aquatic and terrestrial life and environment (Le Page et al., 2017). In this study, discussion was done on Ciprofloxacin, Chloramphenicol and Diclofenac and their ecotoxic effects.

2.3.1. Diclofenac

Diclofenac, whose chemical name is 2-[2-(2,6-dichloroanilino) phenyl] acetic acid with a molecular formula of $C_{14}H_{11}Cl_2NO_2$, is a secondary amino compound, an amino acid, a dichlorobenzene, an aromatic amine and a monocarboxylic acid as shown in Figure 2.3. It has a

molecular weight of 296.148 g/mol. It is produced as Diclofenac potassium or Diclofenac sodium to enhance its solubility, stability, and bioavailability for pharmaceutical use. Diclofenac Sodium is primarily used in many oral formulations, ideal for sustained-release preparations due to its slightly slower dissolution rate compared to the potassium variant. Diclofenac Potassium, being more water-soluble than the sodium type, enables faster absorption and a quicker onset of action, making it suitable for immediate-release topical formulations for acute pain relief.

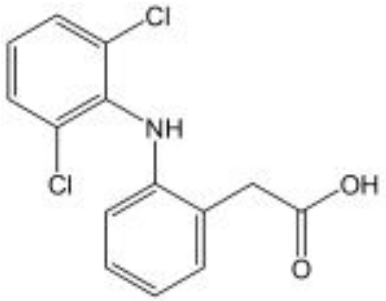

Figure 2.3: The chemical structure of Diclofenac

It is acidic with a pKa value of 3.99. It slightly soluble in water (2.37 mg L^{-1} at 25 °C) hence the relatively high *n*-octanol-water partition coefficient (log K_{ow})of 4.51 (National Library of Medicine, 2023). It is used as an analgesic to alleviate pain by primarily inhibiting cyclooxygenase enzymes, thus reducing prostaglandin synthesis and subsequent inflammation (Wiffen & Xia, 2020).

2.3.1.1. Ecotoxicity of Diclofenac

Diclofenac caused a sharp decline in Asian Gyps vulture populations by poisoning them as they scavenged diclofenac-medicated livestock. This was its first known detrimental effect on the ecosystem followed by a case reported in Europe (Herrero-Villar et al., 2021). Some of the reported toxic effects of Diclofenac on aquatic life include teratogenesis and embryotoxicity in the American bullfrog (Cardoso-Vera et al., 2017) and negative genotoxic effects in the marine copepod *Gladioferens pectinatus* (Guyon et al., 2018). Studies have also shown that Diclofenac

can also induce oxidative stress and cause damage in aquatic organisms like zebrafish even at environmentally realistic exposure levels (Bio & Nunes, 2020). Ecotoxicogenomic assessments have revealed that Diclofenac exposure can reduce survival and reproduction rates in soil-dwelling organisms like *Folsomia candida* (Chen et al., 2015). Additionally, studies have reported that Diclofenac impacts negatively on the development of maize (Hammad et al., 2018).

2.3.2. Chloramphenicol

Chloramphenicol's IUPAC name is 2,2-dichloro-*N*-[(1*R*,2*R*)-1,3-dihydroxy-1-(4-nitrophenyl) propan-2yl]acetamide has a molecular formula is $C_{11}H_{12}C_{l2}N_2O_5$, is an organochlorine compound with nitro, amido and alcoholic substituents as shown in Figure 2.4. It has a molecular weight of 323.132 g/mol.

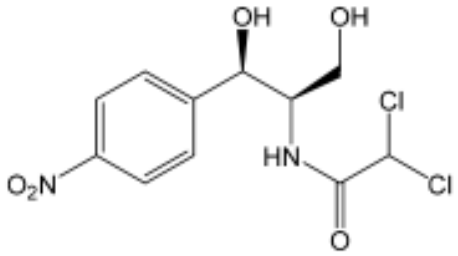

Figure 2.4: The chemical structure of Chloramphenicol

Chloramphenicol appears as white needle-like fine crystals. It sublimes in low pressure. It is fairly soluble in water (25 mg/mL at room temperature) and is soluble in organic solvents. It has a low log K_{ow} of 1.14. It is an antibiotic of broad spectrum against disease causing germs (Roushani et al., 2020). Chloramphenicol acts by inhibiting the synthesis of protein, causing bacterial death by binding to their ribosome (Bayrakci et al., 2021). It is a highly polar compound exhibiting high stability especially in neutral and weakly acidic solutions (Stolker & Danaher, 2011). Since Chloramphenicol has good stability and a relatively low production

cost, it is widely used in developing nations (Van et al., 2020). Chloramphenicol is listed as an emergent antibiotic pollutant by the World Health Organization (Gu et al., 2021).

2.3.2.1. Ecotoxicity of Chloramphenicol

Chloramphenicol was reported as a contributing factor in aplastic anaemia in human beings and animals. Its detrimental effects on the ecology led to its ban from application in all major food- producing animals in numerous countries including China, Japan, USA, Australia, Canada and the European Union (Chen et al., 2020). It has been associated with far-reaching toxicity on aquatic organisms (Zhang et al., 2021). Studies have shown that it can disrupt ecosystems and induce microbial resistance (Nguyen et al., 2022). Chloramphenicol has been reported to inhibit growth and development in green algae and blue- green algae (Xiong et al., 2019) thereby upsetting ecological balance. Its effect on non-target aquatic organisms, such as *Brachionus calyciflorus* revealed negative demographic responses across multiple generations (Iqbal et al., 2022). Additionally, some researches have indicated potential genotoxic carcinogenicity of Chloramphenicol (Luo et al., 2018).

2.3.3 Ciprofloxacin

Ciprofloxacin's IUPAC name is 1-cyclopropyl-6-fluoro-4-oxo-7-piperazin-1-ylquinoline-3-carboxylic acid whose molecular formula is $C_{17}H_{18}FN_3O_3$, is a quinolone with a cyclopropyl, carboxylic acid, fluoro and piperazin-1-yl substituents as shown in Figure 2.5. It has a molecular mass of 331.346 g/mol.

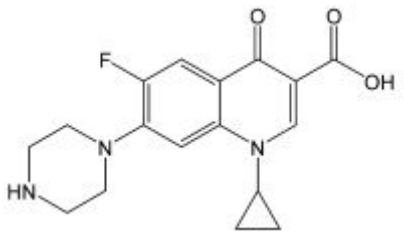

Figure 2.5: The chemical structure of Ciprofloxacin

Ciprofloxacin is a crystalline yellow powder. It is acidic with a pH of 3.5 – 4.6; highly soluble in water, 36 mg/mL at 25 ℃ and has a log K_{ow} of 0.28. It is a broad-spectrum fluoroquinolone antibiotic prescribed for the treatment of diseases like pneumonia, urinary tract infections and other bacterial infections (Cao et al., 2021). It is listed as an emerging antibiotic pollutant in the 4th Watch List under the Water Framework Directive of June 2018 by Commission Implementing Decision (EU) 2018/840 (Gomez Cortes et al., 2022). Aquatic organisms' health, population and diversity is threatened by Ciprofloxacin and its metabolites in the water systems (Yan et al., 2019).

2.3.3.1. Ecotoxicity of Ciprofloxacin

The presence of Ciprofloxacin and its derivatives in aquatic systems poses a significant risk to the human health and ecosystem due to its low biodegradability (Meng et al., 2016). Its presence in the aquatic environment induces resistant strains promoting bacterial resistance, which negatively affects the ecosystem (Adenaya et al., 2025). Furthermore, Ciprofloxacin has been shown to inhibit the growth of aquatic organisms like cyanobacteria and macrophytes (Ebert et al., 2011). Chronic exposure to Ciprofloxacin has been reported to affect the taxonomic diversity of meiobenthic nematode communities (Nasri et al., 2020). Moreover, Ciprofloxacin's presence in aquatic environments contributes to the development and spread of antibiotic resistance, posing additional ecological and human health concerns (Kelly & Brooks, 2018).

A consideration of the operation of conventional WWTPs highlights how they are employed in water purification and their ineffectiveness in remediating pollutants of emerging concern.

2.4. Conventional wastewater treatment process

A schematic representation of a primary and secondary system employed for the remediation of pollutants in conventional wastewater treatment plant as shown in Figure 2.6.

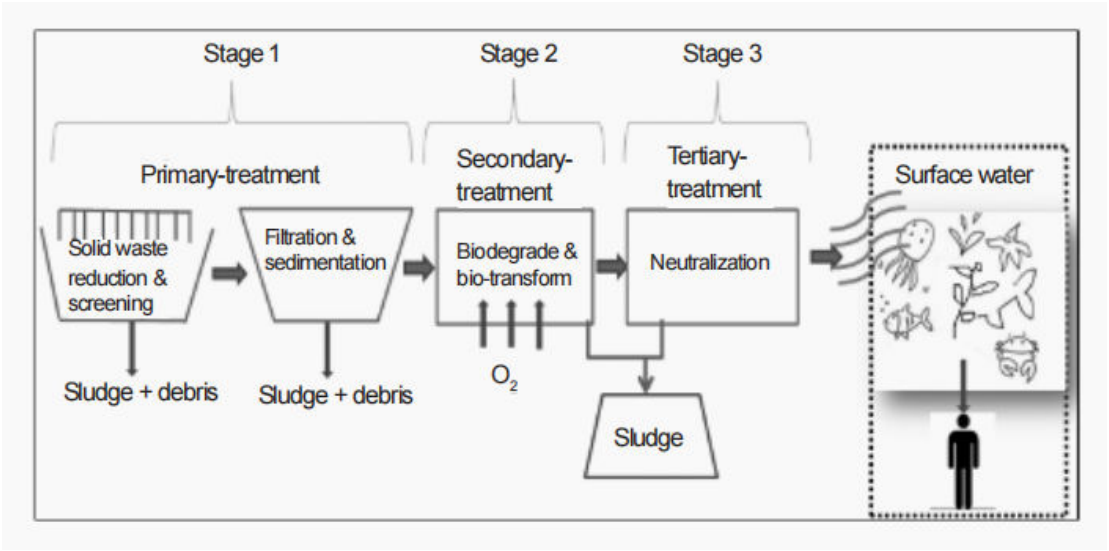

Figure 2.6: Stages and processes involved in a conventional wastewater treatment plant (Orata, 2018)

WWTPs apply primary screens, aerobic and anaerobic digesters, and biological filters in water treatment. They are designed to reliably and efficiently control a variety of pollutants, such as organic waste, particulates and nutrients. However, these plants are not specially made for complete remediation of emerging pollutants. Poor adsorption ability of some of the pharmaceuticals onto the activated sludge limits microbial contact and consequently their biodegradation (Khasawneh & Palaniandy, 2021). Nine WWTPs in the Lake Victoria Basin discharge 0.602 µg/L of pharmaceuticals daily into the lake as reported by Kimosop et al. (2016) which is ten times above the predicted no-effect concentration of 0.05 µg/L (Alliance, 2021) highlighting their inefficiency in pharmaceutical remediation. The daily discharge has likely increased due to population growth in the served towns over the last decade. As a result, conventional WWTPs have been identified as a point source and discharge pathway for biota exposure to emerging pollutants (Orata, 2018).

To remediate micropollutants conventional WWTPs have been supplemented with advanced treatment processes.

2.5. Advanced wastewater treatment process

Owing to the inefficiency of conventional WWTPs in dealing with micro-pollutants, tertiary treatment is increasingly used as the final step before discharging treated water into the environment. Enhanced biological treatment, advanced oxidation processes, electro-oxidative degradation, membrane processes and adsorption have been applied in the remediation of pharmaceuticals and other micropollutants (Orata, 2018).

2.5.1. Enhanced Biological Treatment

Conventional biological treatment applies activated sludge and primarily targets bulk organic compounds achieving only less than 60% removal of micropollutants (Gupta et al., 2021). Conversely, enhanced biological treatment systems incorporate targeted optimizations such as extended sludge retention time, bioaugmentation with specialized microbes, addition of co-substrates to promote co-metabolism, and hybrid configurations like moving bed biofilm reactors to achieve removal efficiencies of up to 100% by enabling effective biodegradation of the micropollutants that conventional systems fail to remediate due to limited microbial contact and metabolic capacity (Luo et al., 2014).

In enhanced biological treatment, pharmaceuticals and their metabolites are degraded by specialized microbes both aerobically and anaerobically. Despite the toxicity of most pharmaceuticals to bacterial strains, some microbial consortia have the ability to biodegrade pharmaceuticals with studies reporting appreciable degradation percentages and complete mineralization by bacterial, algal and fungal cultures (Patel et al., 2019). Phytoremediation is also a biological technique employed in the remediation of pharmaceuticals by maximizing on plants capability to uptake, accumulate and degrade pollutants. The biodegradability of pharmaceutical compounds varies considerably, and many drugs are designed to be stable, which hinders their breakdown by microorganisms (Silva et

al., 2019). The high selectivity of bioremediation is a major drawback when it comes to removing pharmaceuticals from water. This means it only works effectively on pollutants that are easily biodegradable, often resulting in the incomplete removal of many pharmaceutical compounds that are not readily broken down by biological processes (Shah & Shah, 2020). The partial removal of pharmaceuticals, leads to the formation of metabolites that may still pose environmental risks (Ortúzar et al., 2022).

A downside to this treatment technique is its high initial set up cost coupled by high operational cost. Enhanced biological treatment is capital-intensive, requiring large aeration tanks for extended sludge retention times, moving bed biofilm reactors and bioaugmentation dosing systems. Additionally, its operational costs are high due to increased aeration energy, specialized microbial cultures, and co-substrates needed for micropollutant degradation (Srinivasan et al., 2025).

2.5.2. Advanced Oxidation Processes (AOPs)

Advanced oxidation processes offer an appealing technique for the partial and complete degradation of pharmaceuticals, even at trace quantities (Capodaglio et al., 2018). AOPs are categorized into photochemical, non-photochemical and hybrid processes. They comprise a variety of technologies such combination of ultraviolet light and ozone (UV/O_3), Fenton processes (Fe^{2+}/H_2O_2) and Photo-Fenton processes (Deng & Zhao, 2015). AOPs are particularly successful for the remediation of mixed pharmaceuticals pollutants, with removal percentages of $> 99\%$ and effluent concentrations below 1 $\mu g\ L^{-1}$ reported (Anjali & Shanthakumar, 2024). It is however, linked to the generation of by-products whose toxicity may be higher than the parent pollutant. It is an operationally complex process marked by high energy consumption hence high operational and maintenance costs (Water Online, 2019).

2.5.3. Electro-oxidative degradation

Electro-oxidative degradation techniques have recently garnered interest as an approach to reduce pharmaceutical pollution by producing reactive species using electricity instead of chemicals (Loos et al., 2018). A platinum electrode showed better performance than a carbon electrode in the degradation of Diclofenac (Sifuna et al., 2016). While electro-oxidative degradation of pharmaceuticals in water has demonstrated success in removing a wide range of pharmaceutical compounds (Oturan, 2014), it is faced by several limitations hindering its widespread adoption. In the first place, the high cost of electrode materials with superior catalytic activity poses a significant challenge (Banham & Ye, 2017). Moreover, the process is highly sensitive to changes in water quality parameters such as pH, conductivity, and the presence of other compounds that compete for oxidation. Also, electrode fouling and passivation can decrease performance and require frequent maintenance (Włodarczyk-Makuła et al., 2023). Lastly, scalability and long-term stability of electrochemical systems remains a challenge due to high initial and operating costs.

2.5.4. Ultrafiltration and Membrane Technology

Filtration has been utilized to enhance advanced treatment methods at the tertiary level. It eliminates micropollutants from water primarily by capturing the suspended solids to which they are adsorbed to. Membrane technology include ultrafiltration, microfiltration, nanofiltration and reverse osmosis (Baker, 2023). Ultrafiltration and microfiltration are characterized by relatively larger pore sizes and low-pressure membranes as compared to reverse osmosis and nanofiltration membranes hence their application in removal of suspended particles in water. Nanofiltration and reverse osmosis, due to their properties, have been the most preferred technology applied in the remediation of pharmaceuticals in water. Ultrafiltration and membrane technology have been proven to generate high-quality discharge

that meets the guidelines for effluents in sensitive applications like wastewater treatment for domestic re-use (Orata, 2018). However, membrane technology is characterized by high operational costs, membrane fouling and is not fully effective as some micropollutants are smaller in size as compared to the membrane pore sizes (Mohammad Boshir Ahmed et al., 2017).

2.5.5. Use of specialized sorbents

Adsorption is the process by which adsorbate molecules from a fluid (liquid or gas) adhere to the surface of an adsorbent i.e., solid phase via physical or chemical forces. The sorption process occurs in four steps namely; sorbate transport in the fluid phase, diffusion across the boundary layer (film diffusion), pore diffusion, and sorption onto the solid by physical interactions e.g., weak van der Waals interactions or chemical bonds such as hydrogen bonding (Pourhakkak et al., 2021). Adsorption is mainly classified into chemisorption and physisorption based on the type of the bonds formed between the sorbent and the sorbate. Chemisorption is characterized by electron transfer and covalent bonding. It is slow, single layered and irreversible. Physisorption is distinguished by weak *Van der Waals* interactions between the pollutant molecules and the adsorbent surface. It is fast, multi layered and reversible (Rápó & Tonk, 2021). Factors that affects adsorption process include initial pollutant concentration, the solution's temperature and pH, adsorbent dose and the sorbent's particle size (Rápó & Tonk, 2021).

Low initial capital investment and maintenance cost, suitability for batch and continuous process, applicability for trace pollutants and ability to reuse and regenerate sorbents are some of the benefits of adsorption as a remediation technique (Crini & Lichtfouse, 2019). Researchers have utilized various modified bio-based adsorbents for removing pharmaceuticals: akageneite-functionalized maize cob biochar for carbamazepine (Jemutai-

Kimosop et al., 2022); acid-activated *Moringa oleifera* seed biomass for progesterone (Ngeno et al., 2024), and water hyacinth biochar for caffeine and Ciprofloxacin (Ngeno et al., 2016).

The use of affordable, readily available minerals like zeolites as sorbents in water treatment has garnered attention recently.

2.6. Zeolites

Zeolites are hydrated aluminosilicates with highly crystalline structures. They are highly porous with network of interconnected tunnels and cages of defined molecular dimensions. The pores are occupied by water, monovalent and divalent cations. They are either formed over long periods of time within sedimentary deposits or through the reaction between alkaline groundwater and volcanic ash. Zeolites' formation conditions such as the parent volcanic material's chemical composition, temperature, pressure, groundwater presence, and geochemical environment vary greatly across geographic locations (Gottardi & Galli, 2012). Based on their elemental compositions and structures, zeolites vary widely in size and shape and over fifty different varieties have been identified globally (Velazquez-Peña et al., 2019).

The general chemical formula of zeolites is $M_{x/n}[Al_x Si_y O_{2(x+y)}]\cdot pH_2O$ where M is an Alkali metal and/or an Alkaline earth metal, n is cation charge; $1 \leq y/x \leq 6$ and $1 \leq p/x \leq 4$. A tetrahedron, whose centre is either occupied by an aluminum or silicon atom, with four atoms of oxygen at the vertices as illustrated in Figure 2.7 is the unit cell of zeolite framework.

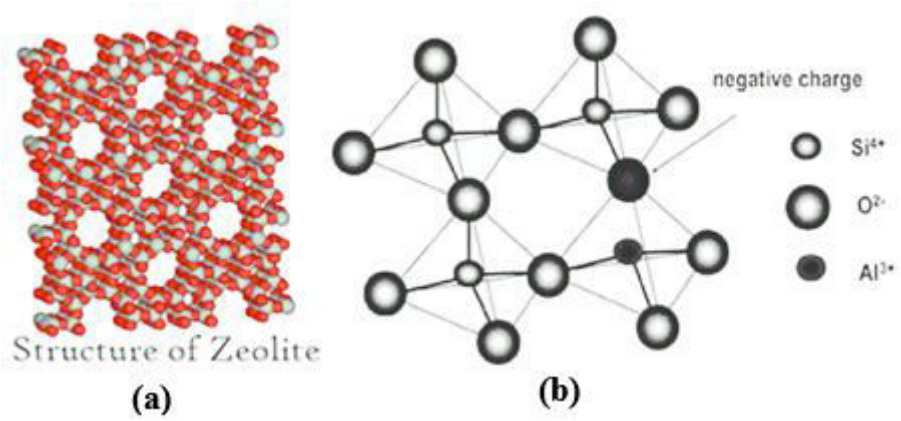

Figure 2.7: The general structure of zeolites highlighting the tetrahedron primary building block and pores in the structure (Maulana & Takahashi, 2018)

The substitution of Si^{4+} by Al^{3+} generates the negative charge of the framework, which is quenched by either monovalent or divalent cations. The structural type of a zeolite is defined by the aluminosilicate framework as it is the most conserved and stable component. The voids in the zeolitic framework house water molecules. Alternately the molecules can be bonded between exchangeable ions and framework ions via aqueous bridges. Table 2.2 shows chemical and physical properties of some zeolites.

Table 2.2: Chemical Formula and Structural Information of Common Zeolites (Wang & Peng, 2010)

Name of Zeolite/ Chemical formula	**Si/Al ratio**	**Symmetry**	**Cation Exchange Capacity (meq/g)**	**Void volume**
Clinoptilolite $(Na,K,Ca_{0.5},Mg_{0.5})_6[Al_6Si_{30}O_{72}]\cdot 20H_2O$	4.0-5.8	Monoclinic	2.16	0.34
Chabazite $(Ca_{0.5},Na,K)_x[Al_xSi_{12x}O_{24}]\cdot 12H_2O$	1.5-4.5	Rhombohedral	3.84	0.47
Mordenite $(Na_2,Ca,K_2)_4\ [Al_8Si_{40}O_{96}]\cdot 28H_2O$	5.4-9.4	Orthorhombic	2.29	0.28
Natrolite $Na_2[Al_2Si_3O_{10}]\cdot 2H_2O$	1.5	Orthorhombic	1.0 - 2.0	0.5
Laumontite $Ca_4[Al_8Si_{16}O_{48}]\cdot 16H_2O$	2.0	Monoclinic	0.8 - 1.5	0.2

Analcime $Na_{16}[Al_{16}Si_{32}O_{96}]\cdot 16H_2O$	2.0	Cubic	4.9	0.2
Phillipsite $(Na,K,Ca)_{1\text{-}2}[Al1\text{-}2Si_{2\text{-}3}O_6]\cdot 2\text{-}6H_2O$	1.0-2.5	Monoclinic	2.0 - 3.5	0.35
Faujasite $(Na_2,Ca,Mg)_{29}[Al_{58}Si_{134}O_{384}]\cdot 240H_2O$	1.0-2.5	Cubic	3.0 - 5.0	0.5
Erionite $(Na_2,K_2,Ca)\ [Al_6Si_{30}O_{72}]\cdot 20H_2O$	4.5-7.0	Hexagonal	2.5 - 3.5	0.30

As illustrated in Table 2.2 zeolite vary in Si/Al ratio, symmetry, cation exchange capacity and void volume. Si/Al ratio controls zeolite's hydrophobicity and surface charge; high ratios increase hydrophobicity, favouring organic pollutant adsorption whereas low ratios correspond with high cation exchange capacity thereby enhancing negative charge, improving heavy metal adsorption (Wang & Peng, 2010). Higher void volumes create larger internal surface area, thereby increasing the adsorbent's capacity because pore filling is a dominant mechanism in zeolite adsorption (Cen et al., 2025).

2.6.1. Applications of zeolites

2.6.1.1. Catalysis

Zeolites are ideal for catalysis due to their unique structural properties, such as high surface area, uniform micropore structure, and tunable acidity. Brønsted acid on -OH- bridging framework between aluminium and silicon channel gives zeolites its catalytic properties. It has also been widely used as a support for catalyst (Limlamthong et al., 2020). Zeolite has been extensively applied to catalyze the conversion of methanol to gasoline (Kianfar & Mazaheri, 2020). Y-zeolites and ZSM-5 containing catalysts, are used in fluid catalytic cracking units of petroleum refineries. They catalyze the cracking of heavy, long-chain hydrocarbons into gasoline, diesel, and other valuable lighter products (Komvokis et al., 2016). Zeolites are also employed in the conversion of methanol to light alkenes (Sofi et al., 2025).

2.6.1.2. Ion-exchange

Substitution of Si by Al in the zeolitic framework results in the negative charge which is quenched by alkali and alkaline earth metal cations. The net negative charge existing on the zeolite ends is balanced by active monovalent or divalent counterions. These positive ions are loosely held and readily exchangeable. This property has been exploited in making zeolite ion exchange resins for water treatment (Guida et al., 2020). Application of zeolite-based fertilizers has been proven to prevent nutrients loss through leaching and volatilization, and slowly release them to plants as needed (Mathur et al., 2022). The use of zeolites in detergent formulations helps to reduce water pollution by minimizing phosphate discharge into waterways (Koohsaryan et al., 2020).

2.6.1.3. Environmental Remediation

Zeolites' high specific surface area, excellent ion exchange capacity, size and shape selectivity, potential for strong acidity, excellent thermal and radiation resistance properties and affordability has made them a choice material for environmental remediation of various pollutants as a sorbent (Barlokova, 2008). Heulandite has been employed to adsorb anions like PO_4^{3-} and NO_3^- (Wanyonyi et al., 2025), heavy metal ions such as Pb^{2+} and Cd^{2+} (Wanyonyi et al., 2024a) from water. Clinoptilolite has been applied for adsorptive remediation Ciprofloxacin and Caffeine from water (Ngeno et al., 2019). Additionally, the adsorptive potential of various types of zeolites was explored for Chloramphenicol, Ciprofloxacin and Diclofenac through simulation studies and gave adsorption energies of -84.46, -173.68 and -78.23 kcal mol^{-1} respectively (Wanyonyi et al., 2020).

To improve on the adsorption properties, zeolites are subjected to modification.

2.7. Zeolite modification

The chemical and structural makeup of a sorbent influences it adsorption properties. In zeolites,

the pore volume, surface area, cation type and the Si/Al ratio are specifically influential in adsorption applications. These properties can be modified by physical, chemical or composite means.

2.7.1. Physical Modification

Mechanical, ultrasonic and thermal treatment are types of physical modification used to improve zeolite performance. Thermal treatment expels domiciled water molecules to increase pore sizes and enhances its exchange adsorption capacity by exposing more cationic sites (Cadar et al., 2020). Ultrasound treatment produces cavitation bubbles that collapse to remove impurities trapped in the pores; restoring pore volume and improving the zeolite's adsorption efficiency (Zieliński et al., 2016). Mechanical crushing of zeolite into a fine powder increases the surface area for adsorption. Merits of physical modification include simplicity, eco-friendliness and low cost.

Physical modification, however, is limited since it does not significantly increase the sorbent's adsorption capacity and efficiency; as a result, other modifying techniques with appreciable results are worth exploring (Xu et al., 2018).

2.7.2. Chemical Modification

Chemical modification can be done by treating the zeolites with either cationic surfactant, rare earth, acid, base and salt. Acid modification is done through acid impregnation. Acids have the ability to partially displace K^+, Ca^{2+} and Mg^{2+} from layers by dissolving impurities in the zeolite pores, thus opening up channels. This increases porosity, which enhances the adsorption capacity (Shi et al., 2018). Base modification of zeolites is usually done to improve its catalytic activity. It is commonly achieved through ion exchange where acidic protons or exchangeable cations within the zeolite structure are replaced with alkali or alkaline earth metal cations (Sarmah et al., 2017). Cationic surfactant modification involves mixing natural zeolite with a cationic surfactant

solution. This helps overcome the low rate at which natural zeolite typically removes anionic pollutants (Jiménez-Castañeda & Medina, 2017). In rare earth modification, a natural zeolite is mixed with a rare earth solution and stirred, then dried and crushed. Hydroxides and oxides of zirconium, lanthanum and cerium are the most common used rare earth metals. Salt modification of zeolite is done by refluxing zeolite with a salt solution. In addition to exchanging zeolite cations with cations in the salt solution, the solution has the ability to remove water and/or inorganic contaminants from the zeolite channel. Surface modification of zeolites increases its hydrophobicity making it ideal for the remediation of many micropollutants (Straioto et al., 2023). Iron has been highly preferred over other elements in the modification of sorbents not only due to its relatively cheap cost but also its environmental compatibility which makes it less likely to pollute the environment or endanger human life. Additionally, its magnetic properties make regeneration of the sorbent easy; its catalytic properties make it ideal for catalytic reduction of pollutants. Studies have indicated that the adsorption performance of zeolite can be improved through iron doping (Maulana & Takahashi, 2018). Iron modified sorbents are known to have extended lifetime and more regeneration cycles as iron is proven to limit biofouling (Lalley et al., 2016). Iron modified activated carbon applied in the removal of a dye from water showed 95% higher adsorption capacity compared to the unmodified and also reasonably high efficiency upon regeneration (Shah et al., 2015). The problem of secondary pollution that is associated with metal ions leaking can easily be countered by performing leaching tests before batch production of the sorbent. The problem of secondary pollution that is associated with metal ions leaking can easily be countered by performing leaching tests before batch production of the sorbent.

Despite the proven efficiency of iron-modified zeolites in adsorption, their application in pharmaceutical remediation remains underexplored, with most studies limited to removal of heavy metals. This knowledge gap necessitates a laboratory study of the adsorptive potential

Kenyan natural zeolite for selected pharmaceuticals so as to avail vital information on the kinetics and mechanisms of adsorption.

2.7.3. Composite modification

Composite modification combines several modifying methods and can be classified as heating, ultrasonic and alkali/acid/salt composite modification. Shortening the reaction time and increasing the adsorption capacity of the zeolite, ultrasound and salt solution composite modification replaces the cation of the bigger radius and dissolves impurities from the surface and pores (Jahani et al., 2023). In heating composite modification, application of high temperature serves to increase the porosity of the zeolites. While composite modification of zeolite, involving pretreatment with either alkali, acid, or salt followed by surfactant or salt modification, offers the merit of reduced adsorption time, it is marked by the key demerit of decreased porosity and surface area, which lowers its adsorption capacity and efficiency (Dionisiou et al., 2013).

Effective adsorption evaluation requires an understanding of the adsorbent's surface chemistry and intrinsic properties, which is achieved via characterization.

2.8. Adsorbent Characterization

Zeolite characterization is a multifaceted process that involves a comprehensive suite of analytical techniques to elucidate their structural, chemical, and textural properties.

2.8.1. Brunauer-Emmett-Teller (BET) analysis

The BET theory applies the Langmuir isotherm to multilayer adsorption, assuming that gas molecules form successive layers on a solid surface with each layer in equilibrium and exhibiting heat of adsorption equal to the liquefaction heat beyond the first monolayer (Pickett, 1945). The specific surface area of zeolite is obtained by measuring the volume of nitrogen gas

adsorbed at various partial pressures near the saturation pressure at 77 K and applying the BET equation to calculate the monolayer capacity (Naderi, 2015). Zeolite specific surface areas range from 10–800 $m^2 g^{-1}$, with natural zeolites like clinoptilolite showing lower values of 20–26 $m^2 g^{-1}$ due to pore blockage by water or impurities while synthetic zeolites such as ZSM-5 much higher values of 600–800 $m^2 g^{-1}$ (Chen et al., 2018).

2.8.2. Energy Dispersive X-ray Spectroscopy (EDS)

This non-destructive technique enables rapid elemental mapping and analysis with detection limits. It works by bombarding a sample with high-energy electrons from a scanning electron microscope, which eject inner-shell electrons from sample atoms and create characteristic X-rays as outer-shell electrons fill the vacancies. The emitted X-rays are collected by a silicon drift detector that measures their energies, producing a spectrum where peak positions identify elements and peak intensities quantify their concentrations (Goldstein et al., 2017). In addition to aluminium and silicon, zeolites have alkali and alkaline earth metal cations and trace metallic impurities like vanadium and arsenic (Shabalin et al., 2023).

2.8.3. Fourier-Transform Infrared (FTIR) Spectroscopy

FTIR spectroscopy works by passing infrared radiation through a sample, where molecules absorb specific wavelengths corresponding to their vibrational transitions, producing a characteristic absorption spectrum that is used in identifying functional groups based on absorption band positions and intensities (Berthomieu & Hienerwadel, 2009). FTIR analysis of zeolites shows characteristic absorption bands for Si-O-Si and Si-O-Al asymmetric stretching vibrations at 950–1250 cm^{-1} and hydroxyl functional groups, crucial for acidity like the bridging Brønsted acid sites (Si-OH-Al) at 3600–3650 cm^{-1} (Flanigen et al., 1971).

2.8.4. X-Ray Diffraction (XRD) analysis

X-Ray Diffractometer works by directing a beam of monochromatic X-rays at a sample, where the rays diffract off parallel atomic planes according to Bragg's law, producing a unique interference pattern of peak intensities at specific angles. The pattern is analyzed to identify crystalline phases, determine lattice parameters, and assess structural features by comparing observed diffraction angles and intensities with known standards (Warren, 1990). Clinoptilolite has been identified in Kenya as reported by Shikuku et al. (2015) as distinct from Faujasite-X.

2.8.5. Scanning Electron Microscopy (SEM)

This technique visualizes the surface morphology, topography, and the microstructure of adsorbents at high resolution, allowing detailed analysis of particle size, shape and texture. Its working principle involves scanning a focused beam of high-energy electrons across a sample surface, where interactions generate secondary electrons, backscattered electrons, and characteristic X-rays that are detected to form high-resolution images with magnifications up to 100,000 times (Mohammed & Abdullah, 2018). SEM analysis of zeolites reveals diverse morphologies such as cubic crystals of 1-5 μm for zeolite-A, hexagonal prisms for mordenite (0.5–10 μm), and spherical aggregates for ZSM-5 (0.2–3 μm) (Cejka et al., 2007).

2.8.6. Point of zero charge (pHpzc)

The point of zero charge is the pH at which an adsorbent's surface carries no net electrical charge, resulting in zero zeta potential and minimal electrostatic interactions with ions present in the solution. It is determined by methods like salt addition method, potentiometric titration and zeta potential measurements and is critical for understanding adsorption behavior, as the surface is positively charged below the pH_{pzc} and negatively charged above it (Kosmulski, 2009). Kragović et al. (2019) documented a rise in pH_{pzc} of natural zeolite to 6.5 from 6.2 upon encapsulating with alginate.

2.8.7. Thermogravimetric analysis

Thermogravimetric analysis assesses the thermal stability and composition by measuring changes in weight as a function of temperature. The resultant plot identifies dehydration, decomposition and structural transitions (Lothenbach et al., 2016). Clinoptilolite demonstrates stability at higher temperature of up to 600 °C while Heulandite's structure collapses at around 350 °C due to its higher aluminum content and high water content (Armbruster, 2001).

Adsorption of adsorbate onto the adsorbent is assessed and described by sorption isotherms, kinetics, mechanisms and thermodynamics.

2.9. Assessment of Adsorption

2.9.1. Adsorption Isotherms

Adsorbate interactions with an adsorbent are described by adsorption isotherms. This is done by observing the correlation between the equilibrium adsorbate concentration and adsorption capacity at constant pH and temperature. Isotherm models provide useful information such as adsorbent capacity and surface properties. Adsorption isotherms are helpful in designing of commercial treatment system that is both efficient and economically feasible as well as optimizing the adsorption mechanism pathways (Sahoo & Prelot, 2020). Langmuir, Freundlich, Redlich-Peterson and Dubinine-Radushkevich are some of the commonly applied isotherm models in the description of experimental adsorption data.

2.9.1.1. Langmuir adsorption isotherm model

The fundamental premise of the Langmuir isotherm is that adsorption occurs at distinct homogeneous sites on an adsorbent, and once an adsorbate occupies a site, further adsorption at that site is precluded (Langmuir, 1916). It is also referred to as monolayer adsorption isotherm (Sahoo & Prelot, 2020). It is expressed by Equation 2.1.

$$Q_e = \frac{K_L Q_{max} C_e}{1 + K_L C_e} \quad \textbf{2.1}$$

Where; $\boldsymbol{Q_e}$ (mg/g) is the sorbent's adsorption capacity at equilibrium; $\boldsymbol{Q_{max}}$ (mg/g or mol/g) and $\boldsymbol{C_e}$ (mol/L) are maximum adsorption capacity and the concentration at equilibrium, respectively, and $\boldsymbol{K_L}$ (L/mol) is the Langmuir constant.

2.9.1.2. Freundlich adsorption isotherm model

At a heterogeneous surface, this isothermal model depicts a non-ideal, multilayer, reversible adsorption. It is predicated on the assumption that the binding energies of the adsorption sites are varied. As a result, the energy distribution for adsorptive sites exhibits an exponential-type function and a spectrum of various binding energies (Sahoo & Prelot, 2020). It is expressed by Equation 2.2.

$$\log(Q_e) = \log(K_F) + \frac{1}{n}\log(C_e)^{1/n} \quad \textbf{2.2}$$

Where; K_F and $1/n$ are Freundlich coefficients relating to the adsorption capacity and intensity, respectively.

2.9.1.3. Temkin adsorption isotherm model

According to this model, adsorption is described by a uniform distribution of binding energies up to a maximum binding energy, and the adsorption heat of all molecules decreases linearly with an increase in coverage of the adsorbent surface (Chu, 2021). It is expressed by Equation 2.3.

$$Q_e = \frac{RT}{b} \ln K_T + \frac{RT}{b} \ln C_e \quad \textbf{2.3}$$

Where; K_T is the equilibrium binding constant (L/mol) and b relates to the adsorption heat

2.9.1.4. Dubinine-Radushkevich adsorption isotherm model

According to this isotherm model, the size of the adsorbate is comparable to the size of the micropores, and the adsorption potential (ε) can be used to define the adsorption equilibrium relation for a particular combination of adsorbate and adsorbent independently of temperature (Altalhi et al., 2022) as shown in Equation 2.4.

$$\varepsilon = RT\ ln\left(1 + \frac{1}{C_e}\right) \quad \text{2.4}$$

Where; ε is the adsorption potential (*J*/mol) and R is the universal gas constant = 8.314 *J*/(mol·K)

2.9.1.5. Redlich-Peterson adsorption isotherm model

This model uniquely combines features of both the Langmuir and Freundlich models through a three-parameter equation with an exponent that allows it to represent adsorption equilibria over a wide range of concentrations, transitioning from heterogeneous to homogeneous behavior (Chu et al., 2024). It is described by Equation 2.5

$$ln\left(K_R\ \frac{C_e}{Q_e} - 1\right) = ln\ a_R + \beta\ ln\ C_e \quad \text{2.5}$$

Where; a_R is the Redlich-Peterson constant (L/mg), K_R is the Redlich-Peterson constant (L/g), and β is an exponent ($0 < \beta < 1$)

2.9.2. Adsorption Kinetics

The retention or release rate of a sorbate from the fluid phase to the solid-phase interface at specified conditions is described by adsorption kinetics. The experimental data is analyzed either linearly or non-linearly and model that best describes the process is identified by applying the goodness of fit index (Musah et al., 2022). Lagergren, Pseudo-second order Elovich and intraparticle diffusion models are some of the models used in description of kinetics of adsorption.

2.9.2.1. Lagergren kinetic model

This model, also known as Pseudo-first order, is based on the assumption that physisorption is the rate-limiting step in the adsorption of particles onto the adsorbent (Liu et al., 2019). The model assumes that the change in sorbate adsorption at a given time is directly proportional to the rate of adsorbate removal and the concentration difference observed over that period. The model is represented by the Equation 2.6.

$$\frac{dQ_t}{dt} = k_1(Q_e - Q_t) \qquad \textbf{2.6}$$

Where; k_1 is the rate constant for *pseudo*-first order adsorption (min^{-1}) and Q_t is the adsorption capacity of the adsorbent at time t (mg/g)

2.9.2.2. *Pseudo*–second order kinetic model

This model predicts behavior across the whole adsorption range and is based on the assumption that chemisorption is the rate-limiting step. The adsorption rate is thus, dependent on adsorption capacity and not on concentration of the sorbate. This model is superior to Lagergren model in that the equilibrium adsorption capacity can be calculated from the model (Sahoo & Prelot, 2020). The *pseudo*–second-order kinetics is expressed by Equation 2.7.

$$Q_t = \frac{k_2 Q_e^2 t}{1 + k_2 Q_e t} \qquad \textbf{2.7}$$

Where; k_2 is the rate constant ($g.mg^{-1}.min^{-1}$)

2.9.2.3. Elovich kinetic model

This model describes chemisorption processes, particularly on surfaces that are energetically heterogeneous, where the adsorption rate decreases exponentially with increasing surface coverage due to reduced active sites (Wu et al., 2009). Second-order kinetics have been

satisfactorily described by the Elovich kinetic model under the assumption that the surface is energetically heterogeneous. It is expressed by Equation 2.8.

$$Q_t = \frac{1}{\beta} ln\,(\alpha\beta) + \frac{1}{\beta} ln\,(t) \qquad \textbf{2.8}$$

Where; α is the initial adsorption rate and β is the desorption constant

2.9.2.4. Intraparticle diffusion kinetic model

This model is used to evaluate the mechanism of adsorption, particularly the role of diffusion within the pores of the adsorbent particles. It helps determine whether intraparticle diffusion is the rate-limiting step in the overall adsorption process (Weber Jr & Morris, 1963). It is expressed by Equation 2.9.

$$qt = k_{id}\, t^{1/2} + C \qquad \textbf{2.9}$$

Where; k_{id} is the Intraparticle diffusion rate constant (mg/g·min$^{1/2}$) and C is a constant related to the boundary layer effects

Compiled in Table 2.3 are the adsorption isotherms and adsorption kinetics for the pharmaceuticals of interest using different sorbents. For chloramphenicol, bamboo charcoal and activated carbon were used, following Dubinin–Radushkevich and Langmuir isotherms respectively. Activated carbon showed a high adsorption capacity of 214.91 mg g^{-1}. Ciprofloxacin was adsorbed by wood biochar and clinoptilolite, both fitting the Langmuir model but with lower capacities of 4.25 and 2.72 mg g^{-1}. Diclofenac showed appreciable adsorption capacities of 42.43 and 62 mg g^{-1} on granular activated carbon and $ZnCl_2$ activated carbon from tea waste respectively, both fitting Langmuir isotherms. In all cases, adsorption kinetics followed the *Pseudo*-second order (PSO) model, indicating chemisorption as the dominant mechanism.

Table 2.3: Adsorption Isotherms and Kinetics of the Selected Pharmaceuticals using different sorbents

Pharmaceutical	Sorbent	Isotherm (max adsorption capacity)	Kinetics	Reference
Chloramphenicol	Bamboo charcoal	Dubinin−Radushkevich (2.3 x 10^{-5} mol g^{-1})	PSO	(Liao et al., 2013)
	Activated carbon	Langmuir (214.91 mg g^{-1})	PSO	(Lach, 2019)
Ciprofloxacin	Wood biochar	Langmuir (4.25 mg g^{-1})		(Srivastava et al., 2022)
	Clinoptilolite	Langmuir (2.717 mg g^{-1})	PSO	(Ngeno et al., 2016)
Diclofenac	Granular activated carbon	Langmuir (42.43 mg g^{-1}) Freundlich (2.018(mg/g)(L/mg)$^{1/n}$		(de Franco et al., 2018)
	$ZnCl_2$ activated carbon from tea waste	Langmuir (62 mg g^{-1})	PSO	(Malhotra et al., 2018)

2.9.3. Adsorption mechanism

The adsorption mechanism describes how adsorbate molecules interact with and bind to an adsorbent surface (Rouquerol et al., 2013). Adsorption can be broadly classified into physical adsorption (physisorption) and chemical adsorption also called chemisorption (Alaqarbeh, 2021). Physisorption involves weak van der Waals forces and is typically reversible, while chemisorption involves stronger chemical bonds and is often irreversible (Alaqarbeh, 2021). The adsorption process is influenced by factors such as the surface area and pore structure of the adsorbent (Chulliyil et al., 2024), the chemical properties of both the adsorbent and adsorbate (Akhtar et al., 2024), and environmental conditions like temperature and pH (Shikuku et al., 2018). Adsorption isotherms, such as Langmuir, Freundlich, Temkin, and Dubinin-Radushkevich models, are used to describe the equilibrium relationship between the amount of adsorbate adsorbed and its concentration in the surrounding fluid at a constant temperature, providing insights into the adsorption mechanism and allowing for the optimization of adsorption processes (Wang & Guo, 2020).

2.9.4. Adsorption Thermodynamics

Adsorption thermodynamics involves the study of energy changes and equilibrium during the adsorption process, where adsorbate molecules adhere onto the adsorbent surface. It utilizes thermodynamic principles to understand the spontaneity, energy requirements, and equilibrium conditions of adsorption with changes in temperature (Ngeno et al., 2019). The key thermodynamic parameters provide insights into the nature of the adsorption process and are Gibbs free energy, enthalpy, and entropy (Atkins et al., 2023) as expressed in Van't Hoff's Equation 2.10.

$$lnK = \frac{\Delta H^{\circ}}{RT} + \frac{\Delta S^{\circ}}{R} \qquad \textbf{2.10}$$

Where; K is the reaction's equilibrium constant (dimensionless); T is the absolute temperature (K); R is the universal gas constant (8.314 J/mol·K); $\Delta H°$ is the reaction's standard enthalpy change and $\Delta S°$ is the reaction's standard entropy change.

2.10. Analytical tools for monitoring adsorption studies

Choosing an appropriate analytical technique is important in determining the residual pollutant concentration, which is necessary to assess the extent of removal achieved by the adsorbent. Liquid chromatography-mass spectrometry known for its high sensitivity and selectivity is particularly effective for detecting and quantifying a wide range of pharmaceuticals at trace levels (ng/L to µg/L) in complex environmental matrices (Fernandes et al., 2021). For volatile pharmaceutical compounds, Gas chromatography-mass spectrometry is commonly employed; however, further derivatization may be required to enhance the volatility of semi-volatile pharmaceutical compounds (Koek et al., 2011). Additionally, spectrophotometric techniques – particularly Ultra Violet-Visible spectrophotometry, are often applied in quantifying pharmaceuticals since most absorb light in the Ultraviolet or visible region. This technique is valued for its simplicity, rapid analysis, and cost-effectiveness (Eneş et al., 2024).

CHAPTER THREE

METHODOLOGY

3.1. Chemicals, Standard Reagents

High purity reference standards for Diclofenac potassium (≤99%), Ciprofloxacin (≤99.8%), and Chloramphenicol (≤98.9%) were purchased from Merck through Kobian Kenya Ltd. Additionally, analytical grade HCl, NaOH, $FeCl_3 \bullet 6H_2O$ and glass fiber filters (pore size 0.5 μm) were locally purchased from Kobian Kenya Ltd.

3.2. Collection and Preparation of the Kenyan natural Zeolite

The Kenyan natural zeolite (NZe) used for this study was among eleven rocks samples collected from Eburru area (0.648 ° S, 36.267 ° E) in Naivasha, Nakuru County. The zeolite was pretreated before application as described by Widiastuti et al. (2011). The pretreatment entailed washing the zeolite with deionized water to remove dust and soluble impurities followed by oven drying the washed zeolite at 105°C for 24 hours. The zeolite was then crushed before sieving through 50 -100 μm mesh strainers to homogenize the size.

3.3. Modification of Zeolite with Fe^{3+}

Iron (III) Chloride hexahydrate was used to modify the natural zeolite, following the method outlined by by Sukmasari and Azmiyawati (2018). In the method, 120 g of natural zeolite (NZe) was activated by soaking in 1000 mL of 6N HCl for 24 hours to dissolve counter-ions materials, and increases and porosity by dealumination. The zeolite was then filtered, washed with distilled water until attainment of neutral pH, and dried in an oven at 100 °C for 4 hours. Subsequently, approximately 100 g of the activated zeolite was mixed with 500 mL of 0.2 M

$FeCl_3 \cdot 6H_2O$ solution and refluxed at 90 °C for 5 hours. The resulting material was filtered, dried at 100 °C for 4 hours, and calcined at 500 °C for 2 hours.

3.3.1. Adsorbent Characterization

Both the modified and the unmodified zeolites were characterized using Scanning Electron Microscope for surface morphology; Energy dispersive X-Ray for elemental composition, X-Ray Diffractometer for crystallinity, and Fourier Transform Infrared Spectroscopy for surface functional groups. The pH of the point of zero charge (pH_{pzc}) was determined by the salt addition method as described by (Al-Maliky et al., 2021). The method involved preparing a series of 20 cm^3 0.01 M NaCl solutions and adjusting their initial pH values across a range of 2–10 using 0.01 M HCl or 0.01 M NaOH and then adding a 0.4 g of the adsorbent to each solution. After equilibrating for 24 hours with agitation, the final pH of each suspension was measured, and pH_{pzc} was identified as the initial pH value where the change in pH was zero.

3.4. Batch Adsorption Studies

The research design was experimental achieved through laboratory experiments. The decontaminating effect of the adsorbent under different conditions was investigated by conducting batch adsorption experiments. The volume of the adsorbate concentration used for the experiments was 20 cm^3. The effects of contact time, reaction temperature, adsorbent dose, initial concentration and pH value were studied. The amount adsorbed were determined by the difference between initial concentration and the final concentration. Residual pollutant concentration was determined by filtering the supernatant through glass fiber filter and placed in a quartz curvette for analysis in UV 1609 UV/VIS Spectrophotometer (Shanghai Metash Instruments)

3.4.1. Effect of pH

The influence of pH was investigated in the range of 2 – 10 while all the other conditions are held constant. To adjust the solutions' initial pH, 0.1 M HCl and 0.1 M NaOH solutions were used.

3.4.2. Effect of Contact Time

The influence of contact time was studied by holding other parameters constant while varying contact time from 0 to 180 minutes. An aliquot was drawn at pre-determined times for concentration analyses. *Pseudo*-first order (Equation 2.6), *pseudo*-second order (Equation 2.7), Elovich (Equation 2.8) and Intraparticle diffusion (Equation 2.9) models were used for kinetic data fitting.

3.4.3. Effect of Initial Pollutant Concentration

The effect of initial concentration of the model wastewater samples on adsorption were studied by varying initial concentrations from 2 to 20 mg/L while holding other parameters constant. Langmuir (Equation 2.1), Freundlich (Equation 2.2) and Temkin (Equation 2.3) isotherm models were applied in description of adsorption isotherm data.

3.4.4. Effect of Adsorbent Dose

The influence of adsorbent dose was investigated by varying mass of adsorbent from 0.01 to 2.0 g/L while maintaining all other parameters constant.

3.4.5. Effect of Temperature

The effect of temperature was studied for range of 298 – 318 K maintaining other parameters constant. Entropy, enthalpy and Gibbs free energy were applied in the description of the data from Van't Hoff plot (Atkins et al., 2023).

3.5. Quality Control and Assurance

To ensure the accuracy, reliability and reproducibility of the adsorption study results, several methodological steps were applied. To mitigate the effect of adsorbent heterogeneity which can introduce significant measurement differences, the adsorbent was prepared in bulk and homogenized by thorough mixing to minimize variability arising from differences in particle size or surface properties. Fresh stock and working adsorbate solutions were prepared before each experiment to prevent degradation or changes in concentration, ensuring consistency across experiments. Calibration curves were generated for the expected adsorbate concentration range of 1 – 20 mg/L, with a coefficient of determination (R^2) > 0.995 deemed acceptable. Calibration verification standards were periodically run during the analysis to check for potential instrumental drift.

To enhance the statistical reliability of the reported data and experimental repeatability, all adsorption experiments were conducted in triplicates, with means, standard deviations, and confidence intervals calculated for replicate measurements. Blank solutions were employed to account for potential background effects, such as analyte loss through degradation, or adsorption onto container walls.

3.6. Quantum Chemical studies of the adsorbates

The molecular structures were optimized using Gaussian 09 suite of software, employing the B3LYP hybrid functional with the 6-31G(d,p) basis set for all atoms. B3LYP is a hybrid density functional theory method that combines the Becke's three-parameter exchange functional (B3) with the Lee-Yang-Parr correlation functional (LYP), incorporating 20 % of Hartree-Fock exchange to improve accuracy for molecular geometries, energies, and properties (Becke, 1993). Geometry optimizations were performed in the gas phase with the convergence criteria

set for default values for energy and force. Vibrational frequency calculations were conducted at the same level of theory to confirm that the optimized structures correspond to true minima on the potential energy surface, as indicated by the absence of imaginary frequencies. All calculations utilized tight convergence and an ultrafine integration grid to ensure high accuracy in the results (Caricato et al., 2009).

3.7. Statistical Analyses

The data obtained were analyzed and processed using Origin Pro. Statistical analyses were performed to evaluate data variance and evaluate the goodness-of-fit for adsorption models using parameters such as the adjusted R-squared $(R_{adj})^2$, root mean square error (RMSE), and chi-squared test (χ^2). Paired t-test at 95% confidence level were carried out to determine whether adsorption by unmodified and modified zeolite were statistically different. It was also carried to determine whether the adsorption of the three analytes onto iron modified zeolite where statistically different.

CHAPTER FOUR

RESULTS AND DISCUSSION

4.1. Adsorbent characterization

4.1.1. Physical appearance of the zeolites

The adsorbents were distinguishable by their physical appearance; NZe (A) was beige while ImZe (B) was light brown in colour as shown in Figure 4.1. Zeolite appears in volcanic tuffs with colours ranging from tan light beige (Coldham & Ivey, 2020). The brown colour of ImZe is characteristic of iron (III) species used in the modification.

Figure 4.1: Photographs of NZe (A) and ImZe (B)

4.1.2. Elemental composition of the sorbent

Table 4.1 shows the chemical composition of NZe and ImZe while their corresponding Energy-Dispersive Spectroscopy (EDS) spectra are illustrated in Figure 4.2. Additional elemental distribution was confirmed through EDS mapping, as shown in Appendices 1, 2, 3 and 4.

Table 4.1: Elemental composition of NZe and ImZe

Element	% Weight	
	NZe	ImZe
Al_2O_3	46.962	39.442
SiO_2	35.969	34.810
Fe_2O_3	8.947	19.464
K_2O	6.617	5.072
TiO_2	0.889	0.892
CaO	0.403	Not detected
ZrO_2	0.098	0.165
SO_3	0.065	0.100
V_2O_5	0.050	0.055

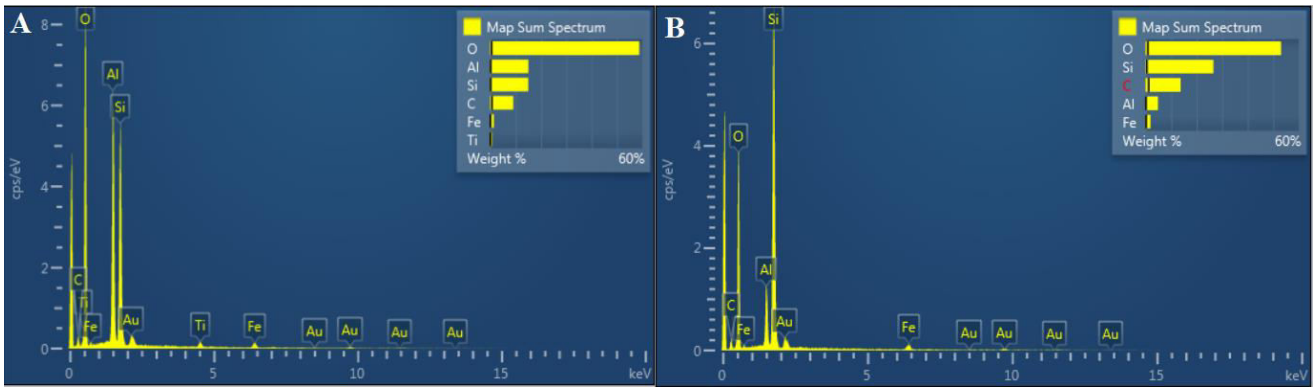

Figure 4.2: EDS spectrum for NZe (A) and ImZe (B)

The EDX results showed that Al, Si, K, Ti, Zr, S, V and Fe were present in both NZe and ImZe. The gold signals detected in the EDS spectra (Figure 4.2) are attributed to the gold foiling applied to the sorbents to enhance conductivity (Stoch, 2015). Based on the results, both NZe and ImZe are categorized as low-silica zeolite with Si/Al ratios of 0.7659 and 0.8744 calculated from their respective oxides, (Wang et al., 2019). In contrast, Ngeno et al. (2019) reported a zeolite with a Si/Al ratio of 4.2.

As shown in Table 4.1, a significant decrease in aluminum content was observed following the modification of NZe with iron, decreasing from 46.96 % to 39.44 %. This is attributed to the leaching out of aluminium during the acid treatment phase of the modification process (Tao et al.,

2006) followed by the incorporation of iron in place of aluminum. Similarly, Izoitko et al. (2025) documented a slight increase in the Si/Al ratio upon introduction of iron into the zeolitic framework and concluded that iron partly substitutes for aluminum. Dealumination of zeolites has been shown to enhance their hydrophobic characteristics (Pálinkó et al., 2013). Moreover, the Fe_2O_3 mass percent on the surface of ImZe (19.464%) exceeded double that of NZe (8.947%), indicating the successful immobilization of Fe onto the NZe surface following modification with Fe^{3+} as indicated in Table 4.1.

Furthermore, following NZe's impregnation of with Fe^{3+}, the levels of Ca, K, and V decreased, suggesting that cation exchange took place between the zeolite's exchangeable cations and Fe^{3+} ions in the solution during the modification process (Ugrina et al., 2015). This is similar to a study on the incorporation of iron into the β-zeolite framework which involved ion exchange of Na and Ca (Boroń et al., 2013).

4.1.3. Point of zero charge

At the pH corresponding to the point of zero charge, pH_{pzc}, the sorbent surface exhibits a net zero charge (Al-Maliky et al., 2021). The pH_{pzc} of the ImZe was 6.9 compared to 5.2 of NZe as shown in Figure 4.3. These results corroborate with previous studies that reported an increase in pH_{pzc} following modification with iron, from 6.8 to 7.5 according to Kragović et al. (2012) and from 6.8 to 9.8 as reported by Ugrina et al. (2015). This is attributed to the incorporation of iron, which is characterized by high pH_{pzc} values ranging from pH 6 to 9 (Kosmulski, 2016).

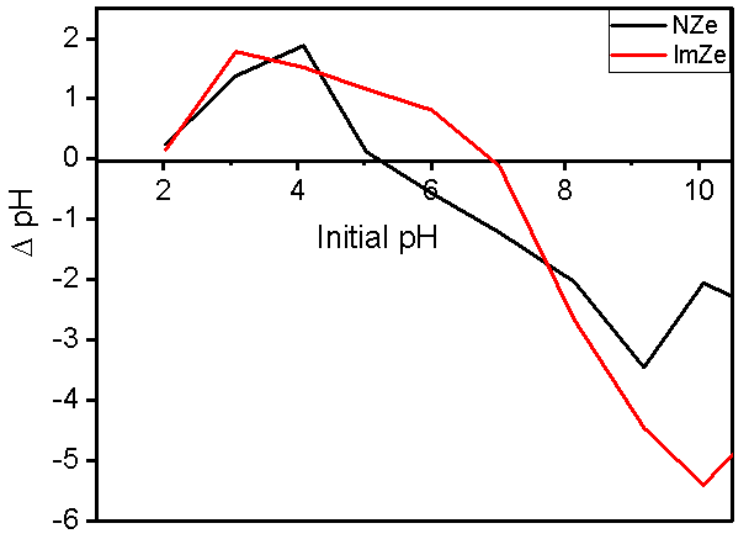

Figure 4.3: Point of zero charge plots for NZe and ImZe

The pH_{pzc} provides insight into the ionization of the sorbent's functional groups and their interactions with adsorbate in solution. The sorbent's surface attracts the electrophilic groups of the sorbate when the solution pH > pH_{pzc} because it is negatively charged; conversely, when the pH is lower, the surface is positively charged and interacts with the sorbate's nucleophilic groups (Adeola et al., 2024). A higher pH_{pzc} indicates that the surface of ImZe retains positive charge over a wider pH range as compared to NZe enhancing its adsorption of negatively charged species (Ugrina et al., 2015).

4.1.4. Fourier Transform Infrared Spectroscopy

The Figure 4.4 shows the FTIR spectra of NZe and ImZe. The broad bands observed between 3850 and 2855 cm^{-1} are indicative of O–H stretching of hydroxyl groups of silanol groups. The bands at 1631(NZe) and 1589 (ImZe) cm^{-1} are characteristic of O-H bending of the water molecules domiciled in the zeolitic pores (Kikuvi et al., 2025).

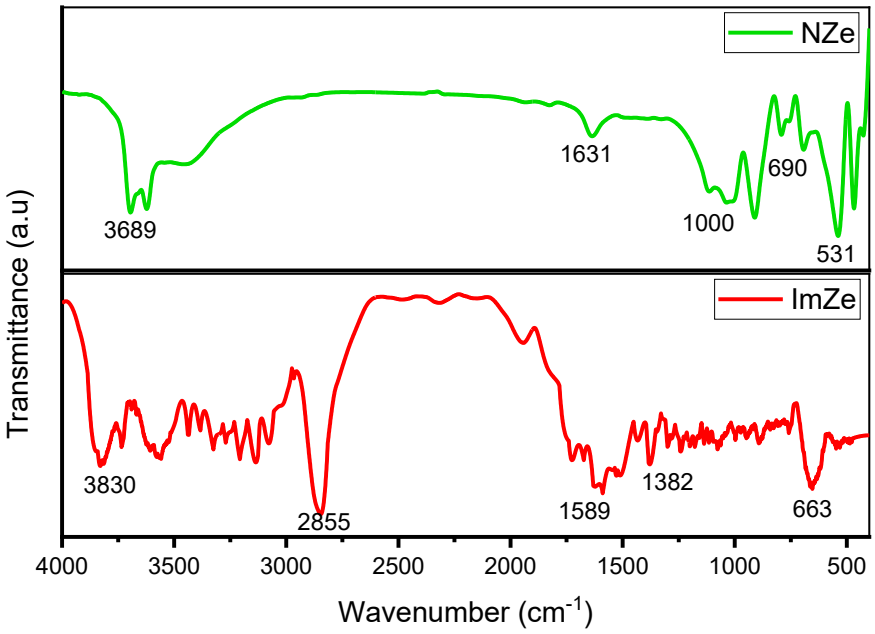

Figure 4.4: FTIR spectra for NZe and ImZe

The moderate bands below 700 cm^{-1} corresponds to the stretching vibrations of Si-O-Al bonds in the zeolite (Carro et al., 2024). The effect of iron impregnation is evident from the shifts in the characteristic clinoptilolite bands, specifically from 3689 to 3830 cm^{-1} and 1000 to 1382 cm^{-1}, suggesting interactions between the iron and the zeolite framework (Ugrina et al., 2015). The FTIR spectra of both sorbents exhibits notable similarities, with slight shifts observed particularly in the fingerprint region (600–1200 cm^{-1}), which is indicative of Si-O-Fe bonds in the iron-modified species (Kumon et al., 2017). This illustrates that the zeolite framework remains intact after modification with iron, consistent with findings from a previous study (Bencheqroun et al., 2022). Our findings align with Kumon et al. (2017) where FTIR analysis revealed characteristic Si-O-Fe bond bands, confirming successful iron incorporation into the Na-P1 zeolite framework during hydrothermal synthesis, while retaining bands typical of Na-P1 zeolite. Additionally, a study on natural mordenite modification with iron reported an

increase in iron loading without significant alterations to the zeolite's crystallinity and textural properties (Chávez Rivas et al., 2019).

4.1.5. X-Ray Diffraction analysis

Figure 4.5 shows the XRD patterns for NZe and ImZe. The peaks are sharp and well-defined indicating that ImZe and its unmodified variant have a high crystalline structure.

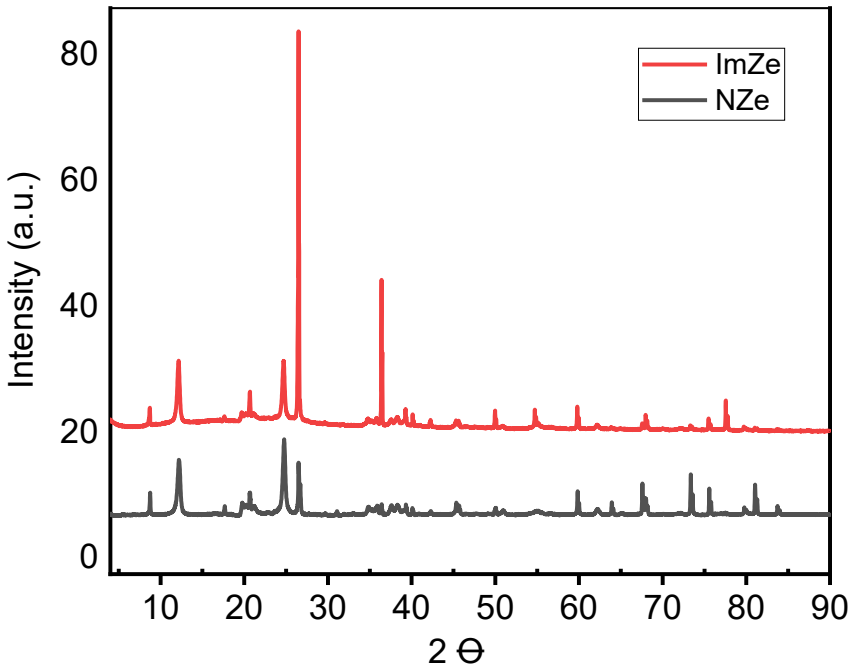

Figure 4.5: X-ray diffractograms of NZe and ImZe

XRD analysis-derived Miller indices identified clinoptilolite as the main phase (79.38%), with quartz (14.27%) and kaolinite (6.35%) as minor phases of the sorbents. The distinct peaks observed at specific 2θ values of 7, 10, 14, 25 and 40° and their corresponding Miller indices are all characteristic of clinoptilolite (Mansouri et al., 2013). Clinoptilolite is the most abundant natural zeolites and has been previously reported in Kenya (Ngeno et al., 2019; Shikuku et al., 2015). The marked increase in peak intensities at 2θ values of 25° and 40° in the ImZe pattern

suggests the successful impregnation of iron into the zeolite structure (Kragović et al., 2013). The lack of significant peak shifts in the ImZe diffractogram compared to that of NZe indicates that the modification process did not alter the structural integrity of the zeolite, supporting the findings previously observed through FTIR spectroscopy. This highlights NZe's quality in preserving its structural properties even after functional modifications.

4.1.6. Scanning Electron Microscope analysis

Figure 4.6 shows the SEM images of the NZe and ImZe at x500 and x1000 magnifications.

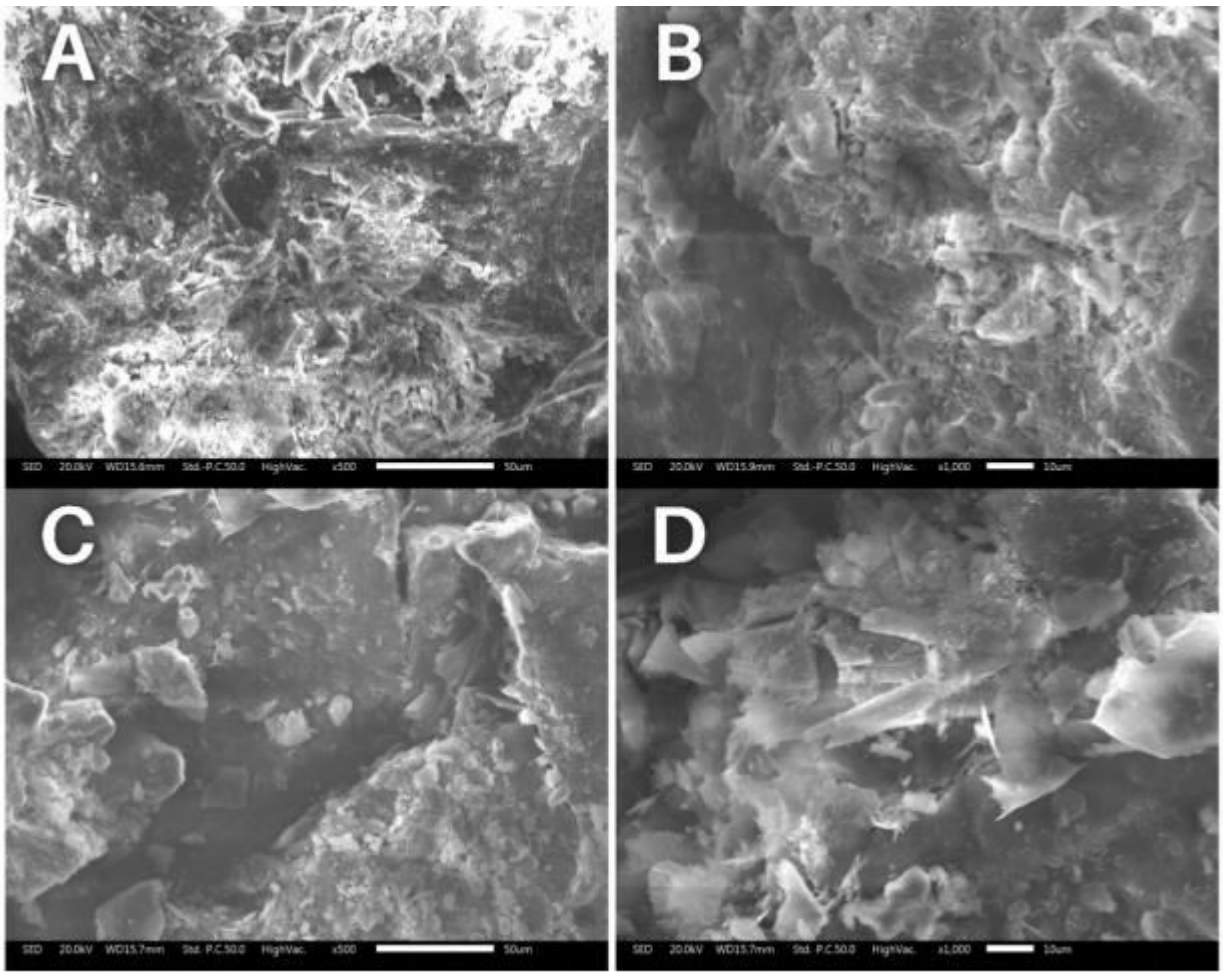

Figure 4.6: SEM micrographs of NZe A .x500 & B. x1000 and ImZe C. x500 & D. x1000

Micrographs A and C reveal aggregated particles with noticeable voids between them, whereas B, which a greater magnification of micrograph A, displays a more granular, porous, and densely packed structure, and D (a higher magnification of micrograph B) features flaky-like particles with well-defined edges. The rough and irregular surface observed in the micrographs indicates apparent porosity, which is essential to the material's ability to adsorb molecules (Kikuvi et al., 2025). The micrographs of both sorbents clearly show crystal aggregates and reveal the presence of macropores within the zeolite structure. The alteration of the ImZe surface can be attributed to the modification, resulting from the precipitation of iron complexes on the zeolitic surface (Mockovčiaková et al., 2006).

4.1.7. Thermogravimetric analysis

The Thermogravimetric and Derivative Thermogravimetric analyses (TG-DTG) curves for the sorbents is as shown in Figure 4.7. The thermogravimetric (TG) curves exhibited significant similarities with only minor differences. These negligible variations in mass loss can be attributed to the conservation of the zeolitic framework even after iron modification of NZe. The TG curve depicts the percentage of weight loss relative to temperature, allowing the assessment of mass reduction over a specific temperature range (Kikuvi et al., 2025). The TG plots start slightly below 100% due to initial nitrogen purging, which removes potential volatile impurities, causing minor weight loss before recording begins (Bottom, 2008). The notable observations include a little mass loss of 0.62% and 0.98% for NZe and ImZe respectively in the temperature range of 50-200 °C corresponds to the desorption of weakly sorbed water molecules in the pores. This was followed by greater mass losses of 7.54% and 6.37% for NZe and ImZe respectively as indicated by a sharp decline in the TG curve in the range 200-700 °C. This observation is ascribable to the dehydration of silanol hydroxyl groups and the release of

chemisorbed water (Alver et al., 2010). The high energy requirement for this process reflects the strength of the bonds binding the water molecules to the zeolitic framework. Beyond 700 °C, the curve flattens range suggesting that no further structural degradation or decomposition occur beyond this temperature indicating the thermal stability of the basic zeolitic structure (Zvereva et al., 2022).

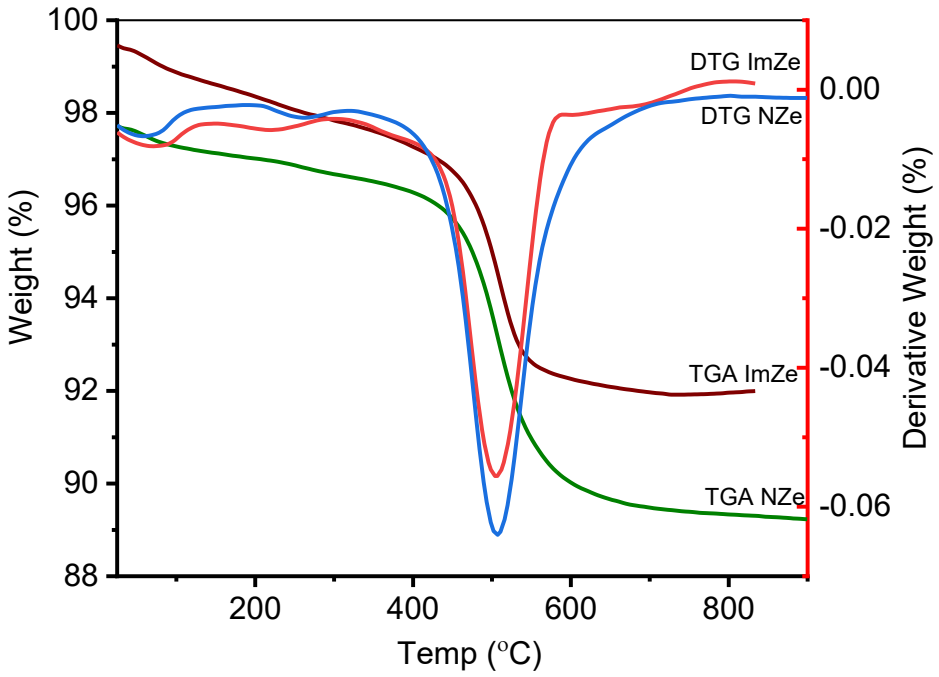

Figure 4.7: TG-DTG curves for NZe and ImZe

On the other hand, the DTG curve shows the rate of weight loss versus temperature, with peaks indicating the temperature ranges where significant weight loss occurs (Bottom, 2008). Distinctive and sharp peaks observed within the 400–600°C range for both NZe and ImZe indicate that the maximum weight loss event occurred in this range. There are no additional observable peaks beyond 600°C suggesting that there is no further decomposition of the sorbents thereby highlighting their thermal stability at higher temperatures (Wan Ngah et al., 2012). The

similarities observed in the TG–DTG curves of the two sorbents indicate a retained framework even after iron modification. This suggests that modification does not compromise the integrity of the adsorbent supporting earlier findings (Ivanova & Knyazeva, 2013). These findings underscore the thermal stability of both sorbents, with negligible variations in weight loss attributable to the incorporation of iron into the zeolitic framework for ImZe.

4.2 Adsorbates' quantum chemical properties

The frontier orbitals for the optimized molecular structures of Ciprofloxacin, Diclofenac potassium, and Chloramphenicol, obtained through molecular simulations, are presented in Figure 4.8. The atoms in white, grey, red, blue, green color represent hydrogen, carbon, oxygen, nitrogen and halogen respectively. Blue and yellow regions correspond to negative and positive values of the orbital.

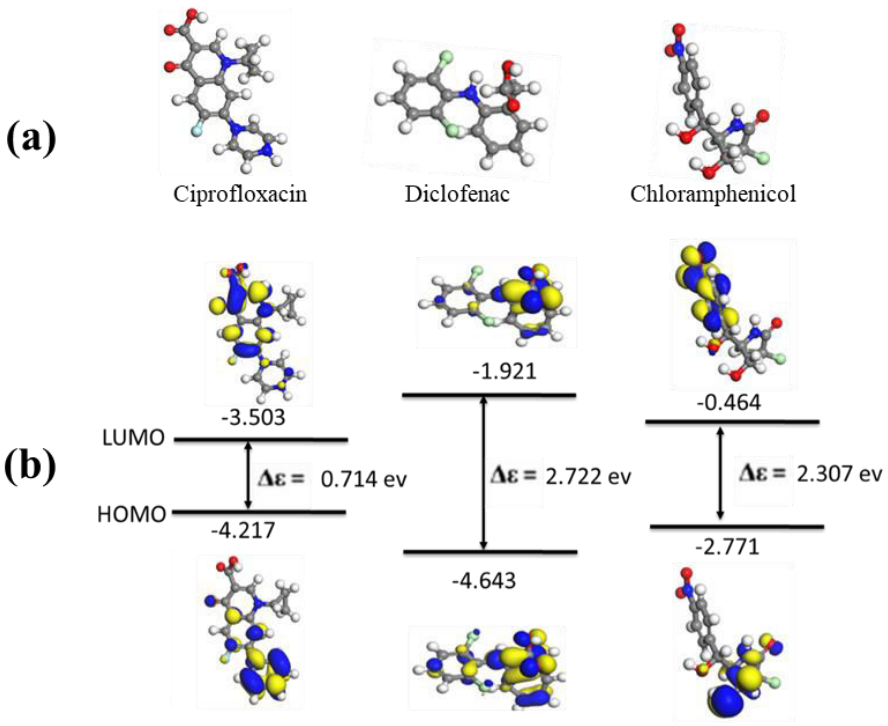

Figure 4.8: (a) Optimized structures of Ciprofloxacin, Diclofenac and Chloramphenicol **(b)** Frontier molecular orbitals of Ciprofloxacin, Diclofenac and Chloramphenicol

The LUMO energy (E_{LUMO}) corresponds to a molecule's electron-accepting capacity while HOMO energy (E_{HOMO}) pertains to its electron-donating ability from which the global hardness (η) can be calculated. The energy gap between LUMO and HOMO elucidates the electrical properties and chemical behavior of molecules, with lower energies indicating lower stability and therefore higher reactivity (Mebi, 2011). Observably, the HOMO of Diclofenac is localized on benzene ring and around N- and OH- groups, resembling the LUMO but with less intensity.

While the LUMO in Ciprofloxacin is on the higher phenyl ring, which has nitrogen in the ring that extends to the -OH group and O-, which are connected to the phenyl ring, the HOMO is centered on the dinitro-phenyl ring. For Chloramphenicol, the HOMO is concentrated on the lower part of the molecule, around the benzene ring, OH group, and acetamide group, with a δ-interaction bonding system forming a semicircle on the ring, while the LUMO is primarily located on the nitro-phenyl ring (Wanyonyi et al., 2020). Table 4.2 shows the quantum chemical descriptors of the three adsorbates.

Table 4.2: Key quantum chemical descriptors obtained for the adsorbates

Pharmaceuticals	Chemical hardness (eV)	Chemical potential (eV)	Chemical softness (eV)
Chloramphenicol	1.15	-1.62	0.87
Ciprofloxacin	0.36	-3.86	2.80
Diclofenac	1.36	-3.28	0.74

Calculations of electron orbital energy levels enabled quantification of HOMO and LUMO energies, with Diclofenac exhibiting the lowest HOMO energy (-4.64 eV) and chloramphenicol the highest (-2.77 eV). A larger HOMO–LUMO energy gap indicates a harder, more stable, and less reactive molecule (Mebi, 2011). The study revealed that Diclofenac exhibits the highest chemical hardness of 1.3609 eV, indicating greater stability and resistance to charge transfer.

Conversely, Chloramphenicol and Ciprofloxacin, with smaller HOMO-LUMO gaps, are highly polarizable and thus more reactive (Al-Sehemi et al., 2016). These descriptors determine the interactions of the adsorbates with the binding sites on the adsorbent.

4.3. Batch Studies

4.3.1. Effect of Dosage

Figure 4.9 illustrates the impact of adsorbent dosage on the removal efficiency of the three pollutants, investigated within the range of 0.01 to 1.0 g/L.

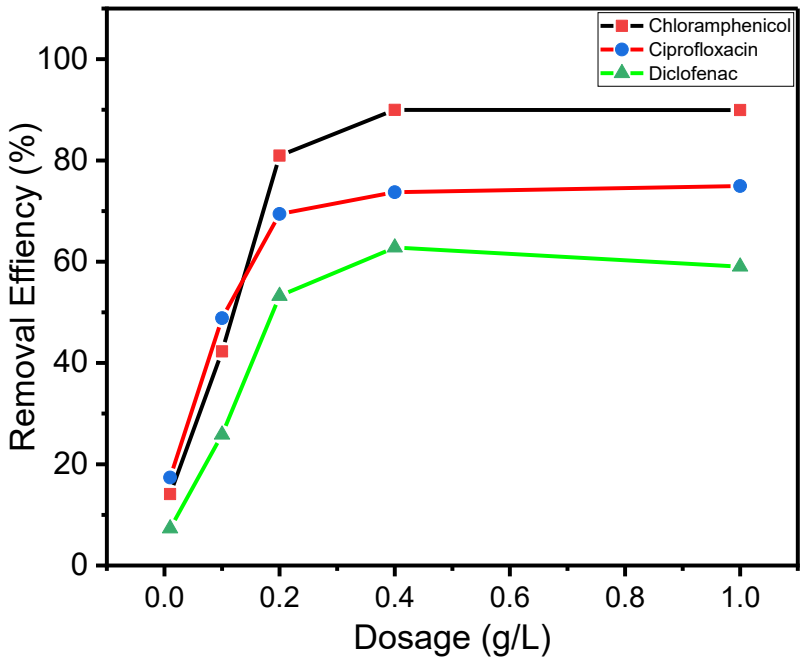

Figure 4.9: The effect of adsorbent dosage on the removal efficiency of the pollutants

The removal efficiency improved with the rise in adsorbent dosage. At dosage of 0.4 g/L, optimal removal efficiency was attained, as shown in Figure 4.9, beyond this point, the efficiency for Chloramphenicol plateaued, while it slightly declined for Ciprofloxacin and

Diclofenac potassium. The initial increase in efficiency is linked to increase in number of active sites and surface area as the adsorbent dosage increases, creating more room for adsorption of the pollutant molecules. However, beyond the optimum dosage, the adsorbent particles aggregate, due to increased particle-particle collisions in the crowed suspension thereby reducing the total effective surface area accessible and therefore lowers the overall adsorptive removal effectiveness removal effectiveness (Nethaji et al., 2010). Therefore, a dosage of 0.4 g/L was used for all subsequent adsorption reactions.

4.3.1. Effect of Contact Time

Figure 4.10 illustrates how contact time influences the removal efficiency of Chloramphenicol, Ciprofloxacin, and Diclofenac potassium through adsorption onto NZe and ImZe. The adsorbate removal percentage surged rapidly with increasing contact time up to 45 minutes for the two adsorbents. This is ascribed to the numerous vacant sites of adsorption on the adsorbents available initially (Parlayici & Pehlivan, 2019). This was followed by a plateau phase where removal efficiency showed no significant change, indicating that equilibrium conditions were attained at this point. During this phase, the adsorption of adsorbates slowed down, likely due to a reduction in available active sites and repulsion between adsorbed pollutant molecules on the sorbents and those in the solution (Shikuku et al., 2018). A paired t-test at a 95% confidence level demonstrated that ImZe markedly surpassed NZe in pollutant removal efficiency, with removal rates of 90% for Chloramphenicol, 74% for Ciprofloxacin, and 63% for Diclofenac potassium, compared to NZe's 32, 22, and 27%, respectively, supported by *p*-values of 0.00472 and 0.00944, confirming statistical significance.

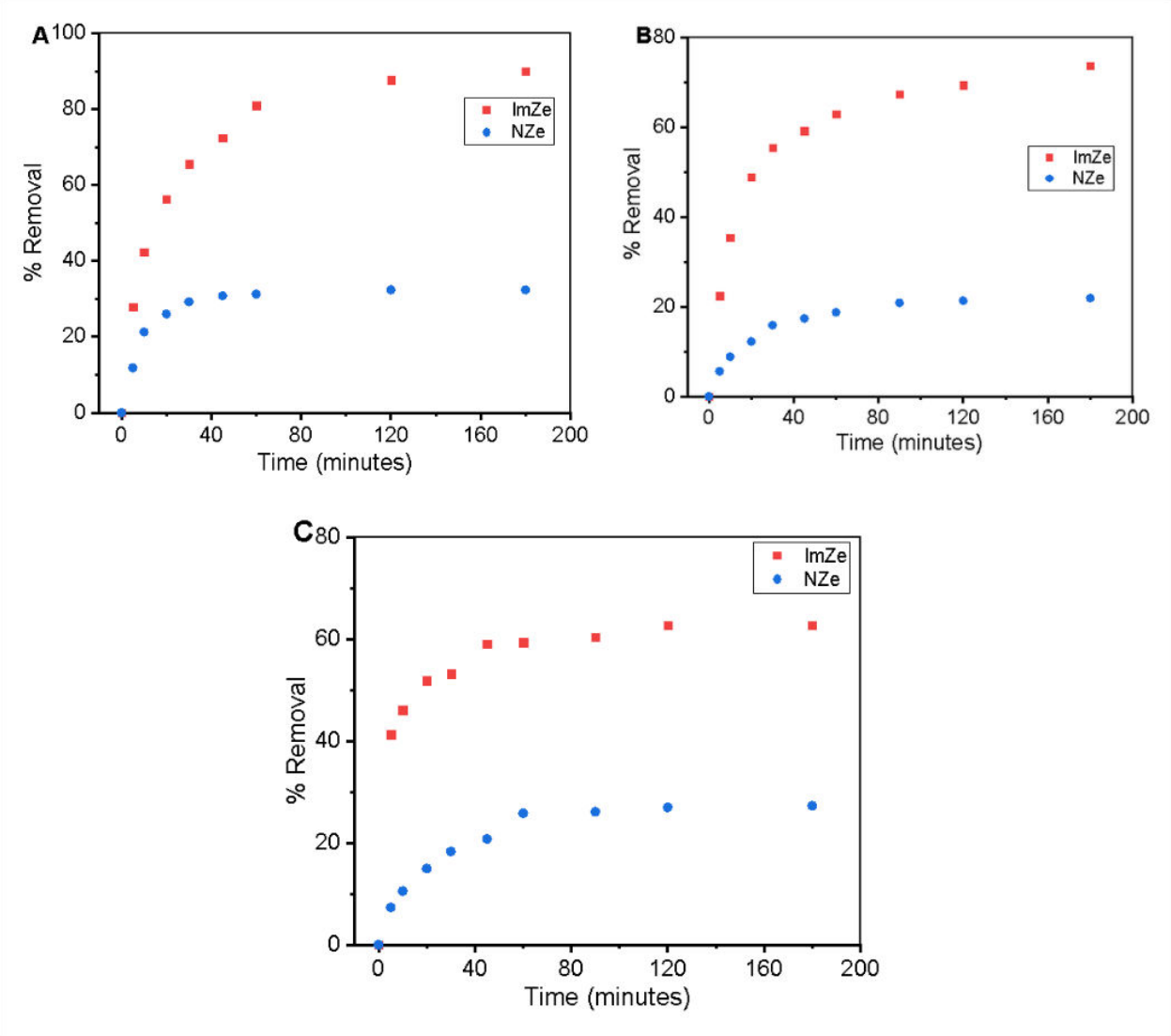

Figure 4.10: Removal efficiencies of NZe and ImZe for (A.) Chloramphenicol, (B.) Ciprofloxacin and (C.) Diclofenac potassium

Furthermore, ImZe demonstrated a greater ability to adsorb the pollutants than NZe. For Chloramphenicol, Ciprofloxacin, and Diclofenac potassium, ImZe's adsorption capacities were 22.49, 18.43, and 15.70 mg/g, respectively, compared to NZe's 7.71, 4.35, and 5.19 mg/g. The impact of iron modification on the zeolite was substantial, resulting in an enhanced adsorption capacity which agrees with other studies (Jannat Abadi et al., 2019). This is due to the impregnation of iron species into the zeolite structure, which not only creates additional active

sites but also shifts the pH_{pzc} toward pH 7.0. This results in a positively charged zeolite surface over a wider pH range, thereby improving its organic pollutant adsorption capacity (Wang & Peng, 2010). It should be noted that the study was an exception to the rule of the Hard and Soft Acids and Bases (HSAB) theory, which predicts stronger interactions between hard-hard or soft-soft species (Pearson, 1963). The Fe^{3+} species, employed to modify the sorbent, is classified as a hard acid (Kiprono et al., 2023). In contrast, the adsorbates; Chloramphenicol and Diclofenac are softer bases, exhibiting pKa values of 5.5 and 4.0, respectively. Ciprofloxacin is a soft basic zwitterionic molecule with pKa values of 6.09 and 8.62. The strong and favorable interactions observed between the hard and soft species can be explained by the high polarizability of the soft species and the presence of half-filled d orbitals in the Fe^{3+} species, which facilitate enhanced bonding.

Figure 4.11 shows a comparison of ImZe's adsorption capacities for Chloramphenicol, Ciprofloxacin and Diclofenac potassium. The order of the adsorption capacity from highest to lowest is: Chloramphenicol > Ciprofloxacin > Diclofenac potassium. This can be attributed to the differences in their molecular structures and weights. Chloramphenicol with a molecular mass of 323.132 g/mol is the least bulky of the three pollutants characterized by its additional functional groups being attached to the core benzene ring (Figure 2.4). Ciprofloxacin whose molecular mass is 331.346 g/mol contains a fused bicyclic core and a piperazine ring (Figure 2.5). Diclofenac potassium is the bulkiest with a molar mass of 334.24 g/mol consists two phenylic rings linked by an amine group (Figure 2.3). According to Muir et al. (2017), the adsorption of organic pollutants onto zeolites is characterized by pore filling and therefore adsorption capacity increases with decreasing molecular weight.

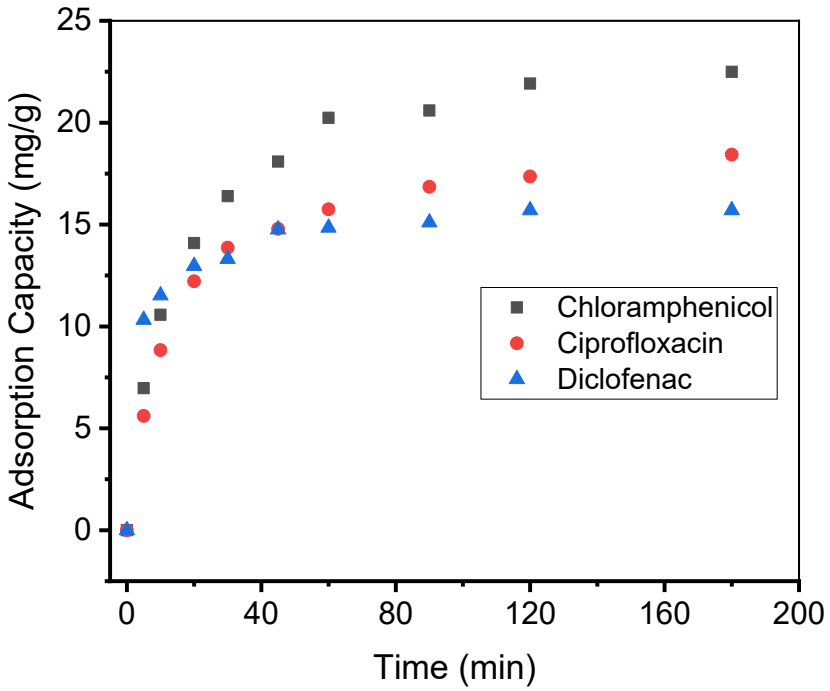

Figure 4.11: Comparative adsorption capacities for the adsorbates onto ImZe

Additionally, Diclofenac potassium has the highest chemical hardness value of 1.36 eV (Table 4.2) meaning it is the least polarizable and opposes charge transfer thereby not allowing strong interactions with adsorbent surface and therefore lowest uptake. Chloramphenicol and Ciprofloxacin have lower chemical hardness values of 1.15 and 0.36 eV, respectively therefore are more polarizable allowing for stronger interactions with ImZe. Despite its higher chemical hardness than Ciprofloxacin, Chloramphenicol was better adsorbed onto ImZe since it has more hydrogen bonding sites (i.e., 8 compared to Ciprofloxacin's 6) in addition to its small molecular weight.

4.3.3. Effect of Initial Pollutant Concentration

Figure 4.12 illustrates the effect of initial pollutant concentration, examined within the range of 2 to 20 mg/L, on the removal efficiency of the three pollutants.

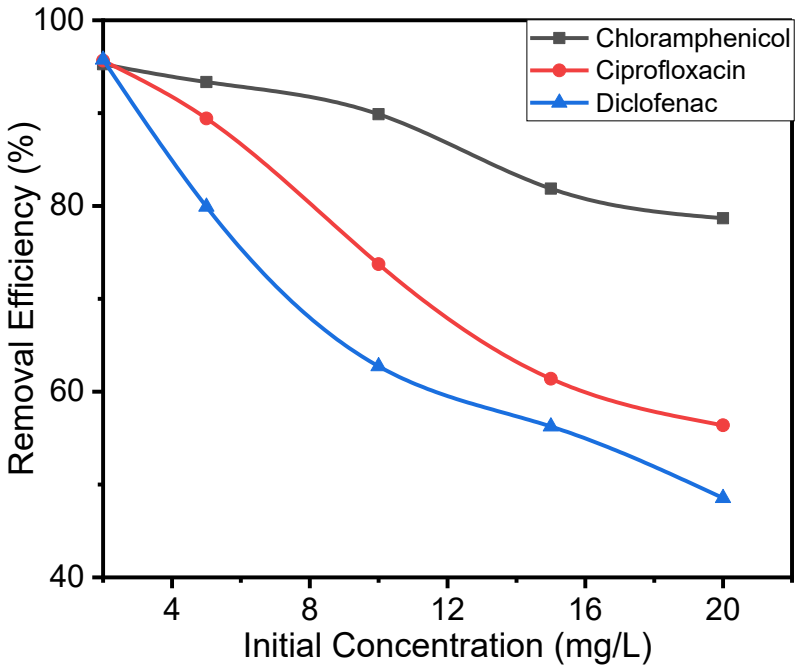

Figure 4.12: The effect of initial pollutant concentration on the removal efficiency

The results showed that increase in initial pollutant concentration corresponded with decreased removal efficiencies. For Chloramphenicol, efficiency dropped from 95.3% to 78.7%; for Ciprofloxacin, it fell from 95.6% to 56.4%; and for Diclofenac potassium, it declined from 95.8% to 48.5%. This suggests that the removal process becomes less effective at higher concentrations, possibly due to saturation (Hassan Ibrahim et al., 2024). Within the examined concentration range, Chloramphenicol was most effectively removed while Diclofenac's remediation was the least effective.

4.3.4. Effect of Temperature

Figure 4.13 illustrates the impact of temperature on the adsorptive removal efficiency of ImZe for the three pollutants. According to the findings, Chloramphenicol and Diclofenac potassium removal efficiency declined from 89.9 to 75.4% and 64.7 to 53.6% respectively as the temperature

rose suggesting that their adsorptive uptake onto ImZe is an exothermic process. Conversely, Ciprofloxacin's adsorption onto ImZe is an endothermic process as the removal increased from 74.2 to 87.2%. At a temperature of 305 K, both Chloramphenicol and Ciprofloxacin are removed adsorptively with the same efficiency, specifically 78%.

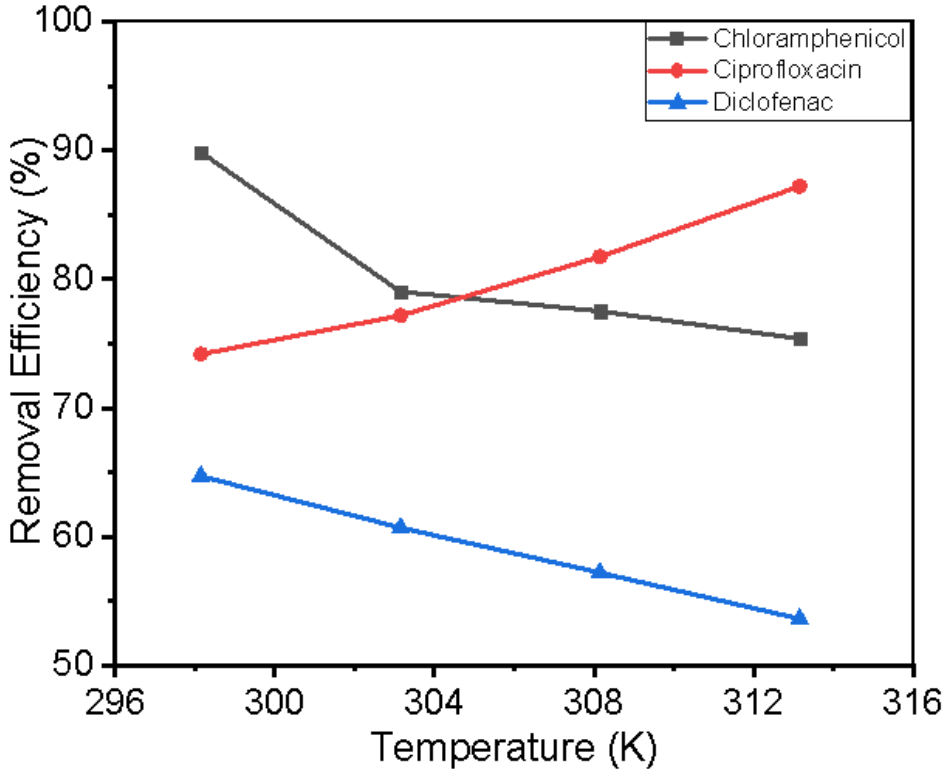

Figure 4.13: The effect of temperature on the pollutants' removal efficiency

In contrast to this study, the adsorption of Chloramphenicol onto porous carbon was marked by increased uptake from 1079 to 1240 mg g^{-1} with increase in temperature from 298 to 318 K (Dai et al., 2018). The adsorptive uptake of Ciprofloxacin by pretreated oat hulls increased from 50 to 90 mg g^{-1} as the temperature rose from 288 to 318 K (Movasaghi et al., 2019) thus corroborating the findings of this study. Similarly, adsorption of Diclofenac onto pine wood biochar decreased from 142.82 to 75.34 µg g^{-1} as the temperature rose from 283 to 323 K (Lonappan et al., 2018).

4.3.5. Effect of pH

The pH of a solution significantly influences the adsorption of organic pollutants by determining the electrical charges on both the adsorbate and the adsorbent's surface. As illustrated in Figure 4.3, ImZe has pH_{pzc} of 6.9, meaning below this pH the surface carries a net positive charge and is negatively charge above it. The influence of pH on the adsorption capacity of the three pollutants examined across a pH range of 2 to 10, is shown in Figure 4.14.

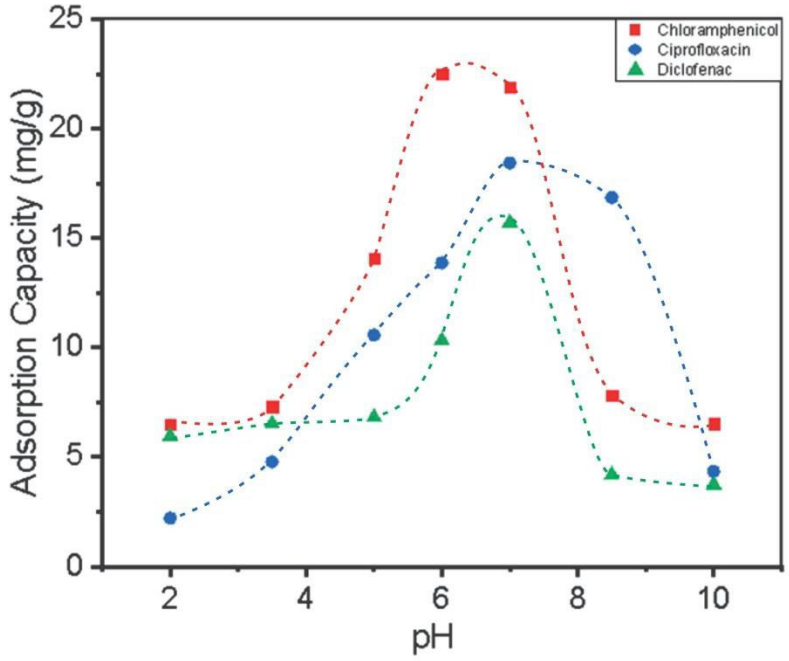

Figure 4.14: Effect of pH on the pollutants' adsorption onto ImZe

ImZe's adsorptive capacity for Chloramphenicol increased with increasing pH showing a peak of 22.4 mg g^{-1}at pH = 6, it drops greatly to 6.5 mg g^{-1}at pH = 10. Ciprofloxacin's removal increased steadily with increasing pH reaching an optimum of 18.4 mg g^{-1}at pH = 7.0 and significantly declines to 4.3 mg g^{-1}at pH = 10. At pH 2 to 5, ImZe's adsorptive potential for Diclofenac potassium remains relatively same from pH 2 – 5 i.e., 6.2 mg g^{-1}; beyond pH 5.0 it increases climaxing at pH =7 having a capacity of 15.7 mg g^{-1}at pH =7and greatly reduces to an

average 3.9 beyond the neutral pH. Further details on the effect of pH on adsorption are discussed under the adsorption mechanism.

4.4. Adsorption Kinetics

Studies on adsorption kinetics are essential for comprehending how fast and effectively adsorbate molecules adsorb to the adsorbent surface. These studies offer insights into the rate-limiting steps and possible adsorption mechanisms such as physisorption or chemisorption. The experimental kinetic data was fitted using non-linear regression models of *pseudo*-first-order, *pseudo*-second-order, Elovich, and intraparticle diffusion kinetic models. The obtained data and the corresponding best fit plots are presented in Figure 4.15, while the calculated parameters of the models are provided in Table 4.3.

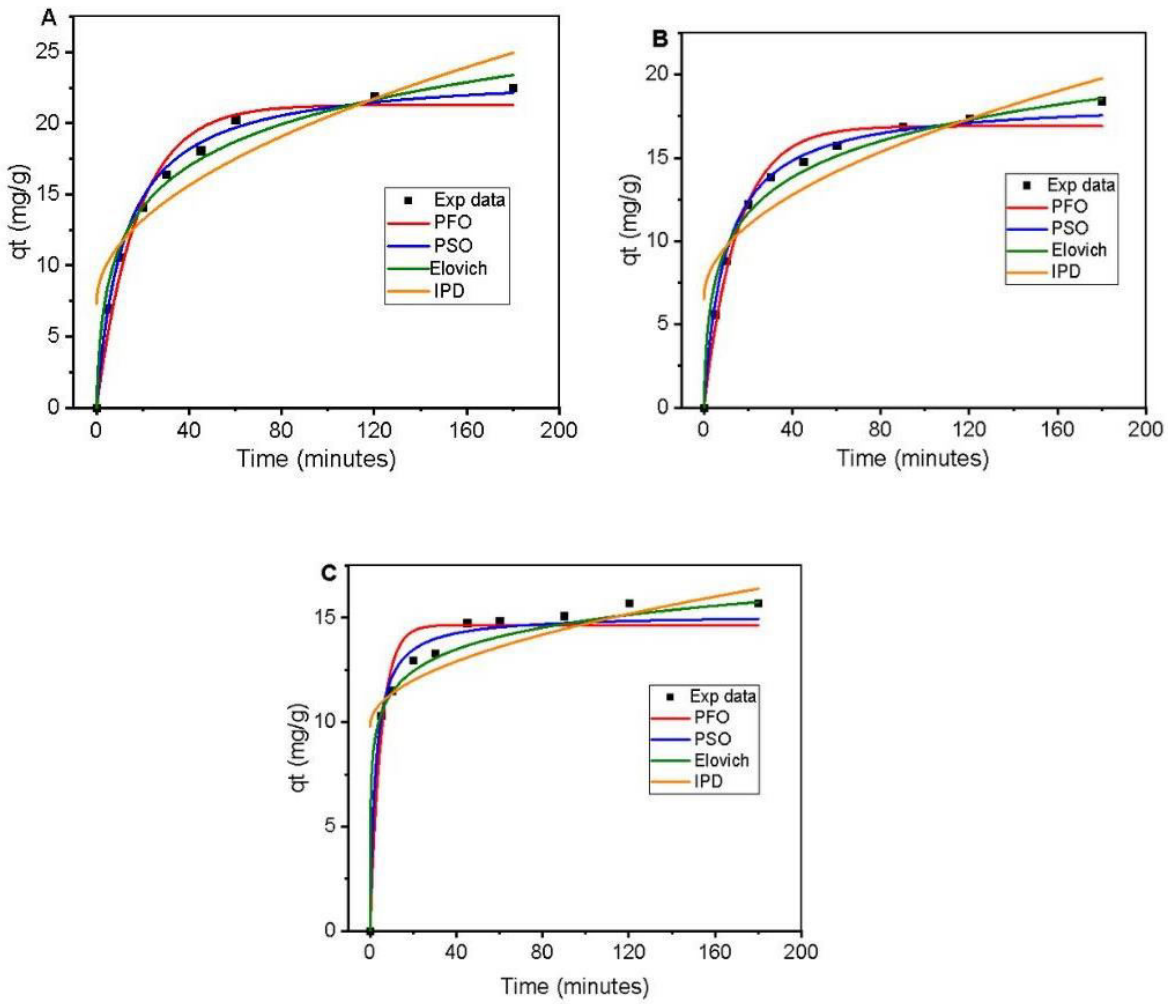

Figure 4.15: Adsorption kinetics fitting of (A) Chloramphenicol, (B) Ciprofloxacin and (C) Diclofenac onto ImZe

Table 4.3: Calculated parameters from the different kinetic models on the adsorption of the pollutants onto ImZe

Model	Parameters	Chloramphenicol	Ciprofloxacin	Diclofenac Potassium
Pseudo-first order	k_1(min^{-1})	0.0569 ± 0.007	0.0652 ± 0.007	0.1966 ± 0.033
	Q_{exp} (mg/g)	22.2924 ± 0.972	18.4345 ± 0.608	15.6997 ± 0.324
	Q_{cal} (mg/g)	21.2857 ± 0.715	16.9090 ± 0.445	14.6493 ± 0.402
	$(R_{adj})^2$	0.9739	0.9766	0.9518
	χ^2	1.4708	0.8113	1.0740
	RMSE	1.7836	0.7308	1.1131
Pseudo-second order	k_2 (g/mg min)	(3.50 ± 0.05)×10^{-3}	(5.40 ± 0.08)×10^{-3}	(2.629 ± 0.05)×10^{-2}
	Q_{cal} (mg/g)	23.6136 ± 0.048	18.5304 ± 0.036	15.1546 ± 0.019
	$(R_{adj})^2$	0.9720	0.9676	0.9358
	χ^2	0.5114	0.3367	0.1921
	RMSE	0.3657	0.1954	0.0842
Elovich	α (mg/g min)	5.5037± 0.143	6.1405 ± 0.189	289.3695 ± 34.149
	β (g/mg)	0.2329 ± 0.0017	0.3154 ± 0.0025	0.6635 ± 0.0094
	$(R_{adj})^2$	0.9696	0.9619	0.8435
	χ^2	0.7607	0.5434	0.6399
	RMSE	0.6635	0.4005	0.5119
Intraparticle diffusion	K_{diff} (mg/g·min$^{1/2}$)	1.3142 ± 0.01142	0.9862 ± 0.0091	0.4909 ± 0.0058
	C	7.3126 ± 0.1033	6.5376 ± 0.0819	9.8026 ± 0.0522
	$(R_{adj})^2$	0.9299	0.9225	0.8799
	χ^2	1.6302	1.0235	0.4154
	RMSE	2.0814	1.0355	0.2678

As depicted in Figure 4.15, during the initial 20 minutes, the *pseudo*-first order, *pseudo*-second order, and Elovich curves for the three pollutants closely matched and effectively aligned with the experimental data. After 20 minutes, however, nonconformities from the experimental findings were noted. The time required to reach equilibrium varied among the pollutants: Diclofenac potassium attained it fastest, in 30 minutes, followed by Chloramphenicol at 45 minutes, and Ciprofloxacin took the longest, at 60 minutes. The variation in the time required for the substances to attain equilibrium is attributable to their distinct physicochemical characteristics, specifically their hydrophobicity (Schwarzenbach et al., 2016). Diclofenac potassium, exhibiting the highest log *P* value of 4.5 and therefore being the most hydrophobic, is likely to adsorb more readily onto the hydrophobic ImZe surface. Conversely, Ciprofloxacin possesses the lowest log *P* value of 1.54, indicating it is the least hydrophobic. Furthermore, its zwitterionic nature contributes to weaker interactions with the hydrophobic sorbent material, thereby extending the contact time needed to attain equilibrium.

The *pseudo*-first order kinetic model is descriptive of physisorption in which the rate of adsorption is directly proportional to the number of available sites (Wang & Guo, 2020). In this model, Diclofenac potassium exhibited the highest k_1 value (0.1966 min^{-1}) suggesting a much faster initial adsorption rate and a shorter time required to reach equilibrium as compared to Chloramphenicol (0.0569 min^{-1}) and Ciprofloxacin (0.0652 min^{-1}). This can be attributed to Diclofenac's lowest water solubility (2.37 mg/L at 25 °C) compared to Chloramphenicol (2500 mg/L) and Ciprofloxacin (36000 mg/L). Lower solubility reduces the inclination to remain in the aqueous phase, promoting faster partitioning onto the solid adsorbent phase, thus increasing k_1 value and reducing equilibration time (Oyege et al., 2024).

However, Diclofenac potassium also showed a relatively lower equilibrium adsorption capacity

(14.65 mg g^{-1}), indicating a poorer overall adsorption capacity compared to the other two pollutants. This model was characterized by high $(R_{adj})^2$ values exhibited by Chloramphenicol, Ciprofloxacin and Diclofenac potassium (0.9739, 0.9766, and 0.9518) and their correspondingly low RMSE values (1.7836, 0.7308, and 1.1131) respectively. This indicates *pseudo*-first order kinetic model can describe the initial adsorption stage for the pollutants however, compared to *pseudo*-second order model, it recorded higher values of χ^2 showing that it cannot satisfactorily describe the kinetics for the whole process.

The *pseudo*-second order kinetic model describes chemisorption where adsorption rate is proportional to the square of available adsorption sites (Bujdák, 2020). Diclofenac potassium exhibited the fastest adsorption rate, shown by its k_2 value of 2.63×10^{-2} g/mg min^{-1}, which was higher than Chloramphenicol's 3.5×10^{-3} g/mg min^{-1} and Ciprofloxacin's 5.40×10^{-3} g/mg min^{-1}. This faster rate indicates Diclofenac attained adsorption equilibrium sooner than the other two pollutants. The relative equilibrium capacities of the three pollutants follows the order earlier discussed (*vide supra* i.e., Section 4.3.2). All pollutants demonstrated a better fit to the *pseudo*- second order model than to the *pseudo*-first order model, as evidenced by low error analysis parameters and the convergence of experimental adsorption capacities and the model's calculated values despite having relatively lower $(R_{adj})^2$ values of 0.9720, 0.9676 and 0.9358. The calculated χ^2 values were 0.5114 for Chloramphenicol, 0.3367 for Ciprofloxacin and 0.1921 for Diclofenac potassium and the corresponding RMSE values for these chemicals were 0.3657, 0.1954, and 0.0842, respectively. This indicates that chemisorption limits the adsorption rate of the pollutants onto ImZe. The findings corroborate an earlier study reporting that the *pseudo*-second order model more precisely characterizes the adsorption of hydrophobic molecules onto hydrophobic surfaces (Xu et al., 2019).

While *pseudo*-first and *pseudo*-second order models are premised on empirical data they lack a theoretical deductions founded in physical principles (Simonin, 2016) the Elovich model elucidates chemisorption kinetics by highlighting surface heterogeneity and the exponential decrease in available adsorption sites as the adsorption process progresses (Elovich & Larinov, 1962). According to the Elovich model, Diclofenac potassium portrayed a notably high initial adsorption rate (α) value of 289.37 mg/g min which indicates a rapid initial adsorption rate. This corroborates the observations from the *pseudo*-first order and *pseudo*-second order models. Additionally, Diclofenac potassium had the highest desorption constant (β) value of 0.6635 g/mg compared to 0.2329 for Chloramphenicol and 0.3154 for Ciprofloxacin suggesting that it experiences the weakest adsorption forces among the three pollutants. The Chloramphenicol's β value was the lowest, indicating that it experiences the strongest adsorption forces (Obayomi et al., 2023). The high initial adsorption rates of the pollutants are indicative of a favourable and fast initial adsorption process, catalysed by strong pollutant-ImZe interactions and plenty of adsorption sites (Khalfaoui et al., 2024). The relatively low desorption values indicate that the adsorption for the pollutants decelerates as the adsorption sites are occupied, leading to decrease in overall adsorption rate. This indicates significant surface heterogeneity, allowing continuation of adsorption thereby rendering the system resistant to effects of saturation (de Vargas Brião et al., 2023). Diclofenac potassium showed a poor fit to the Elovich model as shown by $(R_{adj})^2$ value of 0.8435 compared to Chloramphenicol's 0.9696 and 0.9619 of Ciprofloxacin.

The intraparticle diffusion model specifically examines the physical movement of the adsorbate moves through the pores of an adsorbent, rather than the surface adsorption itself (Weber Jr & Morris, 1963). Chloramphenicol had the highest diffusion constant (K_{diff}) value of 1.3142 $mg/g \cdot min^{1/2}$, indicating the fastest intraparticle diffusion, while Diclofenac potassium exhibited

the slowest as shown by the value of 0.4909. Diclofenac potassium exhibited the highest C value 9.8026, reflecting the greatest boundary layer effect among the three pollutants. This results to increased resistance to mass transfer across the external surface, highlighting that surface adsorption is more dominant in its adsorption process than intraparticle diffusion compared to the other pollutants. This is further corroborated by the $(R_{adj})^2$ values with 0.8799 for Diclofenac potassium showing the least fit to the experimental data compared to 0.9299 and 0.9225 for Chloramphenicol and Ciprofloxacin respectively.

4.4.1. Comparison of kinetics with other adsorbents

Diclofenac's adsorption onto various adsorbents including activated carbon (Petrović et al., 2020), modified clays (Sousa et al., 2022), composite materials (Rigueto et al., 2021), and metal-organic frameworks (Zhuang et al., 2020) has been described by *pseudo*-second order model. A study comparing Ciprofloxacin adsorption's onto activated carbon, bentonite, pumice and zeolite found that the *pseudo*-second order model provided a good fit for all these adsorbents (Genç & Dogan, 2015). A review indicated *pseudo*-second order model's applicability in describing Chloramphenicol adsorption onto a variety of adsorbents (Nguyen et al., 2022).

According to the findings, Diclofenac potassium exhibits a very fast initial adsorption rate (high k_1, k_2 and α) but a low overall equilibrium adsorption capacity (low Q_e). This indicates that Diclofenac potassium quickly binds to readily available adsorption sites, but then encounter limitations, possibly due to steric hindrance. The Elovich model fits poorly, suggesting chemisorption might not be the dominant mechanism for Diclofenac. Ciprofloxacin exhibits intermediate adsorption capacity in all the three kinetic models. Chloramphenicol consistently showed high equilibrium adsorption capacities across the different models. It has

the highest intraparticle diffusion constant, indicating a more efficient movement within the zeolitic pores; this can be attributed to its relatively small size (Kohay & Gazit, 2024).

4.5. Adsorption isotherms

Adsorption isotherms provide insight on the interaction of adsorbate with the adsorbent. Isothermal studies play an important role in optimization processes. Isothermal models are classified on the number of parameters namely: one-parameter, two-parameter and three-parameter models (Ayawei et al., 2017). This work was studied by applying three 2-parameter models i.e., Langmuir, Freundlich and Temkin owing to their ability to describe adsorption mechanism with fewer assumptions. The fittings of the experimental data to the different models is as presented in Figure 4.16 while the calculated parameters of the models are provided in Table 4.4.

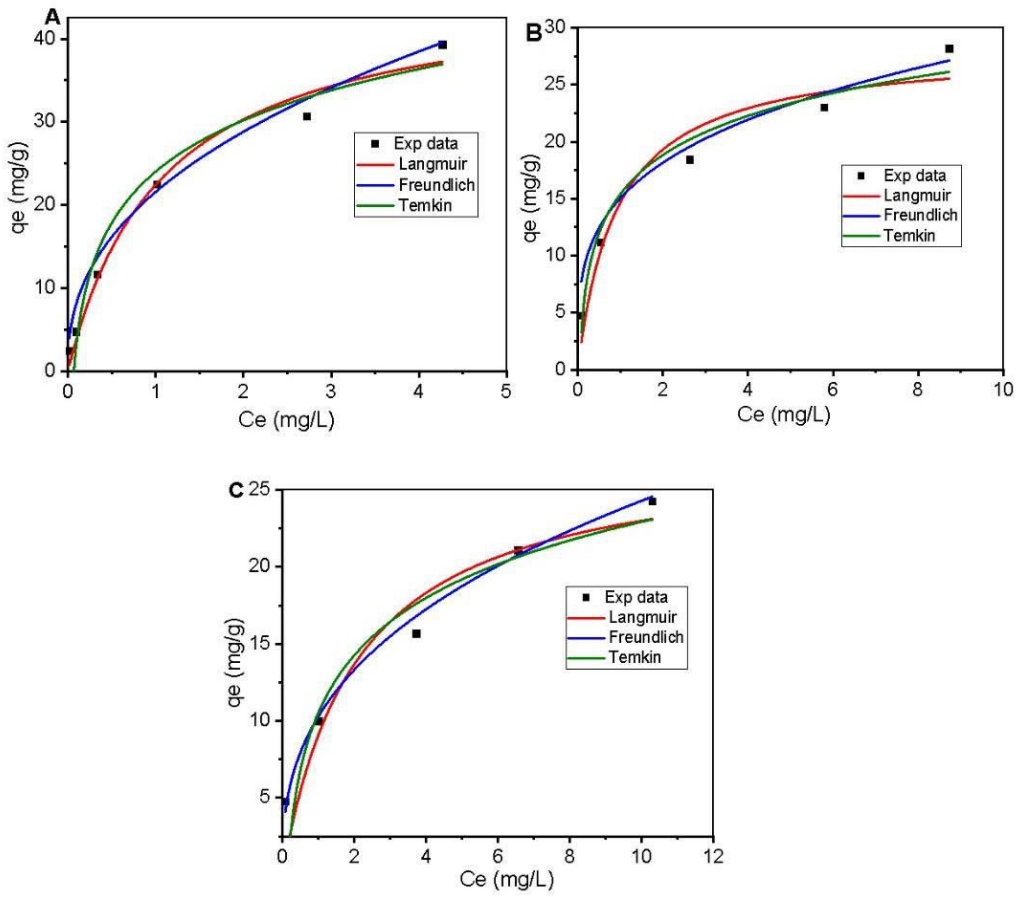

Figure 4.16: Non-linear isothermal fitting of (A) Chloramphenicol, (B) Ciprofloxacin and (C) Diclofenac

Table 4.4: Calculated parameters from the different isotherm models on the adsorption of the pollutants onto ImZe

Isotherm Model	Parameter	Chloramphenicol	Ciprofloxacin	Diclofenac
Langmuir	K_L (L mg^{-1})	0.9241 ± 0.2243	1.0815 ± 0.4968	0.4859 ± 0.2689
	R_L	0.5197 – 0.0513	0.3161 – 0.0442	0.5072 – 0.0933
	Q_{max} (mg g^{-1})	46.6711 ± 3.8539	28.2278 ± 2.9680	27.7209 ± 4.4876
	χ^2	4.0504	7.06581	6.8357
	$(R_{adj})^2$	0.9815	0.9185	0.8918
	RMSE	8.1516	18.7820	17.8721
Freundlich	K_F (L min^{-1})	21.5590 ± 0.0704	15.0282 ± 0.0721	10.2696 ± 0.0585
	n_f	0.4178 ± 0.0031	0.2725 ± 0.0029	0.3738 ± 0.0031
	χ^2	2.4176	1.6195	1.0595
	$(R_{adj})^2$	0.9693	0.9285	0.9601
	RMSE	3.7589	2.0609	1.0906
Temkin	A (L g^{-1})	14.7736 ± 0.4056	22.3766 ± 0.4941	7.0270 ± 0.1590
	B (J mol^{-1})	8.91395 ± 0.0723	4.9540 ± 0.0249	5.3903 ± 0.0361
	χ^2	4.6656	0.4483	1.01753
	$(R_{adj})^2$	0.9384	0.9754	0.9571
	RMSE	10.0777	0.3002	1.0264

From Figure 4.16, it is observed that for all the pollutants, there is an increase in equilibrium adsorption capacity with increasing equilibrium concentration. This is due to the increase in the driving force of the concentration gradient, with increase in the initial pollutant concentration (Shikuku et al., 2018). For Chloramphenicol all three isothermal models seem to align with the experimental data reasonably well, but the Freundlich and Temkin models exhibit a slightly better fit at lower equilibrium concentration (Ce) values. In contrast, Ciprofloxacin exhibits deviations between the models and experimental data, particularly at higher Ce values. The Langmuir and Temkin models seem to underestimate the equilibrium adsorption capacity values for Diclofenac potassium at higher Ce values.

4.5.1. Langmuir isotherm model fitting

The Langmuir isotherm is premised on the assumption that adsorbate adsorption forms a monolayer onto a homogeneous adsorbent surface characterized by energetically identical binding sites with no further lateral interactions between the adsorbed molecules (Langmuir, 1916). It is characterized by two parameters i.e., maximum adsorption capacity (Q_{max}) and Langmuir constant (K_L). Among the three pollutants, Chloramphenicol exhibited the highest Q_{max} (46.67 mg g^{-1}) compared to 28.23 and 27.72 mg g^{-1} for Ciprofloxacin and Diclofenac potassium respectively indicating it has the greatest adsorption capacity. Ciprofloxacin had the highest K_L (1.08) indicating it has a stronger affinity to ImZe as compared to Chloramphenicol and Diclofenac. The R_L values for the three pharmaceutical products fell in the range of 0 to 1 signifying a favourable adsorption process of all the three adsorbates onto ImZe (Musah et al., 2022). The Langmuir model could not satisfactorily describe the adsorption of Chloramphenicol, Ciprofloxacin and Diclofenac onto ImZe. Although $(R_{adj})^2$ values ranged

between 0.8918 and 0.9815 indicating good correlation with the experimental data when adjusted for degrees of freedom, this was outweighed by the other statistical parameters indicating a poor fit. The relative higher χ^2 values i.e., 4.05, 7.07 and 6.84 for Chloramphenicol, Ciprofloxacin and Diclofenac potassium along with large RMSE values i.e., 8.1516, 18.7820, and 17.8721, respectively confirm the model's inadequacy. Langmuir model's unsuitability for describing the adsorption of these pharmaceutical products, likely due to the heterogeneous nature of the ImZe surface or interactions between adsorbed molecules, which violate the model's assumptions (Langmuir, 1916).

4.5.2. Freundlich isotherm model fitting

The Freundlich isotherm is an empirical model that describes adsorption on a heterogeneous surface with adsorption sites of varied energies. Unlike the Langmuir, the Freundlich model allows for multilayer adsorption and lateral interactions between the adsorbed molecules (Freundlich, 1907). K_F and n_f are Freundlich parameters indicative of the relative adsorption capacity and the surface heterogeneity of the sorbent, respectively. Chloramphenicol displayed the highest K_F value 21.56 L min^{-1}, indicating a higher adsorption capacity compared to Ciprofloxacin's 15.03 L $min^{-1}$and Diclofenac's 10.27 L min^{-1}. The adsorptive potential of ImZe for these pollutants decreases in the order Chloramphenicol > Ciprofloxacin > Diclofenac potassium as indicated by their K_F values. Value of $1/n_f < 1$ suggests favorable adsorption, while $1/n_f > 1$ as reported for the pharmaceuticals suggests cooperative adsorption involving several mechanisms (de Souza et al., 2021). The statistical analysis point to this model's fitness to describe the adsorption of the three pharmaceutical products onto ImZe. This is supported by their low calculated χ^2 values ranging between 1.06 and 2.42 in addition to low RMSE values ranging between 1.09 and 3.76. The high $(R_{adj})^2$ values of 0.9693 for Chloramphenicol, 0.9285 for Ciprofloxacin, and 0.9601 for

Diclofenac potassium strongly support a good correlation with the experimental results. The model's suitability to describe adsorption followed the order: Diclofenac potassium > Chloramphenicol > Ciprofloxacin. The Freundlich model's superior fit suggests that the adsorption of these pollutants occurs on a heterogeneous ImZe surface with multilayer coverage.

4.5.3. Temkin isotherm model fitting

This isothermal model relates the amount of adsorbate on the adsorbent after equilibrium to its concentration. It is premised on the supposition that the adsorption heat (ΔH_{ads}) declines linearly with coverage due to adsorbate interactions on the adsorbent's surface (Obaid, 2020). This contrasts with the Langmuir isotherm, which assumes a homogeneous surface and no interactions between adsorbed molecules.

Among the three pharmaceutical products, Ciprofloxacin demonstrated the strongest binding affinity as evidenced by its A value of 22.38 $L\ g^{-1}$ which is the highest. Additionally, Ciprofloxacin exhibited the least change in ΔH_{ads} with surface coverage, a characteristic highlighted by its B value of 4.95 $J\ mol^{-1}$, the lowest recorded. In comparison, Chloramphenicol has an A value of 14.77 $L\ g^{-1}$ and a B value of 8.91 $J\ mol^{-1}$, while Diclofenac's A and B values are 7.03 $L\ g^{-1}$ and 5.39 $J\ mol^{-1}$ respectively. The Temkin model can reasonably describe Ciprofloxacin and Diclofenac potassium adsorption onto ImZe owing to their favourable statistical parameters. They showed χ^2 values of 0.45 and 1.02 respectively along with low RMSE values of 0.30 and 1.03. Whereas Chloramphenicol had good statistical metrics (a high $(R_{adj})^2$ and low χ^2), it's RMSE value of 10.08 indicates that the model is less suitable for Chloramphenicol due to the higher RMSE. Temkin's suitability in describing Ciprofloxacin adsorption onto ImZe is demonstrated by the low value of the error parameters (χ^2 and RMSE). This suggests that as more Ciprofloxacin molecules are adsorbed, the heat of

adsorption decreases, indicating that the process is dominated by chemisorption involving strong interactions (Atkins et al., 2023).

4.6. Adsorption Thermodynamics

Chloramphenicol adsorption onto ImZe decreased from 89.9 to 75.4 % as the solution temperature rose from 298 to 313 K. Ciprofloxacin's removal efficiency increased from 74.2 to 87.2 % while Diclofenac's removal decreased from 64.7 to 53.6 % in the same temperature range as shown in Figure 4.12 (earlier discussed). Consequently, the ImZe's adsorption capacity reduced from 22.5 to 18.8 mg/g and 16.2 to 13.4 mg/g for Chloramphenicol and Diclofenac potassium respectively as indicated in Table 4.5. This is an indication of an exothermic process and therefore temperature increase disfavours adsorption (Atkins et al., 2023); which further aligns with their negative ΔH values. On the other hand, ImZe's adsorptive capacity for Ciprofloxacin increased from 18.5 to 21.8 mg/g as the temperature was varied from 25 to 40 ℃ which is indicative of an endothermic process further corroborated by positive ΔH value obtained (Atkins et al., 2023). The observed decline in the removal efficiency for Chloramphenicol and Diclofenac is due to the weakening of the ImZe-Diclofenac and ImZe–Chloramphenicol interactions with increasing temperature thus favouring desorption. Moreover, elevated temperature results to increase in the mobility of adsorbate molecules, leading to decreased affinity of the pollutant for the sorbent's surface. Resultantly, Chloramphenicol and Diclofenac potassium molecules desorb from the ImZe surface back into the solution phase (Shikuku et al., 2018). Increase in adsorption capacity and consequently the removal efficiency for Ciprofloxacin with increasing temperature indicates that the sorbate requires energy to break existing interactions between the pollutant and the solvent and to facilitate the diffusion of the pollutant into the zeolite's microporous structure, leading to

stronger binding interactions at higher temperatures as reported for malachite green adsorption onto natural zeolite (Han et al., 2010).

Van't Hoff plots (Figure 4.17) were used to ascertain key thermodynamic parameters (ΔG, ΔH and ΔS) for the adsorption process. The results obtained are tabulated in Table 4.5.

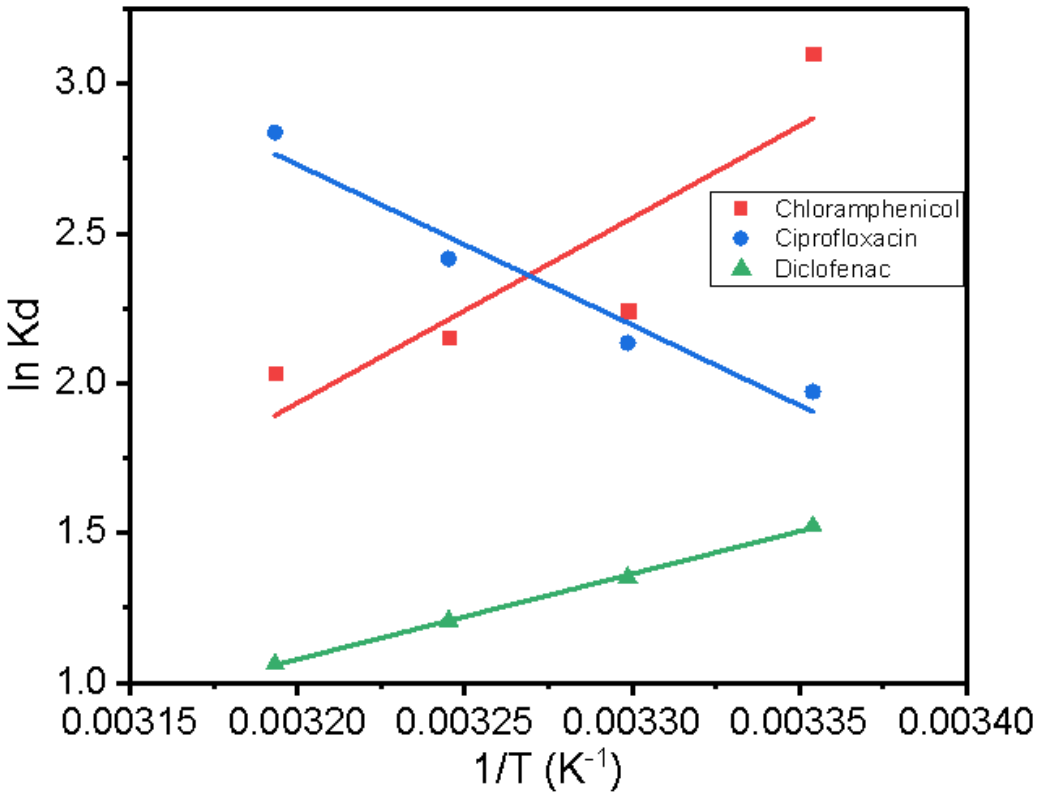

Figure 4.17: Van't Hoff plots for the pollutants' adsorption onto ImZe

Table 4.5: Thermodynamic parameters calculated from Van't Hoff plots

Pharmaceutical	Temp (K)	Adsorption capacity (mg/g)	% Removal	ΔG (kJ mol^{-1})	ΔH (kJ mol^{-1})	ΔS (J mol^{-1} K^{-1})
Chloramphenicol	298.15	22.469	89.90	-7.6795	-55.0072	-148.0522
	303.15	19.759	79.04	-5.6514		
	308.15	19.381	77.50	-5.5168		
	313.15	18.846	75.38	-5.2967		
Ciprofloxacin	298.15	18.546	74.18	-4.7221	44.5475	165.2511
	303.15	19.294	77.18	-5.5483		
	308.15	20.438	81.75	-6.3746		
	313.15	21.807	87.23	-7.2009		
Diclofenac Potassium	298.15	16.177	64.71	-3.7603	-23.7078	-66.9041
	303.15	15.173	60.70	-3.4258		
	308.15	14.302	57.21	-3.0913		
	313.15	13.407	53.63	-2.7568		

From Table 4.5, all the ΔG were negative indicating that the adsorption of all the three pollutants is spontaneous and thermodynamically favourable (Atkins et al., 2023). The negative ΔG values obtained in this study validates a feasible and spontaneous adsorption process of all the pollutants onto the ImZe (Avcı et al., 2019; Cherik et al., 2015; Nguyen et al., 2022). It was also noted that increase in temperature corresponded with the value of ΔG becoming less negative for Chloramphenicol and Diclofenac potassium. This implies that at lower temperatures, the decreasing entropy penalty making the reaction more favourable. Contrariwise, Ciprofloxacin's adsorption onto ImZe is marked by increased spontaneity as the temperature rises.

Enthalpy (ΔH) describes the energy barrier that must be overcome by the sorbate molecules during the adsorption process. The negative ΔH values obtained for Chloramphenicol and Diclofenac potassium suggests that their adsorption process onto ImZe is exothermic in nature whereas the positive value reported for Ciprofloxacin depicts an endothermic process (Han et al., 2010). Barracco et al. (2024), notes that ΔH values in the range of 40–120 kJ/mol as reported for Ciprofloxacin are indicative of chemisorption mechanism, whereas lower ΔH values of -55.00 kJ/mol for Chloramphenicol and -23.71 kJ/mol for Diclofenac potassium are characteristic of physisorption. These findings align with kinetic studies which indicated a physisorption and chemisorption as mechanisms.

The negative ΔS values obtained for Chloramphenicol and Diclofenac potassium suggests an increased order at the solid/solution interphase while a positive ΔS value as reported for Diclofenac potassium points to increased randomness at the solid/solution interface during the adsorption process (Shikuku et al., 2015). The increased orderliness results from adsorbate molecules moving from the disordered bulk solution phase to the ordered sorbent surface during

adsorption. Conversely, the reduction in order is due to sorbed molecules desorbing from the sorbent surface back into the disordered bulk phase.

4.7. Adsorption Mechanism

Adsorption mechanisms provide insights on the interactions between adsorbate and the sorbent's surface. Determining the adsorption mechanism involves analysis of the functional group interactions, the sorbent properties, and the effect of solution's pH and their influence on the adsorption process (Natarajan et al., 2022). Pollutant's adsorption onto adsorbent involves either physical or chemical interactions or a combination of both (Ogbeh et al., 2025). Modification of zeolite with iron has also been reported to increase zeolite's hydrophobicity, thereby further enhancing its capacity for non-polar molecules but also increase the sorbent's pH_{pzc} (Zhang et al., 2022).

The molecular structures of the pollutants have a variety of functional groups which allow many interactions with the ImZe surface. Chloramphenicol's molecular structure (Figure 2.4) has hydroxyl, nitro, chloride, and amide functional groups. Ciprofloxacin (Figure 2.5), a quinolone antibiotic, features cyclopropyl, carboxylic acid, fluoro, and piperazin-1-yl groups. Diclofenac (Figure 2.3), an analgesic, is composed of phenylacetic acid and a dichlorophenyl amino groups. These diverse functional groups in each compound facilitate various interactions with the ImZe surface during adsorption.

The adsorption of solutes onto an adsorbent can occur through electrostatic attractions, electron- donor-acceptor interactions and hydrogen bonding (Nguyen et al., 2022). Additionally some adsorbates' adsorption mechanism is characterized by pore filling (Binh & Kajitvichyanukul, 2019) and complexation with the metal sites (Huang et al., 2019) in the sorbent's surface. Hydrogen bonding is a likely mechanism for the adsorption of all the three

pollutants onto ImZe. This is so because hydrogen bonding which is a special type of dipole-dipole interactions that occur between hydrogen and small electronegative atoms like oxygen, nitrogen or fluorine (Grabowski, 2006). The adsorbates' electronegative atoms can interact with Brønsted acid sites present on the ImZe's surface which are partially positive.

Complexation with iron species of is another likely mechanism. Ciprofloxacin has been reported to form complexes with iron through interaction with its -keto and carboxyl groups (Turel et al., 1996). Chloramphenicol, on the other hand, forms complexes with iron through its electronegative amido group (Al-Khodir & Refat, 2016). Diclofenac potassium chelates with iron via the 2,2′- bipyridine (Agrawal & Shivramchandra, 1991).

The pH of solution plays a key role in the adsorption of pollutants onto sorbents as it determines the electrical charge of the adsorbate and the surface of the adsorbent. The pHpzc of ImZe was determined to be 6.9 (Figure 4.14). When the pH is below the sorbent's pHpzc the surface is positively charged. The surface becomes negatively charged when the solution pH is above the point of zero charge. ImZe exhibited the highest adsorption capacity for Chloramphenicol at pH = 6. At this pH Chloramphenicol is deprotonated as the pH>pKa as illustrated in Figure 4.18 and the ImZe's surface is positively charged allowing electrostatic attractions. At pH 10 the sorbate experiences electrostatic repulsions with the surface as they are all negatively charged and the sorption capacity drops drastically.

Diclofenac potassium showed maximum uptake at pH 7.0. At this pH the Diclofenac molecule was negatively charged (Figure 4.19), while the ImZe surface was positively charged. Above this pH, uptake reduced greatly, indicating electrostatic interactions play a great role in its adsorption onto ImZe.

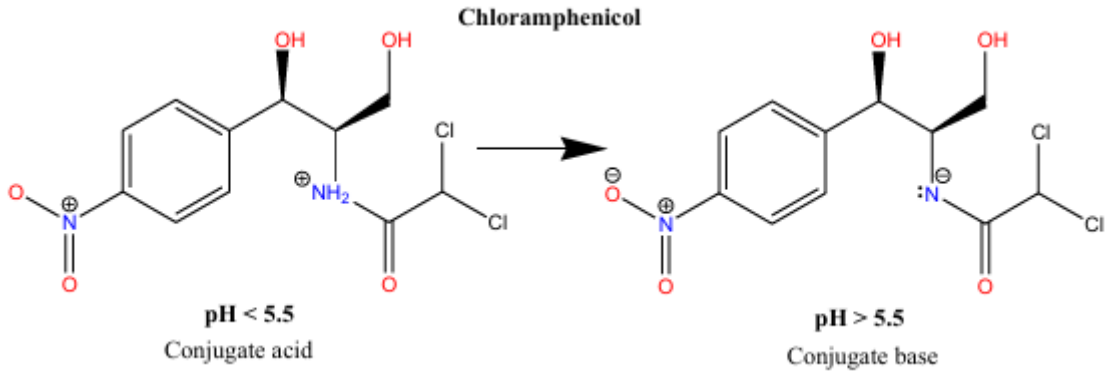

Figure 4.18: Ionic forms of Chloramphenicol based on the pKa (Babić et al., 2007)

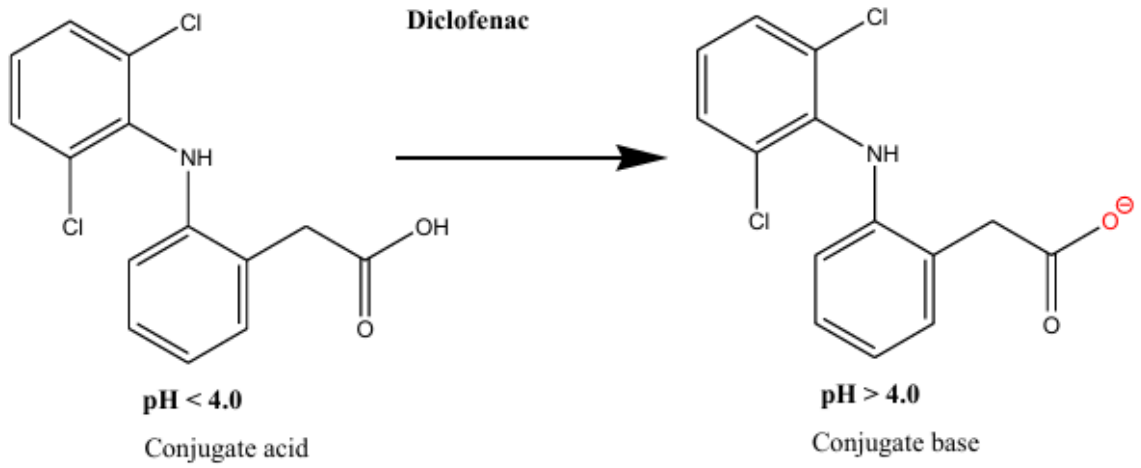

Figure 4.19: Ionic forms of Diclofenac based on the pKa (Babić et al., 2007)

Ciprofloxacin is a unique organic molecule with two pKa values i.e., 5.90 and 8.89. It therefore exhibits three different ionic forms; a cationic species pH < 5.90; zwitterionic form 5.90 < pH < 8.89and the anionic species pH > 8.89 as presented in Figure 4.20. The Zwitterionic species most readily adsorbs onto ImZe compared to the other ionic forms suggesting that electrostatic interactions play a key role in its adsorption and is complemented by mechanisms.

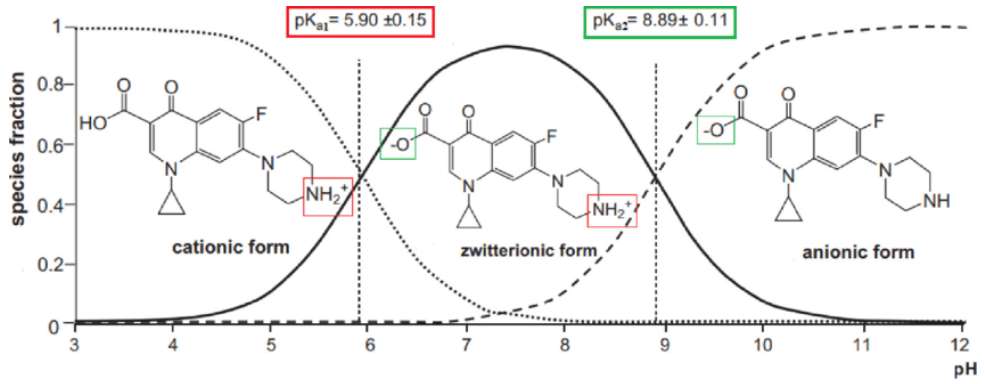

Figure 4:20: Ionic forms of Ciprofloxacin based on its pKa values (Carabineiro et al., 2012)

4.8. Comparison with other zeolitic adsorbents

A comparison with other zeolitic sorbents for the adsorption of the pollutants is compiled in Table 4.6. While all the modified zeolite variants followed the Freundlich model in describing the adsorption of Diclofenac potassium, indicating multilayer adsorption, and the acid-treated ones were equally well-described by the Brunauer-Emmett-Teller (BET) isotherm model, which assumes multilayer adsorption on a homogeneous surface without lateral interactions (Adamson & Gast, 1967). Adsorption onto natural zeolite aligned with the Dubinin-Radushkevich (D-R) isotherm model, signifying a pore-filling mechanism within micropores rather than layer-by-layer adsorption (Dubinin, 1960). Adsorption onto ImZe was best described by the Temkin model, which reflects chemisorption and surface heterogeneity. This distinctive mechanism increases ImZe's adsorption capacity by enabling stronger interactions with the surface across a range of energies, thereby contributing to its relatively high Q_{max}. Increase in the sorbent's surface area corresponds with an increase in adsorption capacity as observed by Peñafiel et al. (2024). Plasma-activated zeolite showed no significant changes in the bulk properties of the natural zeolite (Garcia et al., 2019) which explains why its adsorption capacity remained largely similar to that of the natural zeolite.

Zeolite-modified seaweed demonstrated the highest Q_{max} (93.65 mg/g) for Ciprofloxacin among the zeolite-based sorbents. This results from increased surface area, functionalization of the sorbent's surface with hydroxyl and carboxyl groups which enhance interactions with the Ciprofloxacin molecule (Mohammad B Ahmed et al., 2017). Turkey clinoptilolite followed with a capacity of 40.8 mg/g, while South African clinoptilolite exhibited the lowest adsorption at 5.48 mg/g. The adsorption mechanism of calcium-rich zeolite species primarily involves ion exchange and electrostatic interactions (Kovo et al., 2017). Coating zeolite with magnetite improves its performance by combining magnetite's magnetic properties with zeolite's inherent adsorption capabilities (Maharana & Sen, 2021). Similarly, modifying zeolite with iron enhances its adsorption by incorporating iron's magnetic properties.

Chloramphenicol adsorption onto cobalt-based zeolitic-imidazolate framework is facilitated by π-π interactions between the sorbate's phenyl groups and the sorbent's imidazole linkers, along with electrostatic attractions between cobalt and Chloramphenicol's polar groups (Jalil et al., 2024), making it to outperform ImZe, which mainly depends on electrostatic interactions. Conversely, ionic liquid-modified zeolite exhibited the lowest Q_{max} of 8.40 mg/g for Chloramphenicol, as its adsorption occurs primarily via partitioning and is limited to its surface sorption sites since accessibility of interlayer sites is reduced, resulting in a surface-dominated interaction mechanism only (Sun et al., 2017). This suggests that the adsorption of chloramphenicol onto zeolitic adsorbents is predominantly driven by an electrostatic interaction mechanisms.

Table 4.6: Comparison of zeolitic adsorbents capacity for the pollutants

Adsorbent	Surface Area (m^2/g)	pHpzc	Contact time (min)	Kinetics	pH	Temp (°C)	Conc range (mg/L)	Isotherm	Dosage (g/L)	Q_{max} (mg/g)	Reference
Diclofenac potassium											
Plasma-treated zeolite			60-2160				10-50	Freundlich	100	4.2	(Garcia et al., 2019)
Natural zeolite	41	7.6	2-120	PSO	< 6.0	20	5-50	D-R	2.0	5.1	(Peñafiel et al., 2024)
Nitric acid treated zeolite	89	4.2	2-120	PSO	< 6.0	20	5-50	BET & Freundlich	0.4	11.0	(Peñafiel et al., 2024)
Citric acid treated zeolite	61	4.9	2-120	PSO	< 6.0	20	5-50	BET & Freundlich	1.0	7.5	(Peñafiel et al., 2024)
ImZe		6.9	0-180	PSO	2-10	25-40	2-20	Temkin & Freundlich	1.0	15.70	This study
Ciprofloxacin											
Turkey clinoptilolite	990		0-60	PSO	5.5	22	20		0.25	40.8	(Genç & Dogan, 2015)

Calcium-rich clinoptilolite			5-60	PSO	5.0	10-20	15-75	Langmuir	4	17.30	(Kalebić et al., 2021)
Magnetite-coated clinoptilolite		2.0	5-60	PSO	5.0	10-20		Langmuir	4	14.25	(Kalebić et al., 2021)
Zeolite-modified seaweed	124.359	1.0	1-1440	PSO & Elovich	6.5-8.0	35-45	2.5-150	Langmuir & Freundlich	0.5	93.65	(Atugoda et al., 2021)
South-African clinoptilolite		7.5	5-45	PSO	2.0-12	25-65	2.0-10	Langmuir	2	5.48	(Ngeno et al., 2019)
ImZe		6.9	0-180	PSO	2-10	25-40	2.0-20	Temkin & Freundlich	1.0	18.43	This study
Chloramphenicol											
Cobalt-based zeolitic-imidazolate framework		3-9	0-120	PSO	3-9		0.16-1.62	Langmuir	0.1-1.0	25.73	(Jalil et al., 2024)
Ionic liquid-modified zeolite			120						50	8.40	(Sun et al., 2017)
ImZe		6.9	0-180	PSO	2-10	25-40	2.0-20	Freundlich	1.0	22.49	This study

CHAPTER FIVE

CONCLUSIONS AND RECOMMENDATIONS

5.1. Conclusions

The natural zeolite (NZe) was successfully modified with iron to form iron-modified zeolite (ImZe) as confirmed by EDS and XRD. The structural integrity of NZe was not compromised upon modification with iron as confirmed by the TGA-DTG and XRD. ImZe adsorption capacities for Chloramphenicol, Ciprofloxacin and Diclofenac were 22.49 mg/g, 18.43 mg/g and 15.70 mg/g respectively outperforming NZe's 7.71 mg/g, 4.35 mg/g and 5.19 mg/g respectively.

All the pollutants' adsorption was well described by the *pseudo*-second order kinetic model indicating chemisorption is the rate limiting step. Chloramphenicol and Ciprofloxacin were equally well described by the Elovich kinetic model indicating the ImZe's surface heterogeneity. Chloramphenicol exhibited the fastest intraparticle diffusion rate while Diclofenac showed the slowest indicating its adsorption is largely restricted to surface adsorption.

Freundlich isotherm model well described the experimental data generated from the equilibrium studies of the three pollutants. This is to indicate that the pollutants' adsorption forms a multilayer and the sorbed molecules have lateral interactions. ImZe adsorptive capacity reduced in the sequence Chloramphenicol > Ciprofloxacin > Diclofenac largely due to molecular size. Temkin model revealed Ciprofloxacin binds most strongly onto ImZe.

The adsorption of the three pharmaceutical products onto ImZe was feasible and spontaneous as characterized by negative ΔG values. The adsorption of Chloramphenicol and Diclofenac onto ImZe was an exothermic process confirmed by a negative ΔH values. Contrary,

Ciprofloxacin's adsorption was endothermic and characterized by increased randomness at the sorbent/solution interphase as evidenced by positive ΔS value.

The adsorption of these pollutants onto ImZe can be described by electrostatic interactions, hydrogen bonding and complexation with the iron species on the ImZe surface.

5.2. Recommendations

I would like to recommend:

- A competitive adsorption study involving all pharmaceuticals to demonstrate the adsorbent's selectivity in a competitive environment.
- A column adsorption study to uncover adsorption kinetics, breakthrough curves, and capacity under dynamic flow, offering practical insights for continuous flow systems.
- Batch adsorption studies of other pharmaceuticals onto ImZe to obtain essential data on adsorption capacity, equilibrium, and affinity for individual pharmaceuticals, valuable for preliminary screening.

References

Adamson, A. W., & Gast, A. P. (1967). *Physical chemistry of surfaces* (Vol. 150). Interscience publishers New York.

Adenaya, A., Zumbika, F., Rios-Quintero, R., Lara-Martin, P. A., Wurl, O., Ribas Ribas, M.,…Brinkhoff, T. (2025). Effects of Ciprofloxacin on Bacterial Abundance and Enrichments in Samples from the Sea-Surface Microlayer and Underlying Waters taken in the Southern North Sea. *Frontiers in Microbiology*, *16*, 1624041.

Adeola, A. O., Oyedotun, K. O., Waleng, N. J., Mamba, B. B., & Nomngongo, P. N. (2024). Onion skin–derived sorbent for the sequestration of methylparaben in contaminated aqueous medium. *Biomass Conversion and Biorefinery*, *14*(18), 22909-22920.

Agrawal, Y., & Shivramchandra, K. (1991). Spectrophotometric determination of diclofenac sodium in tablets. *Journal of pharmaceutical and biomedical analysis*, *9*(2), 97-100.

Ahamad, A., Madhav, S., Singh, A. K., Kumar, A., & Singh, P. (2020). Types of water pollutants: Conventional and emerging. *Sensors in Water Pollutants Monitoring: Role of Material*, 21-41.

Ahmed, M. B., Zhou, J. L., Ngo, H. H., Guo, W., Johir, M. A., Sornalingam, K.,…Kallel, M. (2017). Nano-Fe0 immobilized onto functionalized biochar gaining excellent stability during sorption and reduction of chloramphenicol via transforming to reusable magnetic composite. *Chemical engineering journal*, *322*, 571-581.

Ahmed, M. B., Zhou, J. L., Ngo, H. H., Guo, W., Thomaidis, N. S., & Xu, J. (2017). Progress in the biological and chemical treatment technologies for emerging contaminant removal from wastewater: a critical review. *Journal of hazardous materials*, *323*, 274-298.

Akhtar, M. S., Ali, S., & Zaman, W. (2024). Innovative adsorbents for pollutant removal: exploring the latest research and applications. *Molecules*, *29*(18), 4317.

Al-Khodir, F. A., & Refat, M. S. (2016). Synthesis, spectroscopic, thermal and anticancer studies of metal-antibiotic chelations: Ca (II), Fe (III), Pd (II) and Au (III) chloramphenicol complexes. *Journal of Molecular Structure*, *1119*, 157-166.

Al-Maliky, E. A., Gzar, H. A., & Al-Azawy, M. G. (2021). Determination of point of zero charge (PZC) of concrete particles adsorbents. IOP conference series: materials science and engineering,

Al-Sehemi, A. G., Irfan, A., Alrumman, S. A., & Hesham, A. (2016). Antibacterial activities, DFT and QSAR studies of quinazolinone compounds. *Bulletin of the Chemical Society of Ethiopia*, *30*(2), 307-316.

Alaqarbeh, M. (2021). Adsorption phenomena: definition, mechanisms, and adsorption types: short review. *RHAZES: Green and Applied Chemistry*, *13*, 43-51.

Alberts, B., Bray, D., Hopkin, K., Johnson, A. D., Lewis, J., Raff, M.,…Walter, P. (2015). *Essential cell biology*. Garland Science.

Alliance, A. I. (2021). AMR Industry Alliance Antibiotic Discharge Targets List of Predicted No-Effect Concentrations (PNECs). 2018. *Available on: https://www. amrindustryalliance. org/wp-content/uploads/2018/09/AMR_Industry_Alliance_List-of-Predicted-No-Effect-Concentrations-PNECs. pdf [Last accessed: 2021 Apr 5]*.

Altalhi, T. A., Ibrahim, M. M., Mersal, G. A., Mahmoud, M., Kumeria, T., El-Desouky, M. G.,…El-Bindary, M. A. (2022). Adsorption of doxorubicin hydrochloride onto thermally treated green adsorbent: equilibrium, kinetic and thermodynamic studies. *Journal of Molecular Structure*, *1263*, 133160.

Altman, R., Bosch, B., Brune, K., Patrignani, P., & Young, C. (2015). Advances in NSAID development: evolution of diclofenac products using pharmaceutical technology. *Drugs*, *75*(8), 859-877.

Alver, B., Sakizci, M., & Yörükoğullari, E. (2010). Investigation of clinoptilolite rich natural zeolites from Turkey: a combined XRF, TG/DTG, DTA and DSC study. *Journal of Thermal Analysis and Calorimetry*, *100*(1), 19-26.

Anjali, R., & Shanthakumar, S. (2024). Optimization, kinetics, and pathways of pharmaceutical pollutant degradation using solar Fenton technique. *Environmental monitoring and assessment*, *196*(7), 674.

Arman, N. Z., Salmiati, S., Aris, A., Salim, M. R., Nazifa, T. H., Muhamad, M. S., & Marpongahtun, M. (2021). A review on emerging pollutants in the water environment: Existences, health effects and treatment processes. *Water*, *13*(22), 3258.

Armbruster, T. (2001). Clinoptilotite-heulandite: applications and basic research. In *Studies in surface science and catalysis* (Vol. 135, pp. 13-27). Elsevier.

Atkins, P. W., De Paula, J., & Keeler, J. (2023). *Atkins' physical chemistry*. Oxford university press.

Atugoda, T., Gunawardane, C., Ahmad, M., & Vithanage, M. (2021). Mechanistic interaction of ciprofloxacin on zeolite modified seaweed (Sargassum crassifolium) derived biochar: Kinetics, isotherm and thermodynamics. *Chemosphere*, *281*, 130676.

Aus der Beek, T., Weber, F. A., Bergmann, A., Hickmann, S., Ebert, I., Hein, A., & Küster, A. (2016). Pharmaceuticals in the environment—Global occurrences and perspectives. *Environmental toxicology and chemistry*, *35*(4), 823-835.

Avcı, A., İnci, İ., & Baylan, N. (2019). A comparative adsorption study with various adsorbents for the removal of ciprofloxacin hydrochloride from water. *Water, Air, & Soil Pollution*, *230*, 1-9.

Ayawei, N., Ebelegi, A. N., & Wankasi, D. (2017). Modelling and interpretation of adsorption isotherms. *Journal of chemistry*, *2017*.

Babić, S., Horvat, A. J., Pavlović, D. M., & Kaštelan-Macan, M. (2007). Determination of pKa values of active pharmaceutical ingredients. *TrAC Trends in Analytical Chemistry*, *26*(11), 1043-1061.

Baker, R. W. (2023). *Membrane technology and applications*. John Wiley & Sons.

Banham, D., & Ye, S. (2017). Current status and future development of catalyst materials and catalyst layers for proton exchange membrane fuel cells: an industrial perspective. *ACS Energy Letters*, *2*(3), 629-638.

Barlokova, D. (2008). Natural zeolites in the water treatment process. *Slovak J. Civ. Eng*, *2*, 8-12.

Barracco, F., Parisi, E., Pipitone, G., Simone, E., Bensaid, S., & Fino, D. (2024). Valorization of pyrolytic plastic-derived char for adsorption of wastewater contaminants: A kinetic and thermodynamic investigation. *International Journal of Environmental Science and Technology*, *21*(9), 6513-6530.

Baste, I. A. (2021). Making peace with nature: a scientific blueprint to tackle the climate, biodiversity and pollution emergencies.

Bavumiragira, J. P., & Yin, H. (2022). Fate and transport of pharmaceuticals in water systems: A processes review. *Science of the Total Environment*, *823*, 153635.

Bayrakci, M., Keskinates, M., & Yilmaz, B. (2021). Antibacterial, thermal decomposition and in vitro time release studies of chloramphenicol from novel PLA and PVA nanofiber mats. *Materials Science and Engineering: C*, *122*, 111895.

Becke, A. D. (1993). Density-functional thermochemistry. III. The role of exact exchange. *The Journal of chemical physics*, *98*(7), 5648-5652.

Bencheqroun, Z., Sahin, N. E., Soares, O. S., Pereira, M. F., Zaitan, H., Nawdali, M.,…Neves, I. C. (2022). Fe (III)-exchanged zeolites as efficient electrocatalysts for Fenton-like oxidation of dyes in aqueous phase. *Journal of Environmental Chemical Engineering*, *10*(3), 107891.

Berthomieu, C., & Hienerwadel, R. (2009). Fourier transform infrared (FTIR) spectroscopy. *Photosynthesis research*, *101*(2), 157-170.

Binh, Q. A., & Kajitvichyanukul, P. (2019). Adsorption mechanism of dichlorvos onto coconut fibre biochar: the significant dependence of H-bonding and the pore-filling mechanism. *Water Science and Technology*, *79*(5), 866-876.

Bio, S., & Nunes, B. (2020). Acute effects of diclofenac on zebrafish: Indications of oxidative effects and damages at environmentally realistic levels of exposure. *Environmental Toxicology and Pharmacology*, *78*, 103394.

Boroń, P., Chmielarz, L., Gurgul, J., Łątka, K., Shishido, T., Krafft, J.-M., & Dzwigaj, S. (2013). BEA zeolite modified with iron as effective catalyst for N2O decomposition and selective reduction of NO with ammonia. *Applied Catalysis B: Environmental*, *138*, 434-445.

Bottom, R. (2008). Thermogravimetric analysis. *Principles and applications of thermal analysis*, 87-118.

Bottoni, P., Caroli, S., & Caracciolo, A. B. (2010). Pharmaceuticals as priority water contaminants. *Toxicological & Environmental Chemistry*, *92*(3), 549-565. https://doi.org/10.1080/02772241003614320

Bujdák, J. (2020). Adsorption kinetics models in clay systems. The critical analysis of pseudo-second order mechanism. *Applied Clay Science*, *191*, 105630.

Cadar, O., Senila, M., Hoaghia, M.-A., Scurtu, D., Miu, I., & Levei, E. A. (2020). Effects of thermal treatment on natural clinoptilolite-rich zeolite behavior in simulated biological fluids. *Molecules*, *25*(11), 2570.

Cao, D., Shen, Y., Huang, Y., Chen, B., Chen, Z., Ai, J.,…Wei, Q. (2021). Levofloxacin versus ciprofloxacin in the treatment of urinary tract infections: evidence-based analysis. *Frontiers in pharmacology*, *12*, 658095.

Cao, R., Li, J., Liao, Q., Shao, M., Zhang, Q., Zhang, Y.,…Xu, Z. (2025). Enhanced Bioactivity of Natural Products by Halogenation: A Database Survey and Quantum Chemistry Calculation Study. *Journal of Medicinal Chemistry*, *68*(10), 10486-10496.

Capodaglio, A. G., Bojanowska-Czajka, A., & Trojanowicz, M. (2018). Comparison of different advanced degradation processes for the removal of the pharmaceutical compounds diclofenac and carbamazepine from liquid solutions. *Environmental Science and Pollution Research*, *25*, 27704-27723.

Carabineiro, S., Thavorn-Amornsri, T., Pereira, M., Serp, P., & Figueiredo, J. (2012). Comparison between activated carbon, carbon xerogel and carbon nanotubes for the adsorption of the antibiotic ciprofloxacin. *Catalysis today*, *186*(1), 29-34.

Cardoso-Vera, J. D., Islas-Flores, H., SanJuan-Reyes, N., Montero-Castro, E. I., Galar-Martínez, M., García-Medina, S.,…Gómez-Oliván, L. M. (2017). Comparative study

of diclofenac-induced embryotoxicity and teratogenesis in Xenopus laevis and Lithobates catesbeianus, using the frog embryo teratogenesis assay: Xenopus (FETAX). *Science of the Total Environment*, *574*, 467-475.

Caricato, M., Frisch, M. J., Hiscocks, J., & Frisch, M. J. (2009). *Gaussian 09: IOps Reference*. Gaussian Wallingford, CT, USA.

Carro, S., Cabello-Alvarado, C. J., Andrade-Guel, M., Aguilar-Márquez, J. C., García-Morán, P. R., Avila-Orta, C. A., & Quiñones-Jurado, Z. V. (2024). Adsorption Study of Uremic Toxins (Urea, Creatinine, and Uric Acid) Using Modified Clinoptilolite. *Coatings*, *14*(9), 1099.

Cejka, J., van Bekkum, H., Corma, A., & Schueth, F. (2007). *Introduction to zeolite molecular sieves* (Vol. 168). Elsevier.

Cen, W., Wang, B., Huang, Y., Ye, S., Ma, J., Xu, R.,…Lyu, T. (2025). Tailoring mesoporous Y-Zeolite molecular sieve for effective removal of micropollutants from water. *ACS ES&T Water*, *5*(3), 1373-1383.

Chávez Rivas, F., Rodríguez-Iznaga, I., Berlier, G., Tito Ferro, D., Concepción-Rosabal, B., & Petranovskii, V. (2019). Fe speciation in iron modified natural zeolites as sustainable environmental catalysts. *Catalysts*, *9*(10), 866.

Chen, D., Delmas, J.-M., Hurtaud-Pessel, D., & Verdon, E. (2020). Development of a multi-class method to determine nitroimidazoles, nitrofurans, pharmacologically active dyes and chloramphenicol in aquaculture products by liquid chromatography-tandem mass spectrometry. *Food Chemistry*, *311*, 125924.

Chen, G., den Braver, M. W., van Gestel, C. A., van Straalen, N. M., & Roelofs, D. (2015). Ecotoxicogenomic assessment of diclofenac toxicity in soil. *Environmental Pollution*, *199*, 253-260.

Chen, H.-F., Lin, Y.-J., Chen, B.-H., Yoshiyuki, I., Liou, S. Y.-H., & Huang, R.-T. (2018). A further investigation of NH4+ removal mechanisms by using natural and synthetic zeolites in different concentrations and temperatures. *Minerals*, *8*(11), 499.

Cherik, D., Benali, M., & Louhab, K. (2015). Occurrence, ecotoxicology, removal of diclofenac by adsorption on activated carbon and biodegradation and its effect on bacterial community: A review. *World Scientific News*(10), 116-144.

Chu, K. H. (2021). Revisiting the Temkin isotherm: dimensional inconsistency and approximate forms. *Industrial & Engineering Chemistry Research*, *60*(35), 13140-13147.

Chu, K. H., Hashim, M. A., da Costa Santos, Y. T., Debord, J., Harel, M., & Bollinger, J.-C. (2024). The Redlich–Peterson isotherm for aqueous phase adsorption: Pitfalls in data analysis and interpretation. *Chemical Engineering Science*, *285*, 119573.

Chulliyil, H. M., Hamdani, I. R., Ahmad, A., Al Shoaibi, A., & Chandrasekar, S. (2024). Enhanced moisture adsorption of activated carbon through surface modification. *Results in Surfaces and Interfaces*, *14*, 100170.

Coldham, T., & Ivey, J. (2020). A visit to the Indonesian opal fields in 2019—Opal types, mining and treatments, Part 1. *Aust. Gemmol*, *27*, 199-213.

Crini, G., & Lichtfouse, E. (2019). Advantages and disadvantages of techniques used for wastewater treatment. *Environmental Chemistry Letters*, *17*, 145-155.

Dai, C.-m., Geissen, S.-U., Zhang, Y.-l., Zhang, Y.-j., & Zhou, X.-f. (2011). Selective removal of diclofenac from contaminated water using molecularly imprinted polymer microspheres. *Environmental Pollution*, *159*(6), 1660-1666.

Dai, J., Qin, L., Zhang, R., Xie, A., Chang, Z., Tian, S.,…Yan, Y. (2018). Sustainable bovine bone-derived hierarchically porous carbons with excellent adsorption of antibiotics: Equilibrium, kinetic and thermodynamic investigation. *Powder Technology*, *331*, 162-170.

de Franco, M. A. E., de Carvalho, C. B., Bonetto, M. M., de Pelegrini Soares, R., & Féris, L. A. (2018). Diclofenac removal from water by adsorption using activated carbon in batch mode and fixed-bed column: isotherms, thermodynamic study and breakthrough curves modeling. *Journal of Cleaner Production*, *181*, 145-154.

de Souza, R. M., Quesada, H. B., Cusioli, L. F., Fagundes-Klen, M. R., & Bergamasco, R. (2021). Adsorption of non-steroidal anti-inflammatory drug (NSAID) by agro-industrial by-product with chemical and thermal modification: Adsorption studies and mechanism. *Industrial Crops and Products*, *161*, 113200.

Deng, Y., & Zhao, R. (2015). Advanced oxidation processes (AOPs) in wastewater treatment. *Current pollution reports*, *1*(3), 167-176.

Dionisiou, N. S., Matsi, T., & Misopolinos, N. D. (2013). Removal of boron by surfactant modified zeolitic tuff from northeastern Greece. *Journal of Agricultural Science*, *5*(12), 94.

Dubinin, M. (1960). The potential theory of adsorption of gases and vapors for adsorbents with energetically nonuniform surfaces. *Chem Rev*, *60*(2), 235-241.

Ebele, A. J., Abdallah, M. A.-E., & Harrad, S. (2017). Pharmaceuticals and personal care products (PPCPs) in the freshwater aquatic environment. *Emerging contaminants*, *3*(1), 1-16.

Ebert, I., Bachmann, J., Kühnen, U., Küster, A., Kussatz, C., Maletzki, D., & Schlüter, C. (2011). Toxicity of the fluoroquinolone antibiotics enrofloxacin and ciprofloxacin to photoautotrophic aquatic organisms. *Environmental toxicology and chemistry*, *30*(12), 2786-2792.

Elovich, S. Y., & Larinov, O. (1962). Theory of adsorption from solutions of non electrolytes on solid (I) equation adsorption from solutions and the analysis of its simplest form,(II) verification of the equation of adsorption isotherm from solutions. *Izv. Akad. Nauk. SSSR, Otd. Khim. Nauk*, *2*(2), 209-216.

Eneş, D., Daştan, K., Kaplan, O., Çelebier, M., & Dogan, A. (2024). A Comprehensive Examination of UV-VIS Spectrophotometric Methods in Pharmaceutical Analysis Between 2015-2023. *Combinatorial Chemistry & High Throughput Screening*.

Fernandes, S. P., Fonseca, V. F., Romero, V., Duarte, I. A., Freitas, A., Barbosa, J.,…Espiña, B. (2021). Study on the efficiency of a covalent organic framework as adsorbent for the screening of pharmaceuticals in estuary waters. *Chemosphere*, *278*, 130364.

Flanigen, E. M., Khatami, H., & Szymanski, H. A. (1971). Infrared structural studies of zeolite frameworks. In. ACS Publications.

Freundlich, H. (1907). Ueber die adsorption in loesungen. *Z Phys Chem*, *57*, 385-470.

Garcia, J. J. M., Nuñez, J. A. P., Salapare III, H. S., & Vasquez Jr, M. R. (2019). Adsorption of diclofenac sodium in aqueous solution using plasma-activated natural zeolites. *Results in Physics*, *15*, 102629.

Genç, N., & Dogan, E. C. (2015). Adsorption kinetics of the antibiotic ciprofloxacin on bentonite, activated carbon, zeolite, and pumice. *Desalination and Water Treatment*, *53*(3), 785-793.

Goldstein, J. I., Newbury, D. E., Michael, J. R., Ritchie, N. W., Scott, J. H. J., & Joy, D. C. (2017). *Scanning electron microscopy and X-ray microanalysis*. springer.

Gomez Cortes, L., Marinov, D., Sanseverino, I., Navarro Cuenca, A., Niegowska, M., Porcel Rodriguez, E.,…Lettieri, T. (2022). Selection of substances for the 4th Watch List under the Water Framework Directive. *Publications Office of the European Union: Luxembourg*.

Gonzalez Pena, O. I., López Zavala, M. Á., & Cabral Ruelas, H. (2021). Pharmaceuticals market, consumption trends and disease incidence are not driving the pharmaceutical research on water and wastewater. *International journal of environmental research and public health*, *18*(5), 2532.

Gottardi, G., & Galli, E. (2012). *Natural zeolites* (Vol. 18). Springer Science & Business Media.

Grabowski, S. J. (2006). *Hydrogen bonding: new insights* (Vol. 3). Springer.

Gu, X., Xu, Z., Gu, L., Xu, H., Han, F., Chen, B., & Pan, X. (2021). Preparation and antibacterial properties of gold nanoparticles: A review. *Environmental Chemistry Letters*, *19*(1), 167-187.

Guida, S., Potter, C., Jefferson, B., & Soares, A. (2020). Preparation and evaluation of zeolites for ammonium removal from municipal wastewater through ion exchange process. *Scientific reports*, *10*(1), 12426.

Guiloski, I. C., Piancini, L. D. S., Dagostim, A. C., de Morais Calado, S. L., Fávaro, L. F., Boschen, S. L.,…de Assis, H. C. S. (2017). Effects of environmentally relevant concentrations of the anti-inflammatory drug diclofenac in freshwater fish Rhamdia quelen. *Ecotoxicology and environmental safety*, *139*, 291-300.

Gupta, S., Mittal, Y., Panja, R., Prajapati, K. B., & Yadav, A. K. (2021). Conventional wastewater treatment technologies. *Current developments in biotechnology and bioengineering*, 47-75.

Guyon, A., Smith, K. F., Charry, M. P., Champeau, O., & Tremblay, L. A. (2018). Effects of chronic exposure to benzophenone and diclofenac on DNA methylation levels and reproductive success in a marine copepod. *Journal of Xenobiotics*, *8*(1), 7674.

Hammad, H. M., Zia, F., Bakhat, H. F., Fahad, S., Ashraf, M. R., Wilkerson, C. J.,…Shahid, M. (2018). Uptake and toxicological effects of pharmaceutical active compounds on maize. *Agriculture, Ecosystems & Environment*, *258*, 143-148.

Han, R., Wang, Y., Sun, Q., Wang, L., Song, J., He, X., & Dou, C. (2010). Malachite green adsorption onto natural zeolite and reuse by microwave irradiation. *Journal of Hazardous Materials*, *175*(1-3), 1056-1061.

Hassan Ibrahim, A. H., Cihangir, N., Idil, N., & Aracagök, Y. D. (2024). Adsorption of azo dye by biomass and immobilized Yarrowia lipolytica; equilibrium, kinetic and thermodynamic studies. *World Journal of Microbiology and Biotechnology*, *40*(5), 140.

Herrero-Villar, M., Delepoulle, É., Suárez-Regalado, L., Solano-Manrique, C., Juan-Sallés, C., Iglesias-Lebrija, J. J.,…Mateo, R. (2021). First diclofenac intoxication in a wild avian scavenger in Europe. *Science of the Total Environment*, *782*, 146890.

Hong, H., Liu, C., & Li, Z. (2023). Chemistry of soil-type dependent soil matrices and its influence on behaviors of pharmaceutical compounds (PCs) in soils. *Heliyon*, *9*(12).

Huang, D., Wu, J., Wang, L., Liu, X., Meng, J., Tang, X.,…Xu, J. (2019). Novel insight into adsorption and co-adsorption of heavy metal ions and an organic pollutant by

magnetic graphene nanomaterials in water. *Chemical engineering journal*, *358*, 1399-1409.

Iqbal, M. S., Zhu, H., & Xi, Y.-L. (2022). Effect of chloramphenicol on the life table demography of Brachionus calyciflorus (Rotifera): A multigenerational study. *Ecotoxicology and environmental safety*, *237*, 113525.

Ivanova, I. I., & Knyazeva, E. E. (2013). Micro–mesoporous materials obtained by zeolite recrystallization: synthesis, characterization and catalytic applications. *Chemical Society Reviews*, *42*(9), 3671-3688.

Izoitko, A., Koveza, V., & Potapenko, O. (2025). Effects of ZSM-5 Modification with Manganese and Iron Cations on n-Dodecane/2-Methylthiophene Conversion Pathway. *Petroleum Chemistry*, 1-10.

Jahani, F., Sadeghi, R., & Shakeri, M. (2023). Ultrasonic-assisted chemical modification of a natural clinoptilolite zeolite: Enhanced ammonium adsorption rate and resistance to disturbing ions. *Journal of Environmental Chemical Engineering*, *11*(5), 110354.

Jalil, A. A., Rajendran, S., & Vo, D.-V. N. (2024). Adsorption of chloramphenicol onto cobalt-based zeolitic-imidazolate framework (Co-ZIF-67). *INGENIARE-Revista Chilena de Ingeniería*, *32*.

Jannat Abadi, M., Nouri, S., Zhiani, R., Heydarzadeh, H., & Motavalizadehkakhky, A. (2019). Removal of tetracycline from aqueous solution using Fe-doped zeolite. *International journal of industrial chemistry*, *10*(4), 291-300.

Jemutai-Kimosop, S., Okello, V. A., Shikuku, V. O., Orata, F., & Getenga, Z. M. (2022). Synthesis of mesoporous akaganeite functionalized maize cob biochar for adsorptive abatement of carbamazepine: Kinetics, isotherms, and thermodynamics. *Cleaner materials*, *5*, 100104.

Jiang, N., Shang, R., Heijman, S. G., & Rietveld, L. C. (2018). High-silica zeolites for adsorption of organic micro-pollutants in water treatment: A review. *Water research*, *144*, 145-161.

Jiménez-Castañeda, M. E., & Medina, D. I. (2017). Use of surfactant-modified zeolites and clays for the removal of heavy metals from water. *Water*, *9*(4), 235.

K'oreje, K., Vergeynst, L., Ombaka, D., De Wispelaere, P., Okoth, M., Van Langenhove, H., & Demeestere, K. (2016). Occurrence patterns of pharmaceutical residues in wastewater, surface water and groundwater of Nairobi and Kisumu city, Kenya. *Chemosphere*, *149*, 238-244.

Kairigo, P., Ngumba, E., Sundberg, L.-R., Gachanja, A., & Tuhkanen, T. (2020). Occurrence of antibiotics and risk of antibiotic resistance evolution in selected Kenyan

wastewaters, surface waters and sediments. *Science of the Total Environment*, *720*, 137580.

Kalebić, B., Pavlović, J., Dikić, J., Rečnik, A., Gyergyek, S., Škoro, N., & Rajić, N. (2021). Use of natural clinoptilolite in the preparation of an efficient adsorbent for ciprofloxacin removal from aqueous media. *Minerals*, *11*(5), 518.

Kalyva, M. (2017). Fate of pharmaceuticals in the environment-A review.

Kathuria, J., Kaur, J., Babu, N. J., & Arora, M. (2023). Water remediation for pharmaceutical and personal care products (PPCPs) with metal organic frameworks: A review. *Results in Chemistry*, *6*, 101223.

Kelly, K. R., & Brooks, B. W. (2018). Global aquatic hazard assessment of ciprofloxacin: exceedances of antibiotic resistance development and ecotoxicological thresholds. *Progress in molecular biology and translational science*, *159*, 59-77.

Khalfaoui, A., Benalia, A., Selama, Z., Hammoud, A., Derbal, K., Panico, A., & Pizzi, A. (2024). Removal of chromium (VI) from water using orange peel as the biosorbent: experimental, modeling, and kinetic studies on adsorption isotherms and chemical structure. *Water*, *16*(5), 742.

Khasawneh, O. F. S., & Palaniandy, P. (2021). Occurrence and removal of pharmaceuticals in wastewater treatment plants. *Process Safety and Environmental Protection*, *150*, 532-556.

Kianfar, E., & Mazaheri, H. (2020). Methanol to gasoline: a sustainable transport fuel. *Advances in chemistry research*, 66.

Kikuvi, J., Mutua, G., Gembo, R. O., & Orata, F. (2025). Kinetic, isothermal and thermodynamic study on the adsorptive removal of chloramphenicol from water by iron-impregnated Kenyan clinoptilolite zeolite. *Reaction Kinetics, Mechanisms and Catalysis*, 1-23.

Kimosop, S. J., Getenga, Z. M., Orata, F., Okello, V., & Cheruiyot, J. (2016). Residue levels and discharge loads of antibiotics in wastewater treatment plants (WWTPs), hospital lagoons, and rivers within Lake Victoria Basin, Kenya. *Environmental Monitoring and Assessment*, *188*, 1-9.

Kiprono, P., Kiptoo, J., Nyawade, E., & Ngumba, E. (2023). Iron functionalized silica particles as an ingenious sorbent for removal of fluoride from water. *Scientific reports*, *13*(1), 8018.

Koek, M. M., Jellema, R. H., van der Greef, J., Tas, A. C., & Hankemeier, T. (2011). Quantitative metabolomics based on gas chromatography mass spectrometry: status and perspectives. *Metabolomics*, *7*, 307-328.

Kohay, H., & Gazit, O. M. (2024). Regulating adsorption-desorption through controlled modification of the 2D pores in layered double hydroxides. *Surfaces and Interfaces*, *44*, 103810.

Komvokis, V., Tan, L. X. L., Clough, M., Pan, S. S., & Yilmaz, B. (2016). Zeolites in fluid catalytic cracking (FCC). In *Zeolites in Sustainable Chemistry: Synthesis, Characterization and Catalytic Applications* (pp. 271-297). Springer.

Koohsaryan, E., Anbia, M., & Maghsoodlu, M. (2020). Application of zeolites as non-phosphate detergent builders: A review. *Journal of Environmental Chemical Engineering*, *8*(5), 104287.

Kosmulski, M. (2009). *Surface charging and points of zero charge*. CRC press.

Kosmulski, M. (2016). Isoelectric points and points of zero charge of metal (hydr) oxides: 50 years after Parks' review. *Advances in colloid and interface science*, *238*, 1-61.

Kovo, A., Abdulkareem, A., Ogunmola, T., Longtong, D., Isah, A. G., & Eyibio, U. P. (2017). Development of Calcium Rich Zeolite from Ahoko Kaolin for the Adsorption Study of Methylene Blue.

Kragović, M., Daković, A., Marković, M., Krstić, J., Gatta, G. D., & Rotiroti, N. (2013). Characterization of lead sorption by the natural and Fe (III)-modified zeolite. *Applied Surface Science*, *283*, 764-774.

Kragović, M., Daković, A., Sekulić, Ž., Trgo, M., Ugrina, M., Perić, J., & Gatta, G. D. (2012). Removal of lead from aqueous solutions by using the natural and Fe (III)-modified zeolite. *Applied Surface Science*, *258*(8), 3667-3673.

Kragović, M., Stojmenović, M., Petrović, J., Loredo, J., Pašalić, S., Nedeljković, A., & Ristović, I. (2019). Influence of alginate encapsulation on point of zero charge (pHpzc) and thermodynamic properties of the natural and Fe (III)-modified zeolite. *Procedia Manufacturing*, *32*, 286-293.

Kümmerer, K. (2009). The presence of pharmaceuticals in the environment due to human use–present knowledge and future challenges. *Journal of environmental management*, *90*(8), 2354-2366.

Kumon, A., Abidin, Z., & Matsue, N. (2017). Synthesis of iron substituted zeolite with Na-P1 framework. *Journal of Porous Materials*, *24*, 1061-1068.

Küster, A., & Adler, N. (2014). Pharmaceuticals in the environment: scientific evidence of risks and its regulation. *Philosophical Transactions of the Royal Society B: Biological Sciences*, *369*(1656), 20130587.

Lach, J. (2019). Adsorption of chloramphenicol on commercial and modified activated carbons. *Water*, *11*(6), 1141.

Lalley, J., Han, C., Li, X., Dionysiou, D. D., & Nadagouda, M. N. (2016). Phosphate adsorption using modified iron oxide-based sorbents in lake water: kinetics, equilibrium, and column tests. *Chemical engineering journal*, *284*, 1386-1396.

Langmuir, I. (1916). The constitution and fundamental properties of solids and liquids. Part I. Solids. *Journal of the American Chemical Society*, *38*(11), 2221-2295.

Le Page, G., Gunnarsson, L., Snape, J., & Tyler, C. R. (2017). Integrating human and environmental health in antibiotic risk assessment: a critical analysis of protection goals, species sensitivity and antimicrobial resistance. *Environment international*, *109*, 155-169.

Li, J., Corma, A., & Yu, J. (2015). Synthesis of new zeolite structures. *Chemical Society Reviews*, *44*(20), 7112-7127.

Li, Y., Li, L., & Yu, J. (2017). Applications of zeolites in sustainable chemistry. *Chem*, *3*(6), 928-949.

Liao, P., Zhan, Z., Dai, J., Wu, X., Zhang, W., Wang, K., & Yuan, S. (2013). Adsorption of tetracycline and chloramphenicol in aqueous solutions by bamboo charcoal: a batch and fixed-bed column study. *Chemical engineering journal*, *228*, 496-505.

Limlamthong, M., Tesana, S., & Yip, A. C. (2020). Metal encapsulation in zeolite particles: a rational design of zeolite-supported catalyst with maximum site activity. *Advanced Powder Technology*, *31*(3), 1274-1279.

Liu, B., Luo, H., Rong, H., Zeng, X., Wu, K., Chen, Z.,…Xu, D. (2019). Temperature-induced adsorption and desorption of phosphate on poly (acrylic acid-co-N-[3-(dimethylamino) propyl] acrylamide) hydrogels in aqueous solutions. *Desalin. Water Treat*, *160*, 260-267.

Lonappan, L., Rouissi, T., Brar, S. K., Verma, M., & Surampalli, R. Y. (2018). An insight into the adsorption of diclofenac on different biochars: Mechanisms, surface chemistry, and thermodynamics. *Bioresource technology*, *249*, 386-394.

Loos, G., Scheers, T., Van Eyck, K., Van Schepdael, A., Adams, E., Van der Bruggen, B.,…Dewil, R. (2018). Electrochemical oxidation of key pharmaceuticals using a boron doped diamond electrode. *Separation and Purification Technology*, *195*, 184-191.

Lothenbach, B., Durdzinski, P., & De Weerdt, K. (2016). Thermogravimetric analysis. *A practical guide to microstructural analysis of cementitious materials*, *1*, 177-211.

Lu, J., Ji, Y., Chovelon, J.-M., & Lu, J. (2021). Fluoroquinolone antibiotics sensitized photodegradation of isoproturon. *Water research*, *198*, 117136.

Luo, L., Gu, C., Li, M., Zheng, X., & Zheng, F. (2018). Determination of residual 4-nitrobenzaldehyde in chloramphenicol and its pharmaceutical formulation by HPLC with UV/Vis detection after derivatization with 3-nitrophenylhydrazine. *Journal of pharmaceutical and biomedical analysis*, *156*, 307-312.

Luo, Y., Guo, W., Ngo, H. H., Nghiem, L. D., Hai, F. I., Zhang, J.,…Wang, X. C. (2014). A review on the occurrence of micropollutants in the aquatic environment and their fate and removal during wastewater treatment. *Science of the Total Environment*, *473*, 619-641.

Madhav, S., Ahamad, A., Singh, A. K., Kushawaha, J., Chauhan, J. S., Sharma, S., & Singh, P. (2020). Water pollutants: sources and impact on the environment and human health. *Sensors in Water Pollutants Monitoring: Role of Material*, 43-62.

Madikizela, L. M., & Chimuka, L. (2017). Occurrence of naproxen, ibuprofen, and diclofenac residues in wastewater and river water of KwaZulu-Natal Province in South Africa. *Environmental Monitoring and Assessment*, *189*, 1-12.

Maharana, M., & Sen, S. (2021). Magnetic zeolite: A green reusable adsorbent in wastewater treatment. *Materials today: proceedings*, *47*, 1490-1495.

Malhotra, M., Suresh, S., & Garg, A. (2018). Tea waste derived activated carbon for the adsorption of sodium diclofenac from wastewater: adsorbent characteristics, adsorption isotherms, kinetics, and thermodynamics. *Environmental Science and Pollution Research*, *25*, 32210-32220.

Mansouri, N., Rikhtegar, N., Panahi, H. A., Atabi, F., & Shahraki, B. K. (2013). Porosity, characterization and structural properties of natural zeolite-clinoptilolite-as a sorbent. *Environment Protection Engineering*, *39*(1), 139-152.

Massano, M., Salomone, A., Gerace, E., Alladio, E., Vincenti, M., & Minella, M. (2023). Wastewater surveillance of 105 pharmaceutical drugs and metabolites by means of ultra-high-performance liquid-chromatography-tandem high resolution mass spectrometry. *Journal of Chromatography A*, *1693*, 463896.

Mathur, S., Pareek, S., & Shrivastava, D. (2022). Nanofertilizers for development of sustainable agriculture. *Communications in Soil Science and Plant Analysis*, *53*(16), 1999-2016.

Maulana, I., & Takahashi, F. (2018). Cyanide removal study by raw and iron-modified synthetic zeolites in batch adsorption experiments. *Journal of water process engineering*, *22*, 80-86.

Mebi, C. A. (2011). DFT study on structure, electronic properties, and reactivity of cis-isomers of [(NC 5 H 4-S) 2 Fe (CO) 2]. *Journal of Chemical Sciences*, *123*, 727-731.

Meng, X., Liu, Z., Deng, C., Zhu, M., Wang, D., Li, K.,…Jiang, M. (2016). Microporous nano-MgO/diatomite ceramic membrane with high positive surface charge for tetracycline removal. *Journal of hazardous materials*, *320*, 495-503.

Mockovčiaková, A., Orolínová, Z., Matik, M., Hudec, P., & Kmecová, E. (2006). Iron oxide contribution to the modification of natural zeolite. *Acta Montan. Slovaca*, *11*, 353-357.

Mohammed, A., & Abdullah, A. (2018). Scanning electron microscopy (SEM): A review. Proceedings of the 2018 international conference on hydraulics and pneumatics—HERVEX, Băile Govora, Romania,

Movasaghi, Z., Yan, B., & Niu, C. (2019). Adsorption of ciprofloxacin from water by pretreated oat hulls: Equilibrium, kinetic, and thermodynamic studies. *Industrial Crops and Products*, *127*, 237-250.

Muir, B., Wołowiec, M., Bajda, T., Nowak, P., & Czupryński, P. (2017). The removal of organic compounds by natural and synthetic surface-functionalized zeolites: A mini-review. *Mineralogia*, *48*.

Muñoz, E. C., Tseberlidis, G., Husien, A. H., Binetti, S., & Gosetti, F. (2025). Identification and ecotoxicity of the diclofenac transformation products formed by photolytic and photocatalytic processes. *Environmental Science and Pollution Research*, *32*(21), 12700-12712.

Musah, M., Azeh, Y., Mathew, J. T., Umar, M. T., Abdulhamid, Z., & Muhammad, A. I. (2022). Adsorption kinetics and isotherm models: a review. *CaJoST*, *4*(1), 20-26.

Naderi, M. (2015). Surface area: brunauer–emmett–teller (BET). In *Progress in filtration and separation* (pp. 585-608). Elsevier.

Nasri, A., Hannachi, A., Allouche, M., Barhoumi, B., Saidi, I., Dallali, M.,…Beyrem, H. (2020). Chronic ecotoxicity of ciprofloxacin exposure on taxonomic diversity of a meiobenthic nematode community in microcosm experiments. *Journal of King Saud University-Science*, *32*(2), 1470-1475.

Natarajan, R., Saikia, K., Ponnusamy, S. K., Rathankumar, A. K., Rajendran, D. S., Venkataraman, S.,…Banerjee, K. (2022). Understanding the factors affecting adsorption of pharmaceuticals on different adsorbents–A critical literature update. *Chemosphere*, *287*, 131958.

National Library of Medicine. (2023). *Diclofenac*. Retrieved 4 December 2023 from https://pubchem.ncbi.nlm.nih.gov/compound/Diclofenac

Nethaji, S., Sivasamy, A., Thennarasu, G., & Saravanan, S. (2010). Adsorption of Malachite Green dye onto activated carbon derived from Borassus aethiopum flower biomass. *Journal of Hazardous Materials*, *181*(1-3), 271-280.

Ngeno, E., Ongulu, R., Shikuku, V., Ssentongo, D., Otieno, B., Ssebugere, P., & Orata, F. (2024). Response surface methodology directed modeling of the biosorption of progesterone onto acid activated Moringa oleifera seed biomass: Parameters and mechanisms. *Chemosphere*, *360*, 142457.

Ngeno, E. C., Orata, F., Lilechi, D., Shikuku, V. O., & Kimosop, S. (2016). Adsorption of caffeine and ciprofloxacin onto pyrolitically derived water hyacinth biochar: isothermal, kinetic and thermodynamic studies. *J. Chem. Chem. Eng*, *10*, 185-194.

Ngeno, E. C., Shikuku, V. O., Orata, F., Baraza, L. D., & Kimosop, S. J. (2019). Caffeine and ciprofloxacin adsorption from water onto clinoptilolite: Linear isotherms, kinetics, thermodynamic and mechanistic studies. *South African Journal of Chemistry*, *72*, 136-142.

Nguyen, L. M., Nguyen, N. T. T., Nguyen, T. T. T., Nguyen, T. T., Nguyen, D. T. C., & Tran, T. V. (2022). Occurrence, toxicity and adsorptive removal of the chloramphenicol antibiotic in water: a review. *Environmental Chemistry Letters*, *20*(3), 1929-1963.

Obaid, S. A. (2020). Langmuir, Freundlich and Tamkin adsorption isotherms and kinetics for the removal aartichoke tournefortii straw from agricultural waste. Journal of Physics: Conference Series,

Obayomi, K. S., Lau, S. Y., Danquah, M. K., Zhang, J., Chiong, T., Meunier, L.,…Rahman, M. M. (2023). Green synthesis of graphene-oxide based nanocomposites for efficient removal of methylene blue dye from wastewater. *Desalination*, *564*, 116749.

Ogbeh, G. O., Ogunlela, A. O., Akinbile, C. O., & Iwar, R. T. (2025). Adsorption of organic micropollutants in water: A review of advances in modelling, mechanisms, adsorbents, and their characteristics. *Environmental engineering research*, *30*(2).

Oong, G. C., & Tadi, P. (2020). Chloramphenicol.

Orata, F. O. (2018). Conventional wastewater treatment plants as a discharge and source point for biota exposure to micro-pollutants. *Ecotoxicology: perspective on key issues. CRC Press, Boca Raton. https://doi. org/10.1201/b21896 Chapter*.

Ortúzar, M., Esterhuizen, M., Olicón-Hernández, D. R., González-López, J., & Aranda, E. (2022). Pharmaceutical pollution in aquatic environments: a concise review of environmental impacts and bioremediation systems. *Frontiers in Microbiology*, *13*, 869332.

Oturan, M. A. (2014). Electrochemical advanced oxidation technologies for removal of organic pollutants from water. In (Vol. 21, pp. 8333-8335): Springer.

Oyege, I., Wasswa, J., Bhaskar, M. S. B., Nkedi-Kizza, P., & Kasozi, G. N. (2024). Mixed-Solvent Sorption and Moisture-Regime-Dependent Degradation of Chlorpyrifos in Selected Tropical Soils. *International Journal of Environmental Research*, *18*(2), 14.

Pálinkó, I., Kónya, Z., Kukovecz, Á., & Kiricsi, I. (2013). Zeolites. *Springer Handbook of Nanomaterials*, 819-858.

Pang, T., Yang, X., Yuan, C., Elzatahry, A. A., Alghamdi, A., He, X.,…Deng, Y. (2021). Recent advance in synthesis and application of heteroatom zeolites. *Chinese Chemical Letters*, *32*(1), 328-338.

Parlayici, Ş., & Pehlivan, E. (2019). Comparative study of Cr (VI) removal by bio-waste adsorbents: equilibrium, kinetics, and thermodynamic. *Journal of Analytical Science and Technology*, *10*(1), 1-8.

Patel, M., Kumar, R., Kishor, K., Mlsna, T., Pittman, C. U., Jr., & Mohan, D. (2019). Pharmaceuticals of Emerging Concern in Aquatic Systems: Chemistry, Occurrence, Effects, and Removal Methods. *Chem Rev*, *119*(6), 3510-3673. https://doi.org/10.1021/acs.chemrev.8b00299

Pearson, R. G. (1963). Hard and soft acids and bases. *Journal of the American Chemical Society*, *85*(22), 3533-3539.

Peñafiel, M. E., Jara-Cobos, L., Flores, D., Jerves, C., & Menendez, M. (2024). Enhancing adsorptive removal of diclofenac from aqueous solution: Evaluating organic and inorganic acid treatment of zeolite. *Case Studies in Chemical and Environmental Engineering*, *9*, 100575.

Petrović, R., Gajić, D., Levi, Z., Bodroža, D., Sailović, P., & Mlinarević, V. (2020). Kinetics of diclofenac adsorption from aqueous solution on commercial activated carbon. *Journal of Chemists, Technologists and Environmentalists*, *1*(1).

Pickett, G. (1945). Modification of the Brunauer—Emmett—Teller theory of multimolecular adsorption. *Journal of the American Chemical Society*, *67*(11), 1958-1962.

Pourhakkak, P., Taghizadeh, A., Taghizadeh, M., Ghaedi, M., & Haghdoust, S. (2021). Fundamentals of adsorption technology. In *Interface science and technology* (Vol. 33, pp. 1-70). Elsevier.

Prüss-Ustün, A., Wolf, J., Bartram, J., Clasen, T., Cumming, O., Freeman, M. C.,…Johnston, R. (2019). Burden of disease from inadequate water, sanitation and hygiene for selected adverse health outcomes: an updated analysis with a focus on low-and

middle-income countries. *International journal of hygiene and environmental health*, *222*(5), 765-777.

Rápó, E., & Tonk, S. (2021). Factors affecting synthetic dye adsorption; desorption studies: a review of results from the last five years (2017–2021). *Molecules*, *26*(17), 5419.

Rashid, R., Shafiq, I., Akhter, P., Iqbal, M. J., & Hussain, M. (2021). A state-of-the-art review on wastewater treatment techniques: the effectiveness of adsorption method. *Environmental Science and Pollution Research*, *28*, 9050-9066.

Rehman, M. S. U., Rashid, N., Ashfaq, M., Saif, A., Ahmad, N., & Han, J.-I. (2015). Global risk of pharmaceutical contamination from highly populated developing countries. *Chemosphere*, *138*, 1045-1055.

Rigueto, C. V. T., Rosseto, M., Nazari, M. T., Ostwald, B. E. P., Alessandretti, I., Manera, C.,…Dettmer, A. (2021). Adsorption of diclofenac sodium by composite beads prepared from tannery wastes-derived gelatin and carbon nanotubes. *Journal of Environmental Chemical Engineering*, *9*(1), 105030.

Rouquerol, J., Rouquerol, F., Llewellyn, P., Maurin, G., & Sing, K. (2013). *Adsorption by powders and porous solids: principles, methodology and applications*. Academic press.

Roushani, M., Rahmati, Z., Farokhi, S., Hoseini, S. J., & Fath, R. H. (2020). The development of an electrochemical nanoaptasensor to sensing chloramphenicol using a nanocomposite consisting of graphene oxide functionalized with (3-Aminopropyl) triethoxysilane and silver nanoparticles. *Materials Science and Engineering: C*, *108*, 110388.

Rusch, M., Spielmeyer, A., Zorn, H., & Hamscher, G. (2019). Degradation and transformation of fluoroquinolones by microorganisms with special emphasis on ciprofloxacin. *Applied microbiology and biotechnology*, *103*, 6933-6948.

Sahoo, T. R., & Prelot, B. (2020). Adsorption processes for the removal of contaminants from wastewater: the perspective role of nanomaterials and nanotechnology. In *Nanomaterials for the detection and removal of wastewater pollutants* (pp. 161-222). Elsevier.

Sarmah, B., Satpati, B., & Srivastava, R. (2017). Highly efficient and recyclable basic mesoporous zeolite catalyzed condensation, hydroxylation, and cycloaddition reactions. *Journal of Colloid and Interface Science*, *493*, 307-316.

Schwarzenbach, R. P., Gschwend, P. M., & Imboden, D. M. (2016). *Environmental organic chemistry*. John Wiley & Sons.

Shabalin, B., Yaroshenko, K., & Mitsiuk, N. (2023). Composition of chemical elements and ion exchange complex of acid-and alkali-modified natural zeolites from the sokyrnytsky deposit. *Mineralogical Journal-Ukraine*, *45*(2), 116-123.

Shah, A., & Shah, M. (2020). Characterisation and bioremediation of wastewater: a review exploring bioremediation as a sustainable technique for pharmaceutical wastewater. *Groundwater for Sustainable Development*, *11*, 100383.

Shah, I., Adnan, R., Wan Ngah, W. S., & Mohamed, N. (2015). Iron impregnated activated carbon as an efficient adsorbent for the removal of methylene blue: regeneration and kinetics studies. *PloS one*, *10*(4), e0122603.

Sharma, P. C., Jain, A., Jain, S., Pahwa, R., & Yar, M. S. (2010). Ciprofloxacin: review on developments in synthetic, analytical, and medicinal aspects. *Journal of enzyme inhibition and medicinal chemistry*, *25*(4), 577-589.

Shi, J., Yang, Z., Dai, H., Lu, X., Peng, L., Tan, X.,…Fahim, R. (2018). Preparation and application of modified zeolites as adsorbents in wastewater treatment. *Water Science and Technology*, *2017*(3), 621-635.

Shikuku, V. O., Kowenje, C. O., Donato, F. F., Zanella, R., & Prestes, O. D. (2015). A comparison of adsorption equilibrium, kinetics and thermodynamics of aqueous phase clomazone between faujasite X and a natural zeolite from Kenya. *South African Journal of Chemistry*, *68*(1), 245-252.

Shikuku, V. O., Zanella, R., Kowenje, C. O., Donato, F. F., Bandeira, N. M., & Prestes, O. D. (2018). Single and binary adsorption of sulfonamide antibiotics onto iron-modified clay: linear and nonlinear isotherms, kinetics, thermodynamics, and mechanistic studies. *Applied Water Science*, *8*, 1-12.

Sifuna, F. W., Orata, F., Okello, V., & Jemutai-Kimosop, S. (2016). Comparative studies in electrochemical degradation of sulfamethoxazole and diclofenac in water by using various electrodes and phosphate and sulfate supporting electrolytes. *Journal of Environmental Science and Health, Part A*, *51*(11), 954-961.

Silva, A., Delerue-Matos, C., Figueiredo, S. A., & Freitas, O. M. (2019). The use of algae and fungi for removal of pharmaceuticals by bioremediation and biosorption processes: a review. *Water*, *11*(8), 1555.

Simonin, J.-P. (2016). On the comparison of pseudo-first order and pseudo-second order rate laws in the modeling of adsorption kinetics. *Chemical engineering journal*, *300*, 254-263.

Sofi, M., Hamid, M., Jalil, A., Alhebshi, A., Hassan, N., Bahari, M., & Mohamud, M. (2025). Recent advancements of SAPO-34 and ZSM-5 zeolite in converting methanol to olefin: a review. *Arabian Journal for Science and Engineering*, *50*(6), 3671-3697.

Sousa, J. C., Ribeiro, A. R., Barbosa, M. O., Ribeiro, C., Tiritan, M. E., Pereira, M. F. R., & Silva, A. M. (2019). Monitoring of the 17 EU Watch List contaminants of emerging concern in the Ave and the Sousa Rivers. *Science of the Total Environment*, *649*, 1083-1095.

Sousa, M. U., Rodrigues, A. M., Araujo, M. E. B., Menezes, R. R., Neves, G. A., & Lira, H. L. (2022). Adsorption of sodium diclofenac in functionalized palygoskite clays. *Materials*, *15*(8), 2708.

Srinivasan, K., Hariharapura, R. C., & Mallikarjuna, S. V. (2025). Pharmaceutical waste management through microbial bioremediation. *Environmental monitoring and assessment*, *197*(4), 488.

Srivastava, A., Dave, H., Prasad, B., Maurya, D. M., Kumari, M., Sillanpää, M., & Prasad, K. S. (2022). Low cost iron modified syzygium cumini l. Wood biochar for adsorptive removal of ciprofloxacin and doxycycline antibiotics from aqueous solution. *Inorganic Chemistry Communications*, *144*, 109895.

Stoch, A. (2015). Fly ash from coal combustion-characterization. *Praca doktorska*.

Stolker, A. A., & Danaher, M. (2011). Sample Preparation: Extraction and Clean-Up. *Chemical Analysis of Antibiotic Residues in Food*, 125-152.

Straioto, H., Viotti, P. V., Moura, A. A. d., Diório, A., Scaliante, M. H. N. O., Moreira, W. M.,…Bergamasco, R. (2023). Modification of natural zeolite clinoptilolite and ITS application in the adsorption of herbicides. *Environmental Technology*, *44*(26), 3949-3964.

Straub, J. O., Le Roux, J., & Tedoldi, D. (2023). Halogenation of pharmaceuticals is an impediment to ready biodegradability. *Water*, *15*(13), 2430.

Stuart, M., Lapworth, D., Crane, E., & Hart, A. (2012). Review of risk from potential emerging contaminants in UK groundwater. *Science of the Total Environment*, *416*, 1-21.

Sukmasari, E., & Azmiyawati, C. (2018). Modification of natural zeolite with Fe (iii) and its application as adsorbent chloride and carbonate ions. IOP Conference Series: Materials Science and Engineering,

Sun, K., Shi, Y., Xu, W., Potter, N., Li, Z., & Zhu, J. (2017). Modification of clays and zeolites by ionic liquids for the uptake of chloramphenicol from water. *Chemical engineering journal*, *313*, 336-344.

Tao, Y., Kanoh, H., Abrams, L., & Kaneko, K. (2006). Mesopore-modified zeolites: preparation, characterization, and applications. *Chem Rev*, *106*(3), 896-910.

Thai, T., Salisbury, B. H., & Zito, P. M. (2023). Ciprofloxacin. In *StatPearls [internet]*. StatPearls Publishing.

Turel, I., Bukovec, N., & Farkas, E. (1996). Complex formation between some metals and a quinolone family member (ciprofloxacin). *Polyhedron*, *15*(2), 269-275.

Ugrina, M., Medvidović, N. V., & Daković, A. (2015). Characterization and environmental application of iron-modified zeolite from the Zlatokop deposit. *Desalination and Water Treatment*, *53*(13), 3557-3569.

UNEP, A. (2016). A snapshot of the world's water quality: towards a global assessment. *Nairobi, United Nations Environment Programme*.

UNESCO. (2023). *World Water Assessment Programme*. Retrieved October 10 from https://www.unesco.org/en/wwap

United Nations. (2010). *The Human Right to Water and Sanitation*. Retrieved November 15 from https://www.un.org/waterforlifedecade/pdf/human_right_to_water_and_sanitation_media_brief.pdf

van Bokhoven, J. A., & Lamberti, C. (2014). Structure of aluminum, iron, and other heteroatoms in zeolites by X-ray absorption spectroscopy. *Coordination Chemistry Reviews*, *277*, 275-290.

Van, T., Yidana, Z., Smooker, P., & Coloe, P. (2020). Antibiotic use in food animals worldwide, with a focus on Africa: Pluses and minuses. J Glob Antimicrob Resist 20: 170–177. In.

Velazquez-Peña, G. C., Solache-Ríos, M., Olguin, M., & Fall, C. (2019). As (V) sorption by different natural zeolite frameworks modified with Fe, Zr and FeZr. *Microporous and Mesoporous Materials*, *273*, 133-141.

Wada, O. Z., & Olawade, D. B. (2025). Recent occurrence of pharmaceuticals in freshwater, emerging treatment technologies, and future considerations: A review. *Chemosphere*, *374*, 144153.

Wan Ngah, W., Teong, L., Wong, C., & Hanafiah, M. (2012). Preparation and characterization of chitosan–zeolite composites. *Journal of applied polymer science*, *125*(3), 2417-2425.

Wang, C., Leng, S., Guo, H., Yu, J., Li, W., Cao, L., & Huang, J. (2019). Quantitative arrangement of Si/Al ratio of natural zeolite using acid treatment. *Applied Surface Science*, *498*, 143874.

Wang, J., & Guo, X. (2020). Adsorption kinetic models: Physical meanings, applications, and solving methods. *Journal of Hazardous Materials*, *390*, 122156.

Wang, S., & Peng, Y. (2010). Natural zeolites as effective adsorbents in water and wastewater treatment. *Chemical engineering journal*, *156*(1), 11-24.

Wang, Y., Zhang, W., Mhungu, F., Zhang, Y., Liu, Y., Li, Y.,…Zhong, X. (2021). Probabilistic risk assessment of dietary exposure to chloramphenicol in Guangzhou, China. *International journal of environmental research and public health*, *18*(16), 8805.

Wanyonyi, F. S., Orata, F., Mutua, G. K., Odey, M. O., Zamisa, S., Ogbodo, S. E.,…Pembere, A. (2024a). Application of South African heulandite (HEU) zeolite for the adsorption and removal of Pb2+ and Cd2+ ions from aqueous water solution: Experimental and computational study. *Heliyon*, *10*(14).

Wanyonyi, F. S., Orata, F., Ramasami, P., Ngeno, E., Shikuku, V., Gembo, R. O.,…Pembere, A. (2025). Unlocking the adsorptive effectiveness of naturally occurring heulandite zeolite for the removal of PO43− and NO3− anions from wastewater. *Environmental Monitoring and Assessment*, *197*(1), 1-18.

Wanyonyi, F. S., Pembere, A., Mutua, G. K., Orata, F., & Louis, H. (2020). Computational screening of zeolites for the adsorption of selected pharmaceutical pollutants. *SN Applied Sciences*, *2*(11). https://doi.org/10.1007/s42452-020-03694-y

Warren, B. E. (1990). *X-ray Diffraction*. Courier Corporation.

Water Online. (2019). *Benefits And Disadvantages Of The Advanced Oxidation Process*. Water Online. Retrieved 19 January 2024 from https://www.wateronline.com/doc/benefits-and-disadvantages-of-the-advanced-oxidation-process-0001

Weber Jr, W. J., & Morris, J. C. (1963). Kinetics of adsorption on carbon from solution. *Journal of the sanitary engineering division*, *89*(2), 31-59.

Widiastuti, N., Wu, H., Ang, H. M., & Zhang, D. (2011). Removal of ammonium from greywater using natural zeolite. *Desalination*, *277*(1-3), 15-23.

Wiffen, P. J., & Xia, J. (2020). Systematic review of topical diclofenac for the treatment of acute and chronic musculoskeletal pain. *Current medical research and opinion*, *36*(4), 637-650.

Windeck, H., Berger, F., & Sauer, J. (2024). Chemically accurate predictions for water adsorption on Brønsted sites of zeolite H-MFI. *Physical Chemistry Chemical Physics*, *26*(36), 23588-23599.

Włodarczyk-Makuła, M., Myszograj, S., & Włodarczyk, M. (2023). Removal of organic micro-pollutants from wastewater in electrochemical processes. *Energies*, *16*(15), 5591.

Wu, F.-C., Tseng, R.-L., & Juang, R.-S. (2009). Characteristics of Elovich equation used for the analysis of adsorption kinetics in dye-chitosan systems. *Chemical engineering journal*, *150*(2-3), 366-373.

Xie, J., Meng, W., Wu, D., Zhang, Z., & Kong, H. (2012). Removal of organic pollutants by surfactant modified zeolite: Comparison between ionizable phenolic compounds and non-ionizable organic compounds. *Journal of hazardous materials*, *231*, 57-63.

Xiong, Q., Hu, L.-X., Liu, Y.-S., Wang, T.-T., & Ying, G.-G. (2019). New insight into the toxic effects of chloramphenicol and roxithromycin to algae using FTIR spectroscopy. *Aquatic Toxicology*, *207*, 197-207.

Xu, W., Hussain, A., & Liu, Y. (2018). A review on modification methods of adsorbents for elemental mercury from flue gas. *Chemical engineering journal*, *346*, 692-711.

Xu, Z., Yang, Z., Liu, Y., Lu, Y., Chen, K., & Zhu, W. (2014). Halogen bond: its role beyond drug–target binding affinity for drug discovery and development. *Journal of chemical information and modeling*, *54*(1), 69-78.

Yan, Y., Xu, X., Shi, C., Yan, W., Zhang, L., & Wang, G. (2019). Ecotoxicological effects and accumulation of ciprofloxacin in Eichhornia crassipes under hydroponic conditions. *Environmental Science and Pollution Research*, *26*, 30348-30355.

Yang, Y., Zhang, X., Jiang, J., Han, J., Li, W., Li, X.,…Alvarez, P. J. (2021). Which micropollutants in water environments deserve more attention globally? *Environmental Science & Technology*, *56*(1), 13-29.

Yi, H., Feng, Y., Yu, Q., Tang, X., Zhang, Y., & Zhuang, R. (2020). Synthesis of divalent metal-silicalite MEL zeolites as efficient bi-functional adsorbents/catalysts for non-methane hydrocarbon in cooking oil fumes elimination. *Separation and Purification Technology*, *251*, 117363.

Zhang, J., Tang, X., Yi, H., Yu, Q., Zhang, Y., Wei, J., & Yuan, Y. (2022). Synthesis, characterization and application of Fe-zeolite: A review. *Applied Catalysis A: General*, *630*, 118467.

Zhang, Y., Guo, P., Wang, M., Wu, Y., Sun, Y., Su, H., & Deng, J. (2021). Mixture toxicity effects of chloramphenicol, thiamphenicol, florfenicol in Daphnia magna under different temperatures. *Ecotoxicology*, *30*, 31-42.

Zhuang, S., Chen, R., Liu, Y., & Wang, J. (2020). Magnetic COFs for the adsorptive removal of diclofenac and sulfamethazine from aqueous solution: Adsorption kinetics, isotherms study and DFT calculation. *Journal of Hazardous Materials*, *385*, 121596.

Zieliński, M., Zielińska, M., & Dębowski, M. (2016). Ammonium removal on zeolite modified by ultrasound. *Desalination and Water Treatment*, *57*(19), 8748-8753.

Zimmermann, M., Zimmermann-Kogadeeva, M., Wegmann, R., & Goodman, A. L. (2019). Mapping human microbiome drug metabolism by gut bacteria and their genes. *Nature*, *570*(7762), 462-467.

Zvereva, I. A., Shelyapina, M. G., Chislov, M., Novakowski, V., Malygina, E., Rodríguez-Iznaga, I.,…Petranovskii, V. (2022). A comparative analysis of natural zeolites from various Cuban and Mexican deposits: Structure, composition, thermal properties and hierarchical porosity. *Journal of Thermal Analysis and Calorimetry*, 1-13.

APPENDICES

Appendix 1: EDS layered mapping of NZe

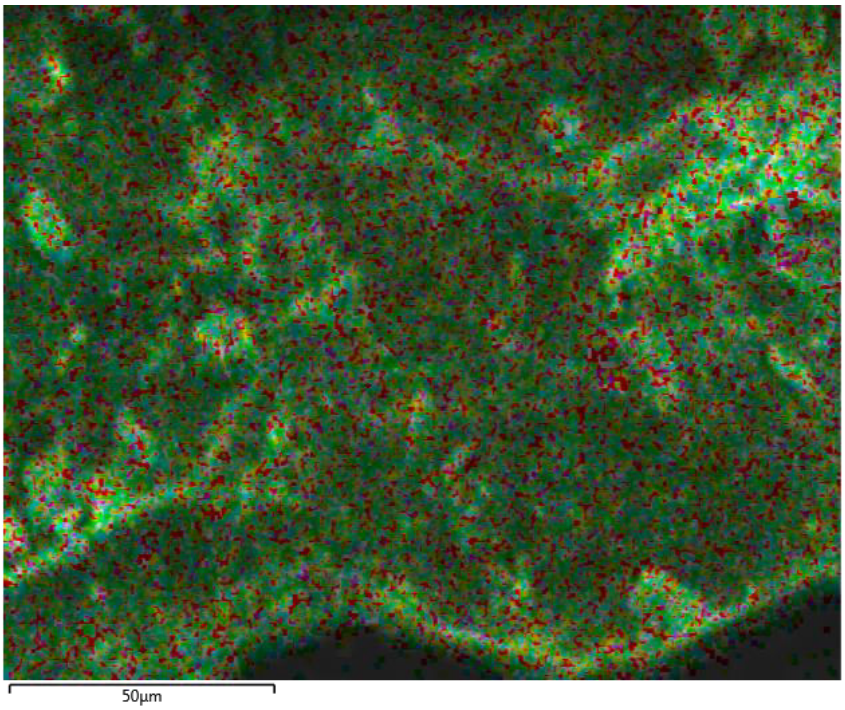

Appendix 2: EDS layered mapping of ImZe

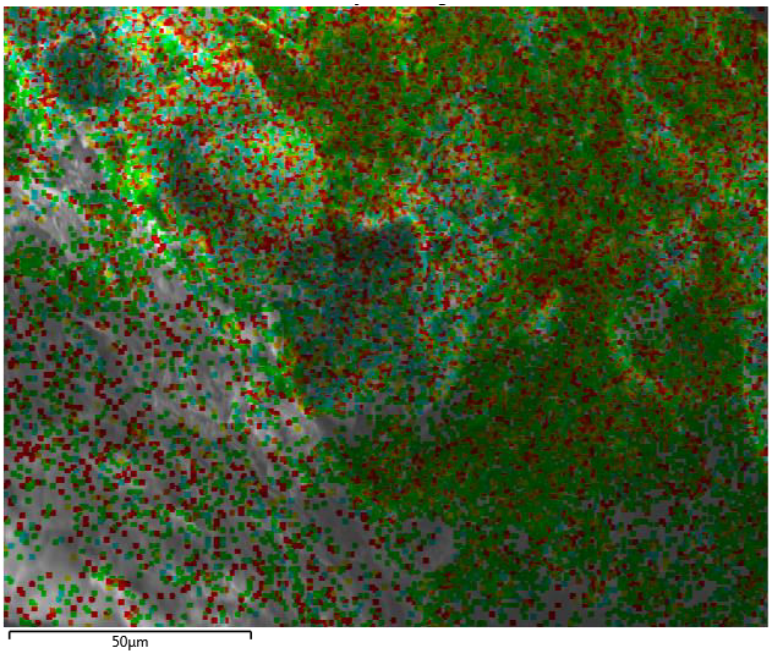

Appendix 3: EDS elemental distribution mapping of NZe

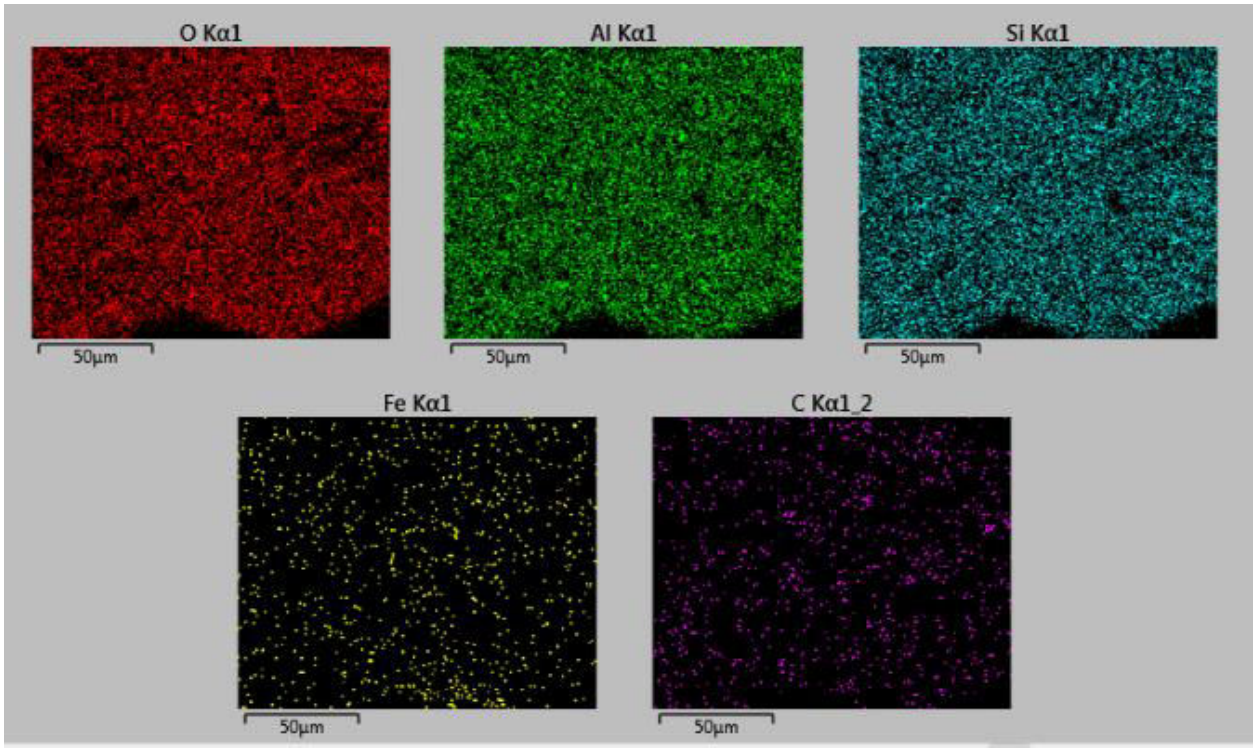

Appendix 4: EDS elemental distribution mapping of ImZe

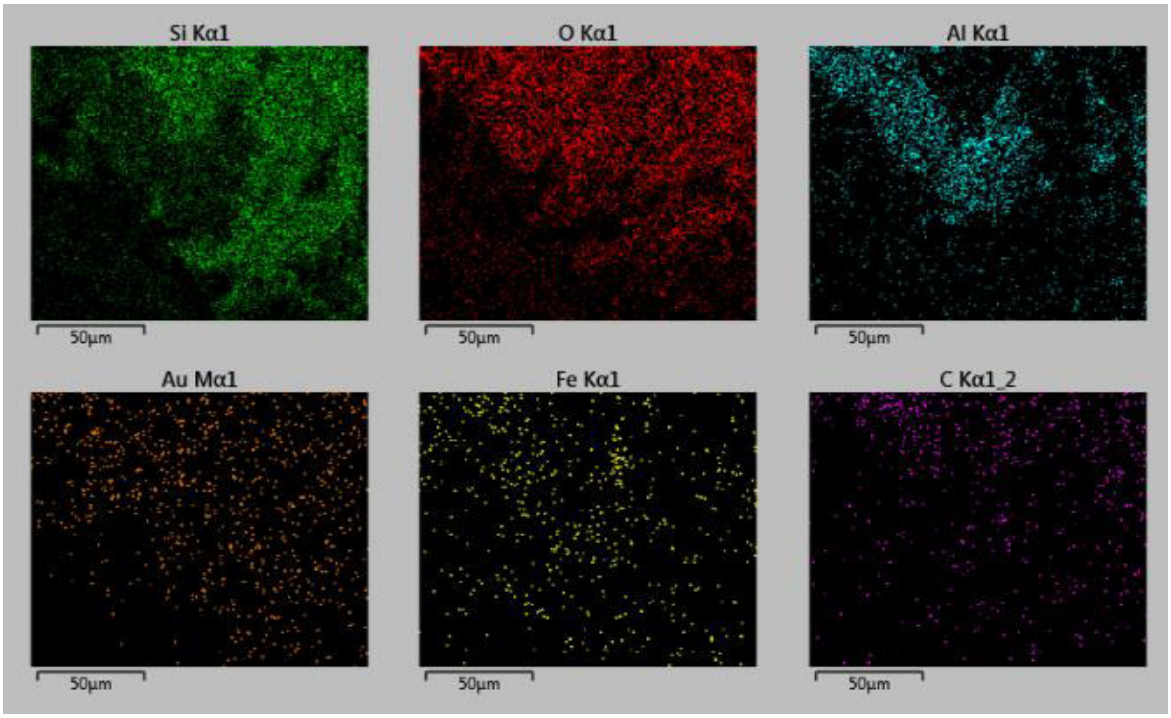

Appendix 5: Calibration Curves of the adsorbates

Standard calibration curves of Chloramphenicol, Ciprofloxacin and Diclofenac potassium (Appendix 5) were prepared by different concentrations starting from 1 to 20 ppm with at 10-point calibration in triplicates.

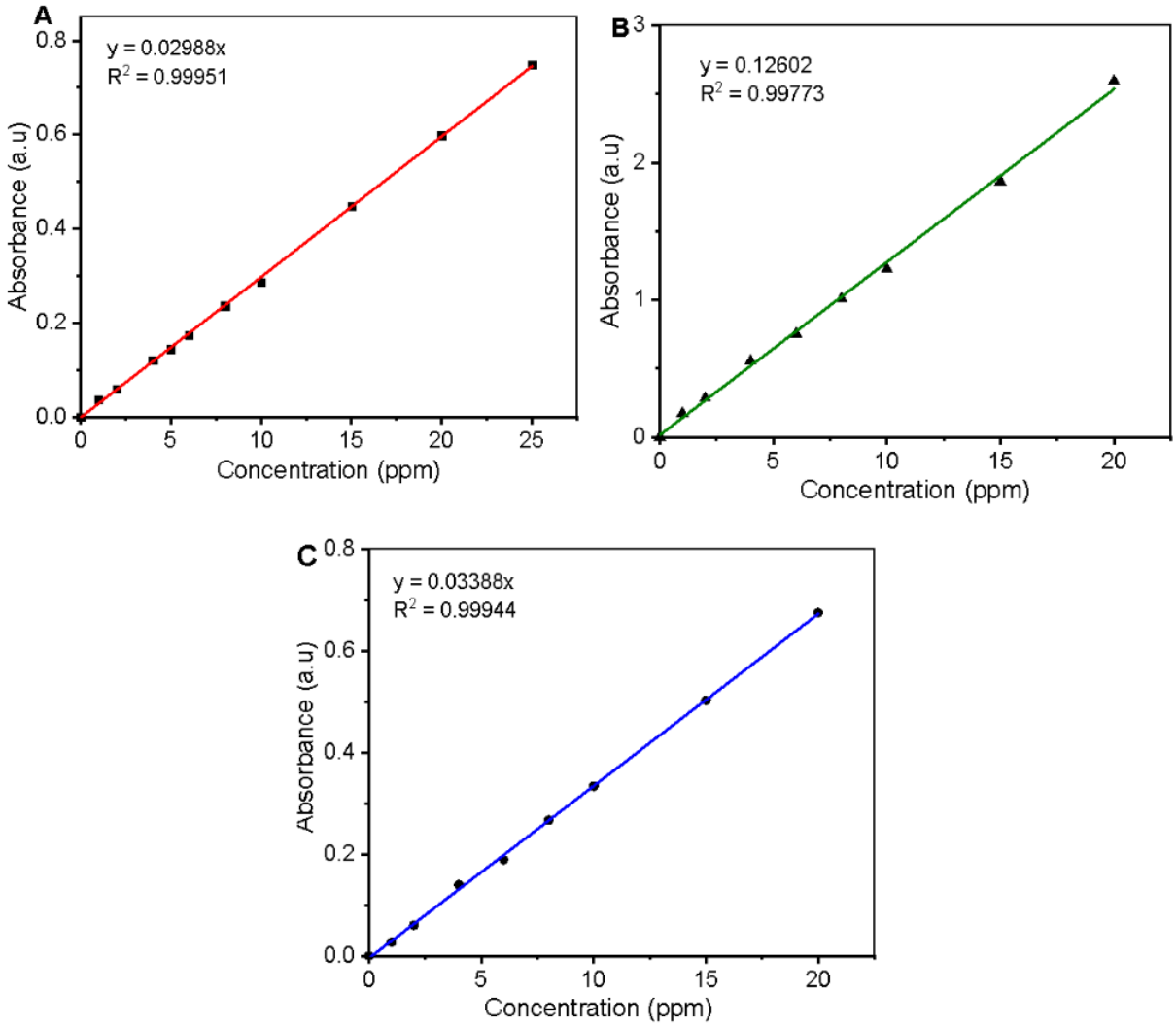

Appendix 5: Calibration curves for A. Chloramphenicol B. Ciprofloxacin C. Diclofenac

The R^2 values were 0.9995 (Chloramphenicol), 0.9973 (Ciprofloxacin) and 0.9999 (Diclofenac potassium) demonstrating an excellent fit of the data with a negligible deviation of 0.049 % for Chloramphenicol, 0.27% for Ciprofloxacin and 0.006% for Diclofenac potassium. Diclofenac potassium exhibited the lowest molar absorptivity with Ciprofloxacin showing the highest. This is to be attributed to a more extended conjugation in Ciprofloxacin owing to its quinoline structure and aromatic ring thus contributing to its higher molar absorptivity while Diclofenac potassium has the lowest overall conjugation. The linearity of the calibration curves indicated

their applicability in accurate determination of unknown concentrations by correlating the absorbance to concentration.

Appendix 6: Raw Kinetic data

Time (min)	Chloramphenicol		Ciprofloxacin		Diclofenac	
	Adsorption capacity (mg/g)					
	NZe	ImZe	NZe	ImZe	NZe	ImZe
0	0	0	0	0	0	0
5	2.954975	6.972259693	1.4020825	5.60832618	1.831058	10.32423208
10	5.3235175	10.5735175	2.2100525	8.84020619	2.62969275	11.51877133
20	6.50060675	14.09246283	3.0541225	12.2164948	3.74232075	12.96928328
30	7.30722	16.39358228	3.96649475	13.8659794	4.57764505	13.3105802
45	7.7064825	18.09232797	4.34536	14.7938144	5.1902725	14.76109215
60	7.8148	20.23439721	4.68685575	15.7474227	6.461604	14.84641638
120	8.092	21.9187005	5.21417525	16.8556701	6.5255975	15.10238908
180	8.092014	22.492375	5.3386645	17.3546584	6.7424	15.6996587
240	8.091991	22.492401	5.3386729	18.4345461	6.819965	15.6996590

Appendix 7: Raw Equilibrium data

Ci (mg/L)	Chloramphenicol		Ciprofloxacin		Diclofenac	
	Ce (mg/L)	Qe (mg/g)	Ce (mg/L)	Qe (mg/g)	Ce (mg/L)	Qe (mg/g)
2	0.09457	4.763575	0.087010309	4.782474228	0.08498294	4.78754265

5	0.33271	11.668225	0.528865979	11.17783505	1.003993174	9.990017065
10	1.0123944	22.469014	2.62618156	18.4345461	3.72696246	15.68259385
15	2.71879	30.703025	5.791600315	23.02099921	6.563139932	21.09215017
20	4.26354	39.34115	8.72365172	28.1908707	10.29351536	24.2662116

Appendix 8: Raw Thermodynamics data

Temperature (°C)	**Chloramphenicol**	**Ciprofloxacin**	**Diclofenac**
	Adsorption capacity (mg/g)		
298.15	22.468571	18.5461	16.1766225
303.15	19.759025	19.29381443	15.1728175
308.15	19.3808525	20.43814433	14.3020475
313.15	18.84553875	21.80670103	13.4069965